Coherent Diffractive Imaging: Principles and Biological Applications

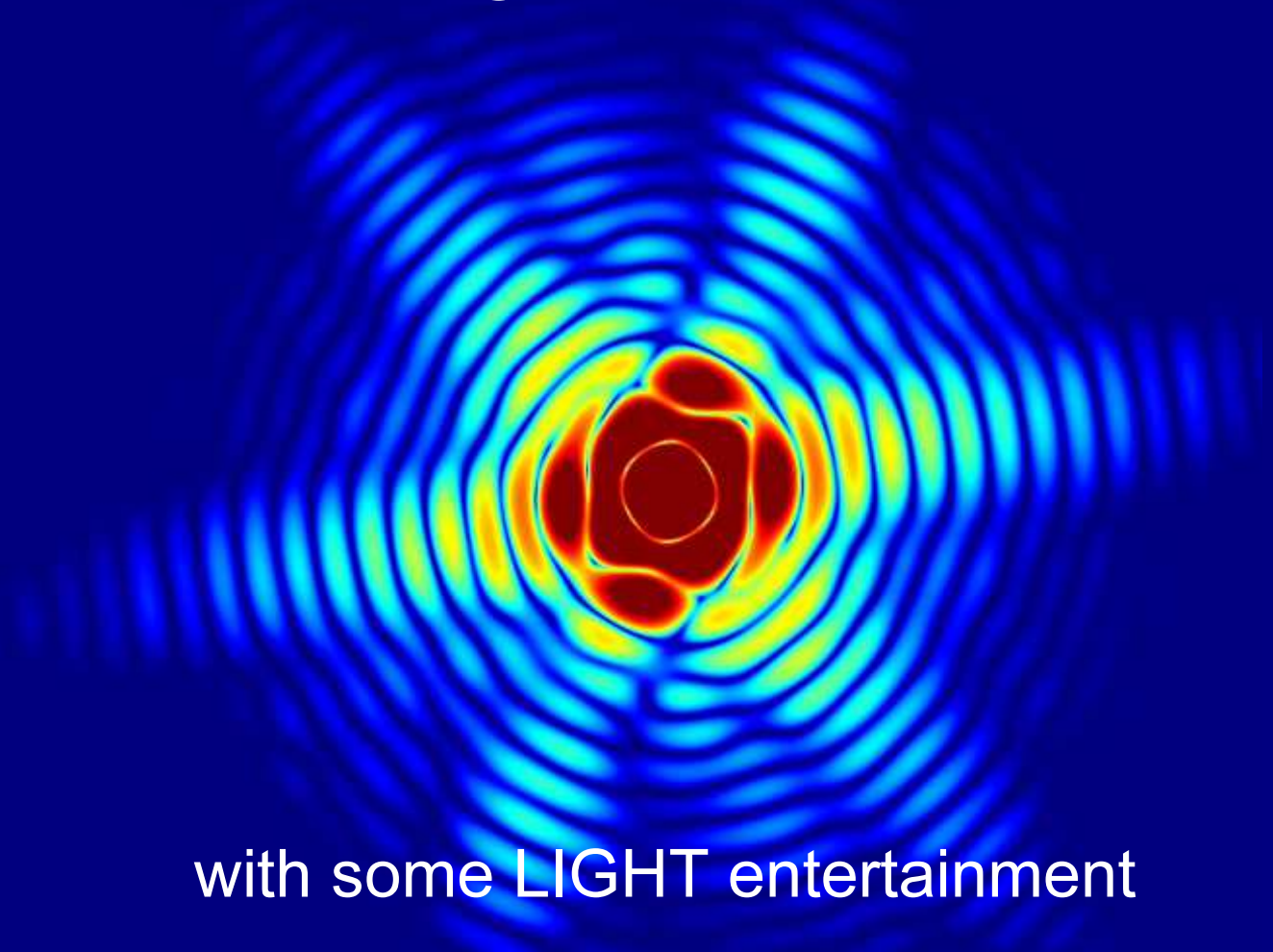

with some LIGHT entertainment

Janos Hajdu
Uppsala University, Sweden, and
the European Extreme Light Infrastructure in Prague

THE ACT OF OBSERVATION CHANGES WHAT IS BEING OBSERVED

AN ATOM

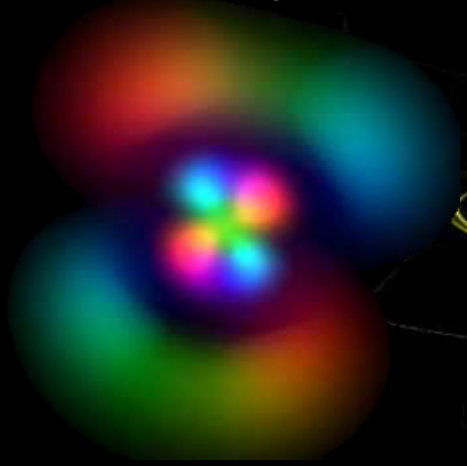

AN ATOM BEEING OBSERVED IN A PARTICLE COLLIDER

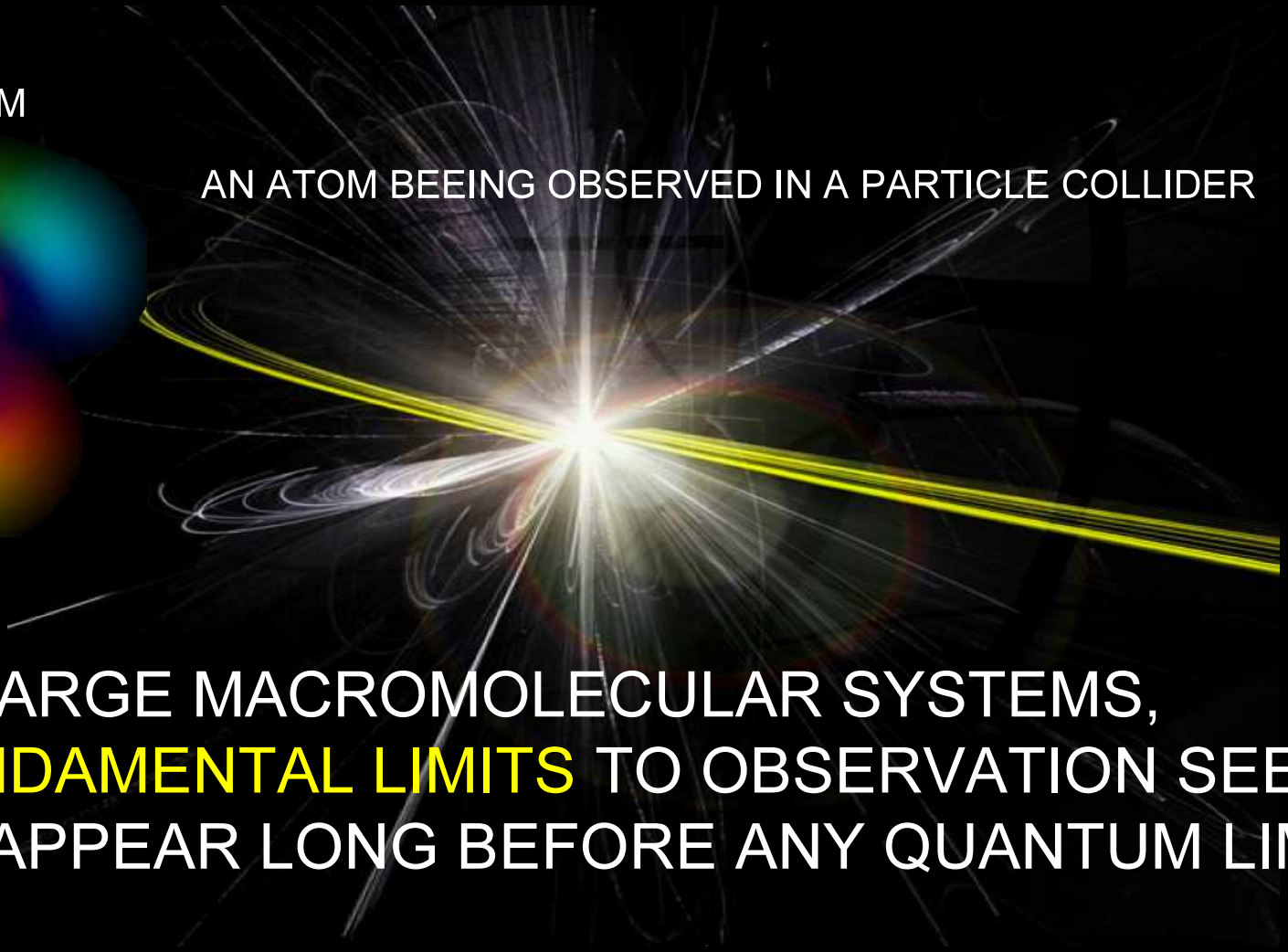

IN LARGE MACROMOLECULAR SYSTEMS, FUNDAMENTAL LIMITS TO OBSERVATION SEEM TO APPEAR LONG BEFORE ANY QUANTUM LIMITS

The changes inflicted can be quite dramatic

OXFROD 1981: Glycogen phosphorylase *b*
A large macromolecular system

Wire works by John Jenkins and Giuseppe Zanotti

The 1st DEDICATED SYNCHROTRON SOURCE for HARD X-RAYS

DARESBURY LABORATORY (1981-2008)

RADIATION DAMAGE TO A CRYSTAL

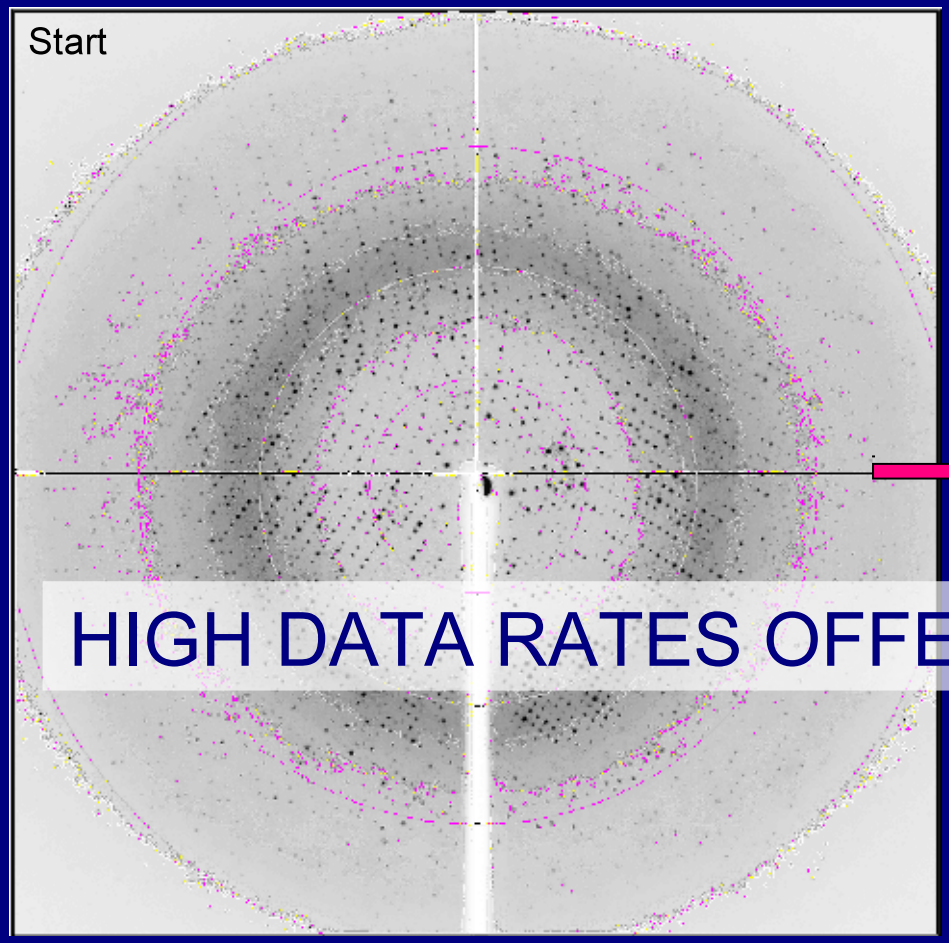

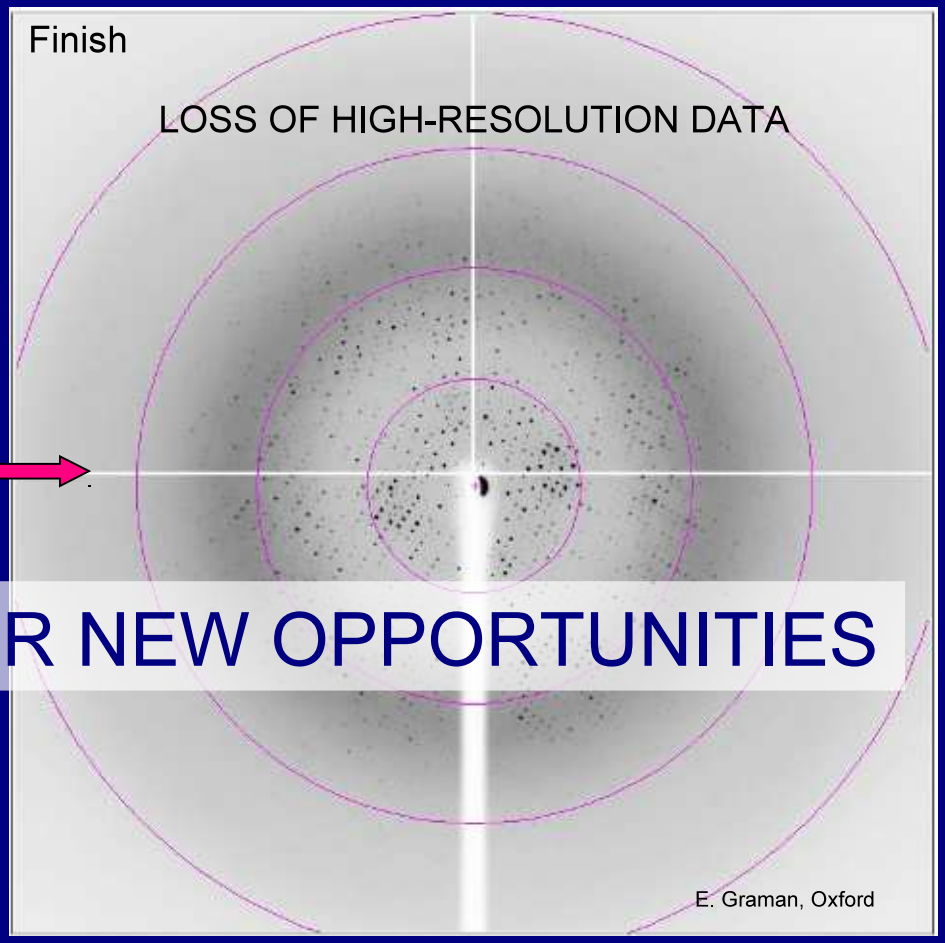

HIGH DATA RATES OFFER NEW OPPORTUNITIES

A REVELATION FROM DARESBURY IN 1981: Data collection was fast (20 min *vs*. 2 weeks), and the crystals lasted much longer at the synchrotron than at home in Oxford.

The 1st hint for a significant time component in damage formation

THE 1st TIME-RESOLVED EXPERIMENT IN XTALLOGRAPHY

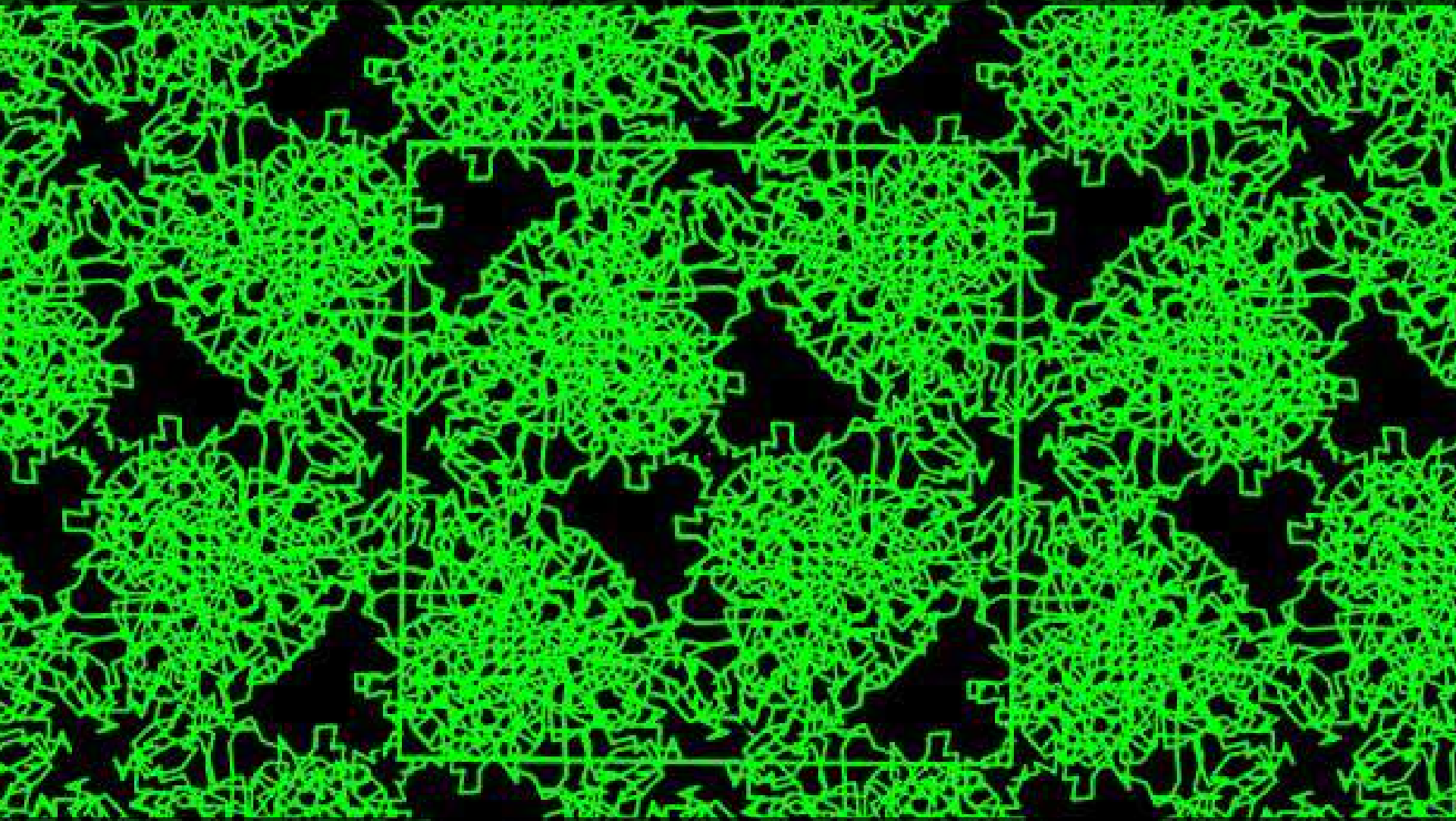

CATALYSIS IN A CRYSTAL OF GLYCOGEN PHOSPHORYLASE

Hajdu, J., Acharya, K. R., Stuart, D. I., McLaughlin, P. J., Barford, D., Oikonomakos, N. G., Klein, H. & Johnson, L. N. (1987) Catalysis in the crystal: Synchrotron radiation studies with glycogen phosphorylase *b*. *EMBO J.*, 6, 539-546.

Hajdu, J., Acharya, K. R., Barford, D., Stuart, D. I., Johnson, L. N. (1988) Catalysis in enzyme crystals. *TIBS*, 13, 104-109.

HEPTENITOL

HEPTULOSE-2-PHOSPHATE

EACH DATA SET REPRESENTS A TIME & VOLUME AVERAGE

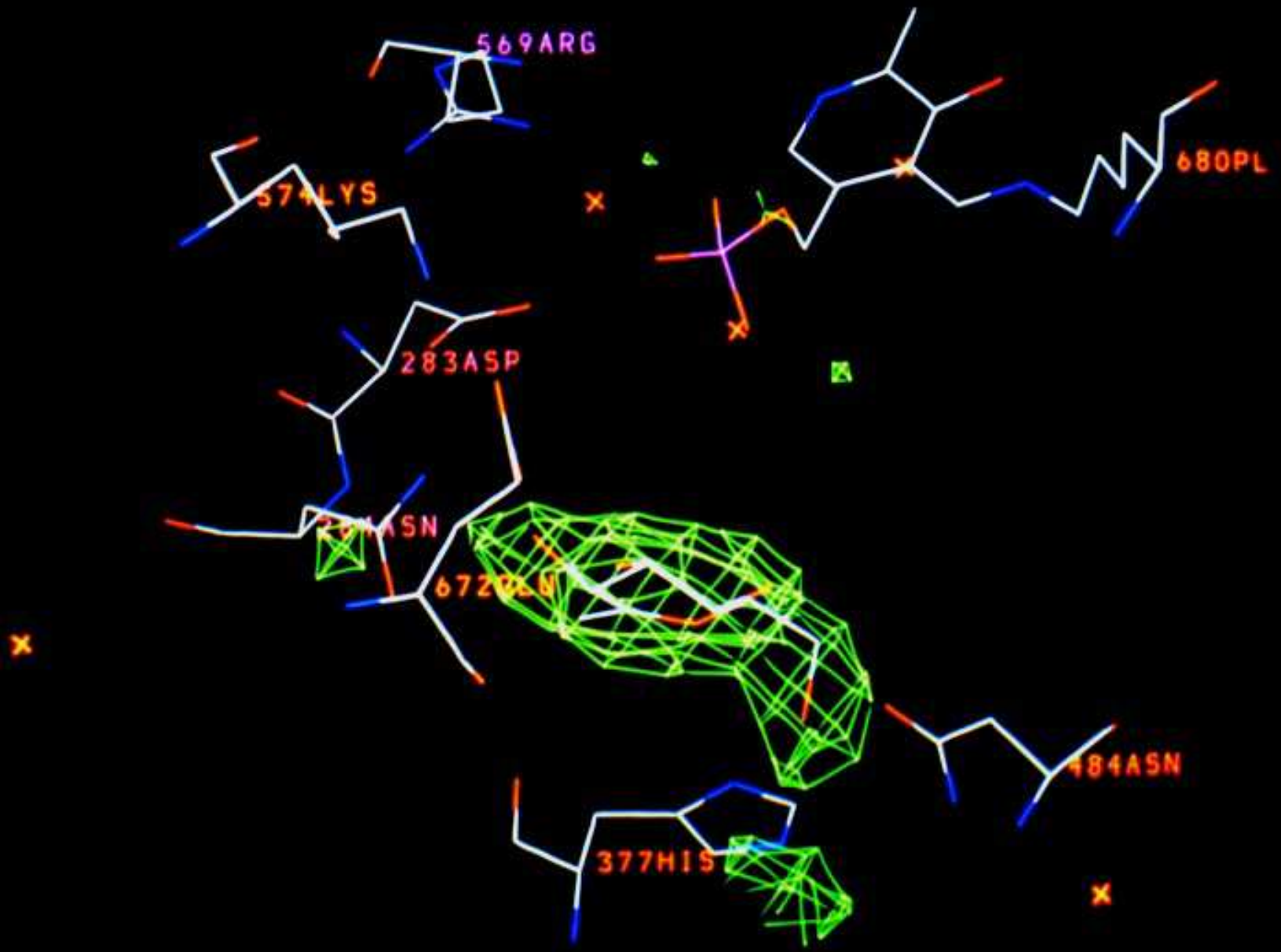

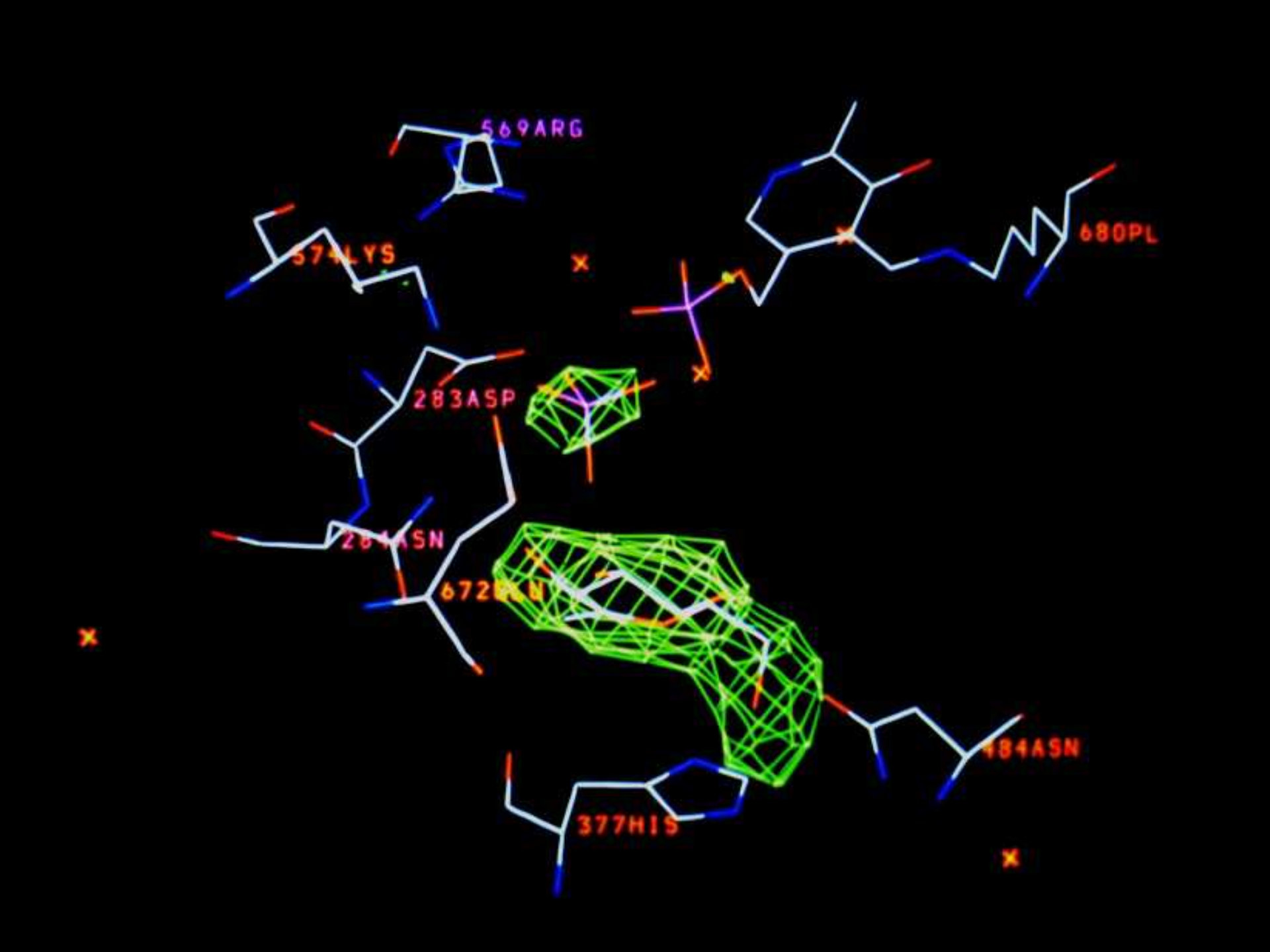
569ARG
574LYS
680PL
283ASP
264ASN
672
484ASN
377HIS

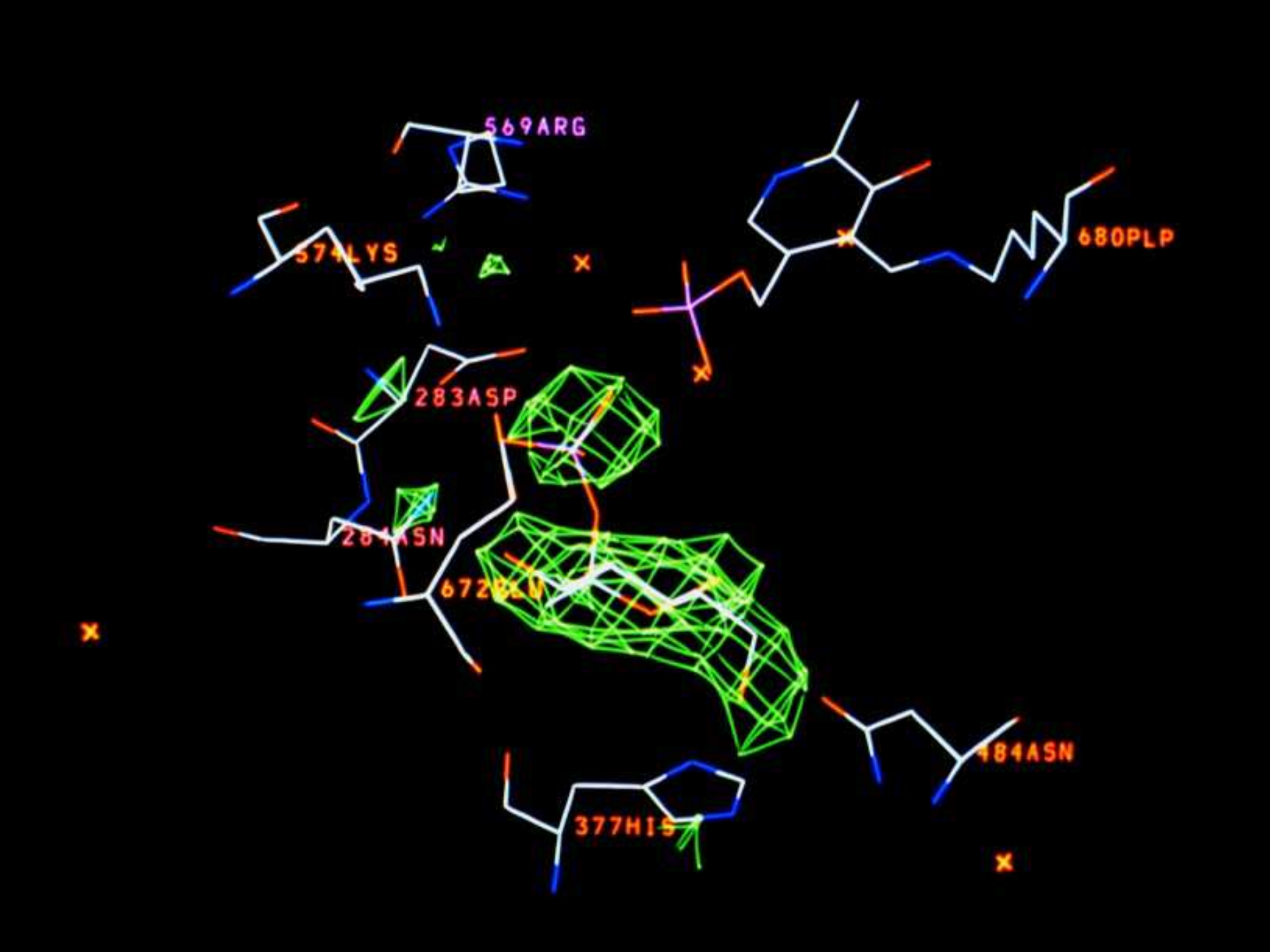
569ARG
574LYS
680PLP
283ASP
284ASN
484ASN
377HIS

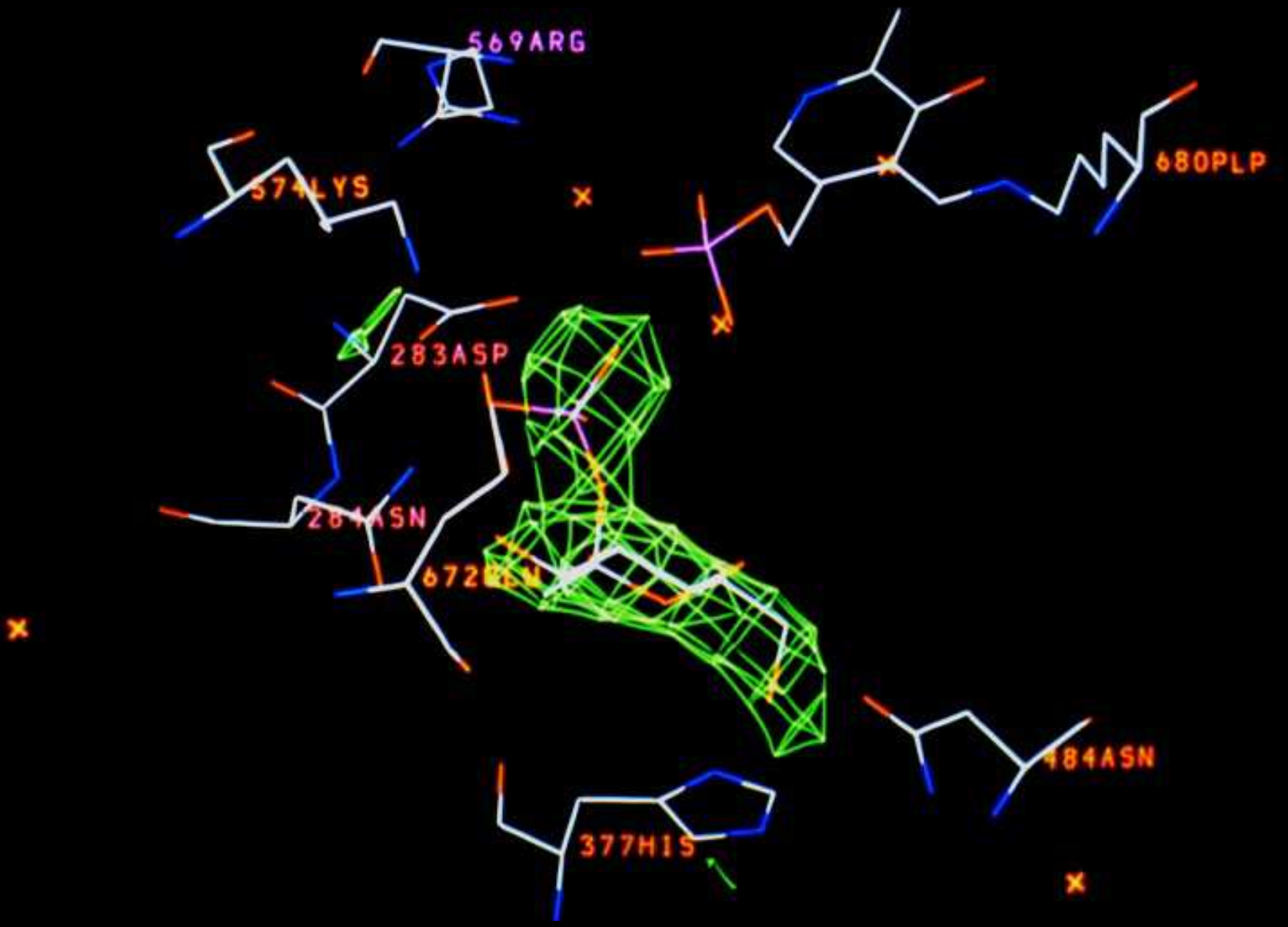
569ARG
574LYS
680PLP
283ASP
284ASN
377HIS
484ASN

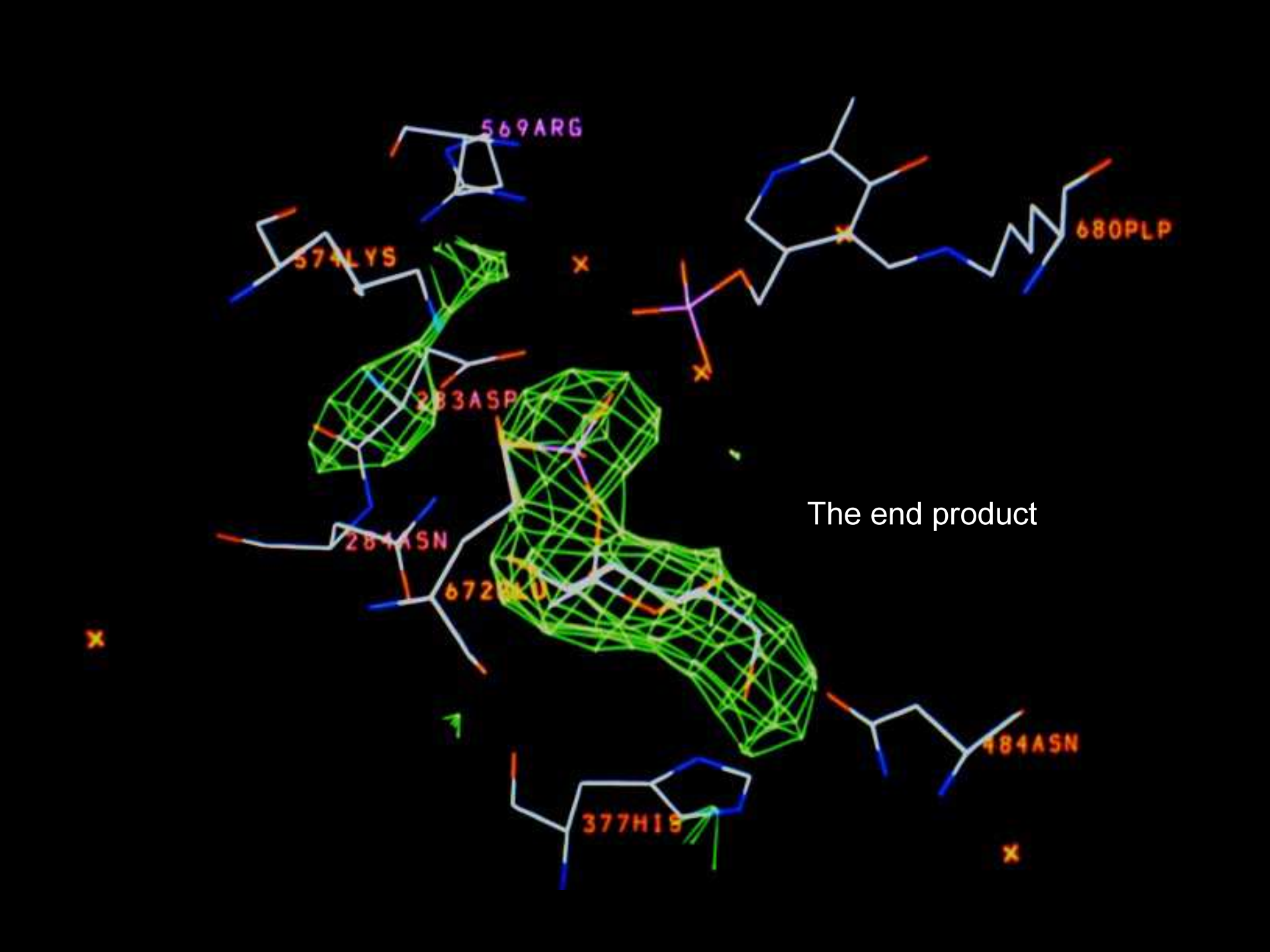

The end product

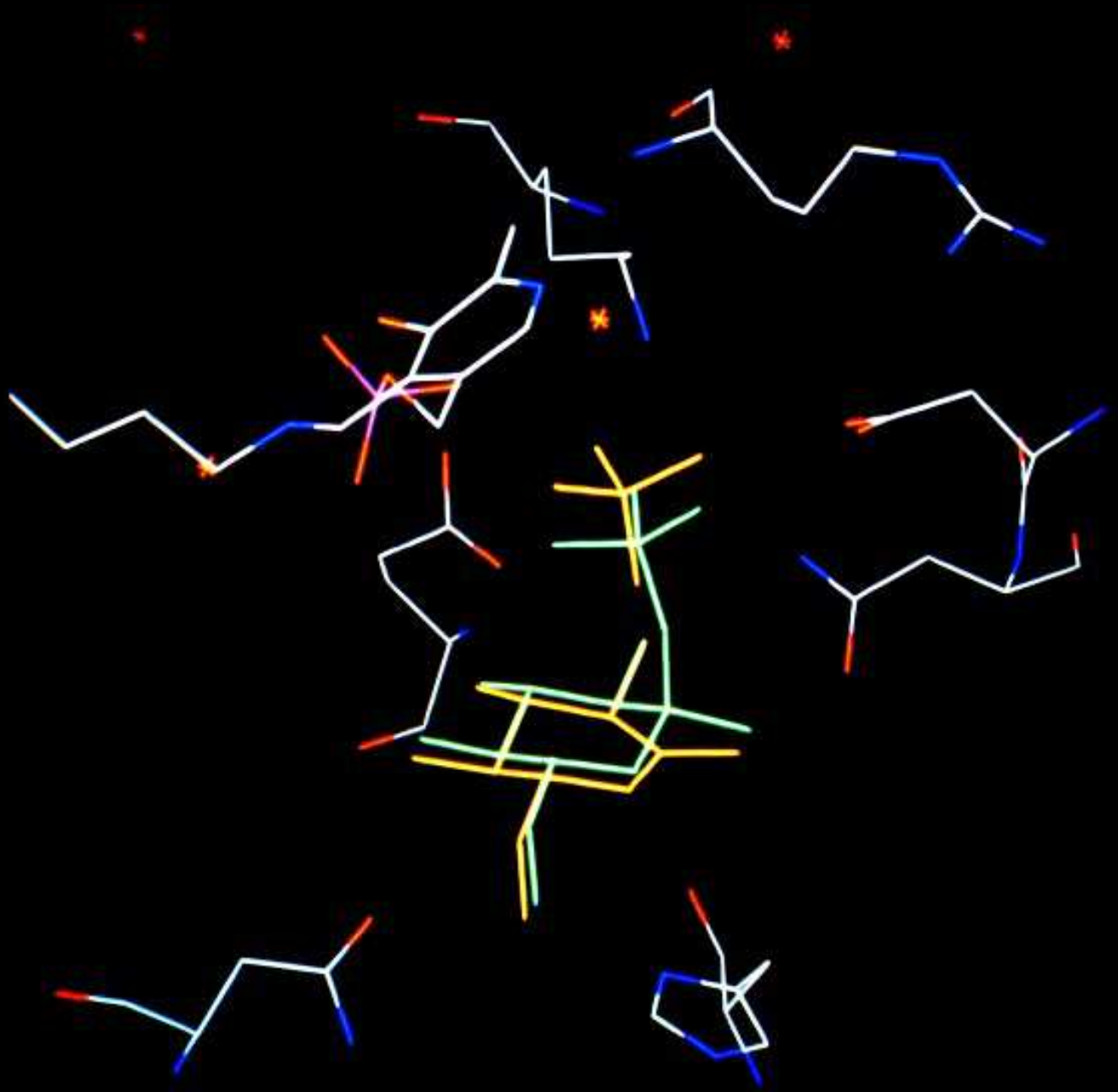

"Catalysis in the crystal: Synchrotron radiation studies with glycogen phosphorylase b"
Hajdu, J. et al. *EMBO J*. **6**, 539-546 (1987).

FASTER DATA COLLECTION BY BRUTE FORCE: WHITE SYNCHROTRON RADIATION (1984)

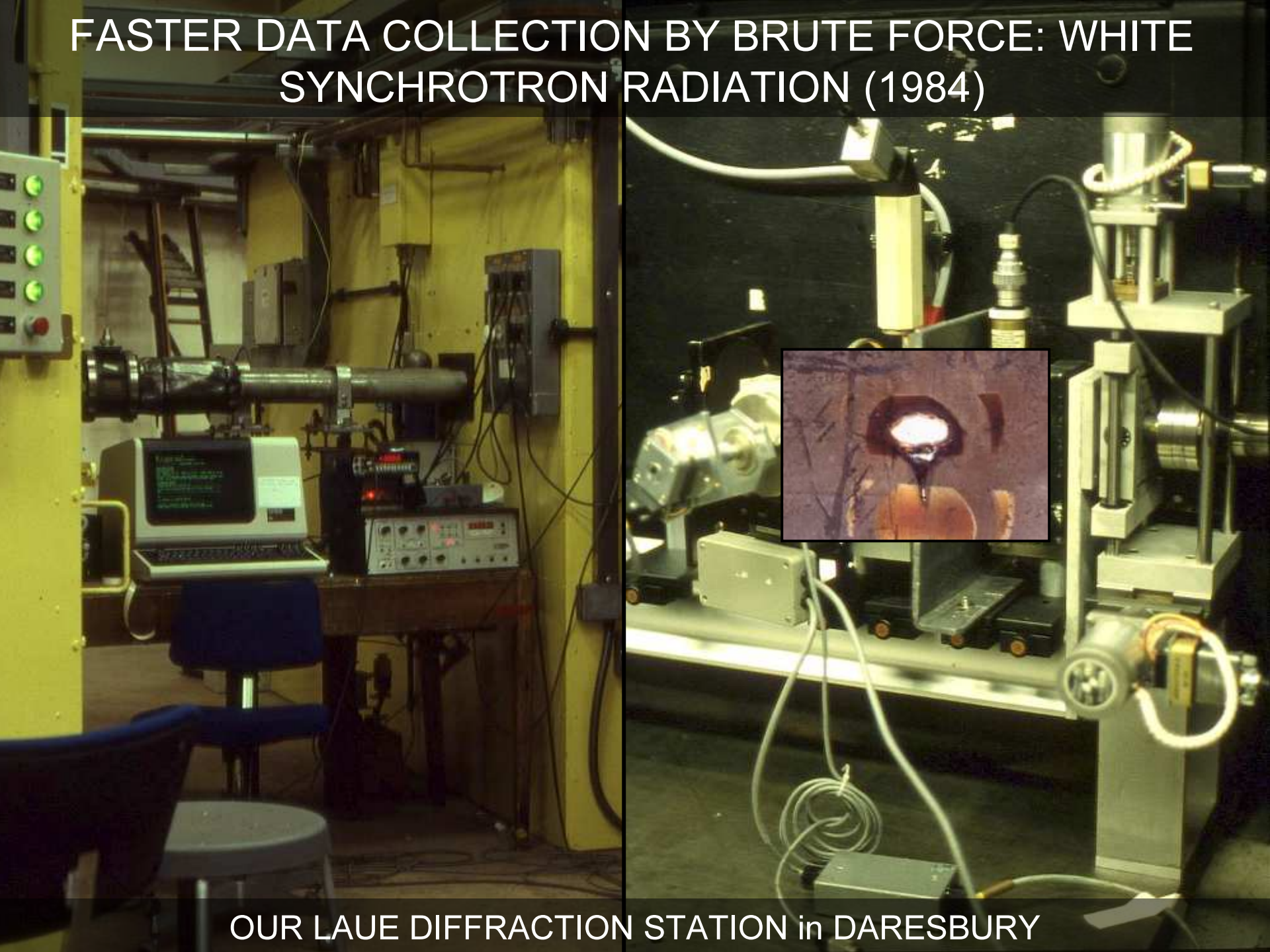

OUR LAUE DIFFRACTION STATION in DARESBURY

“Millisecond X-ray diffraction: First electron density map from Laue photographs of a protein crystal”
Hajdu et al. *Nature* **329**, 178-181 (1987)

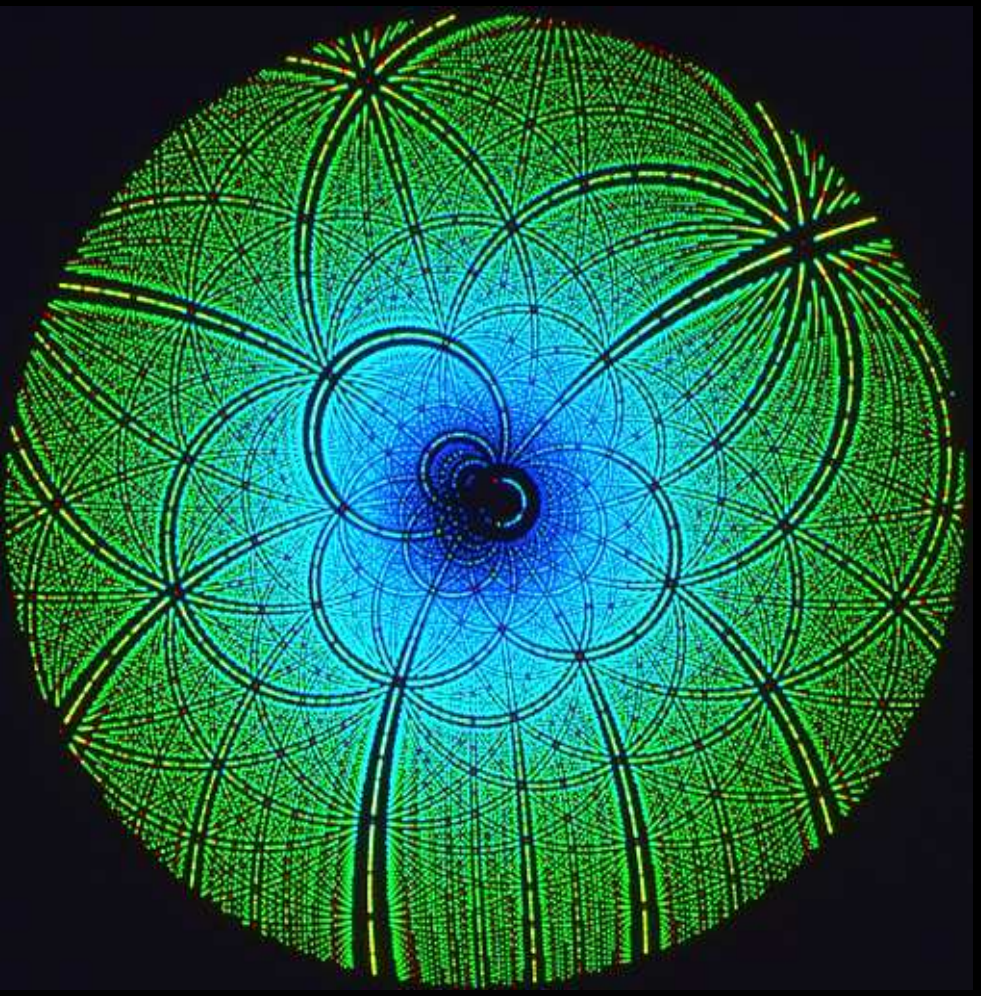

Binding of maltoheptose to
glycogen phosphorylase *b*

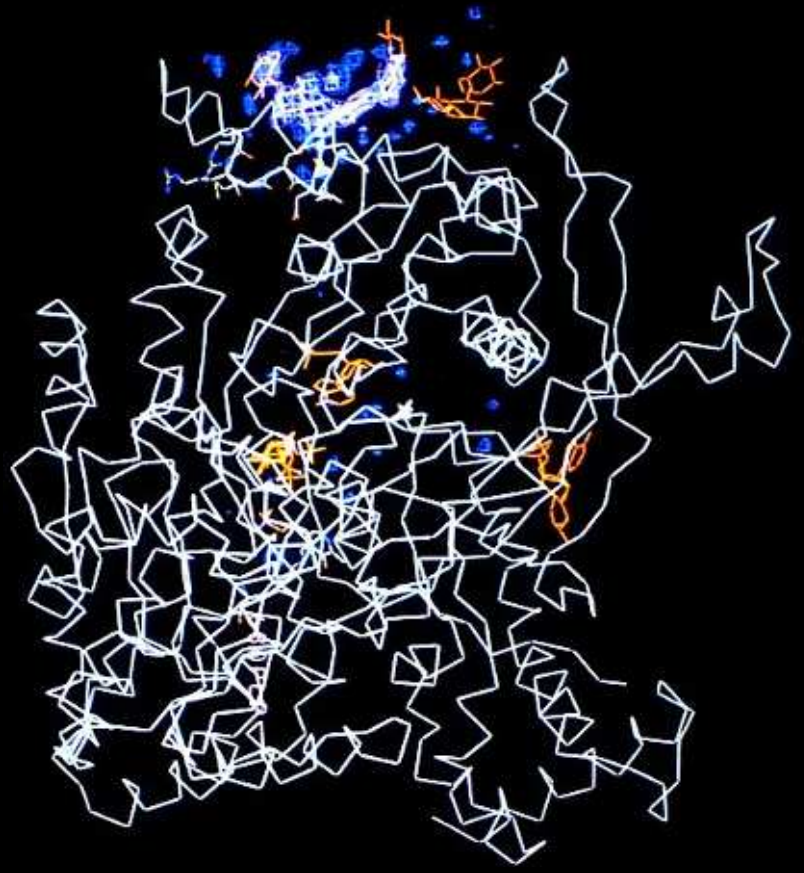

Sensitive to disorder, high background, plenty of corrections - but can be very fast

X-RAY DRIVEN CATALYSIS IN A REDOX ENZYME

EXPLOITING IONISATION BY X-RAYS

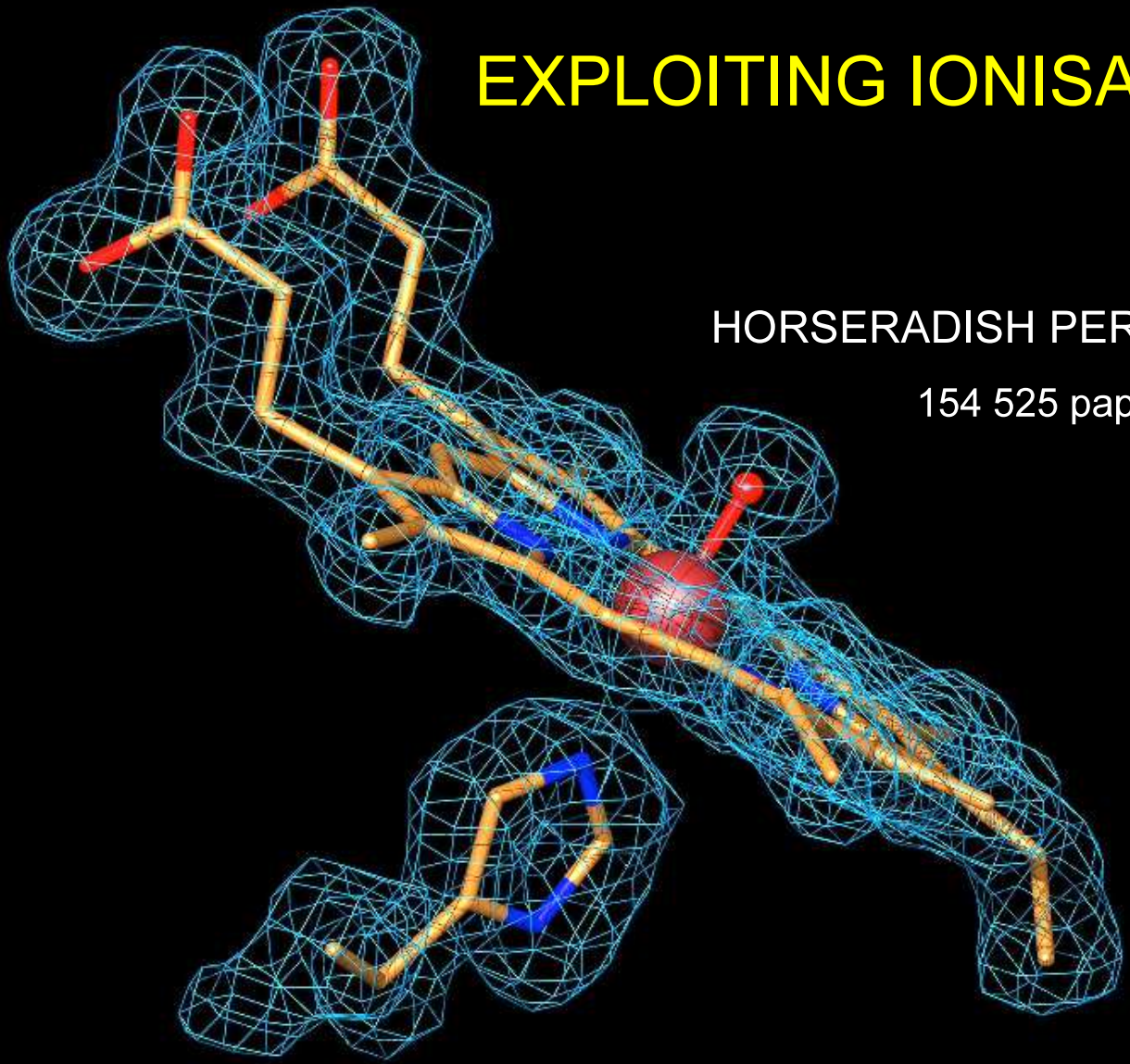

HORSERADISH PEROXIDASE (HRP)

154 525 papers !

Berglund, G.I., Carlsson, G.H., Smith, A.T., Szöke, H., Henriksen, A. & Hajdu, J. (2002) *Nature* 417, 463-468.

PHOTO-IONISATION

UV/VIS PHOTON

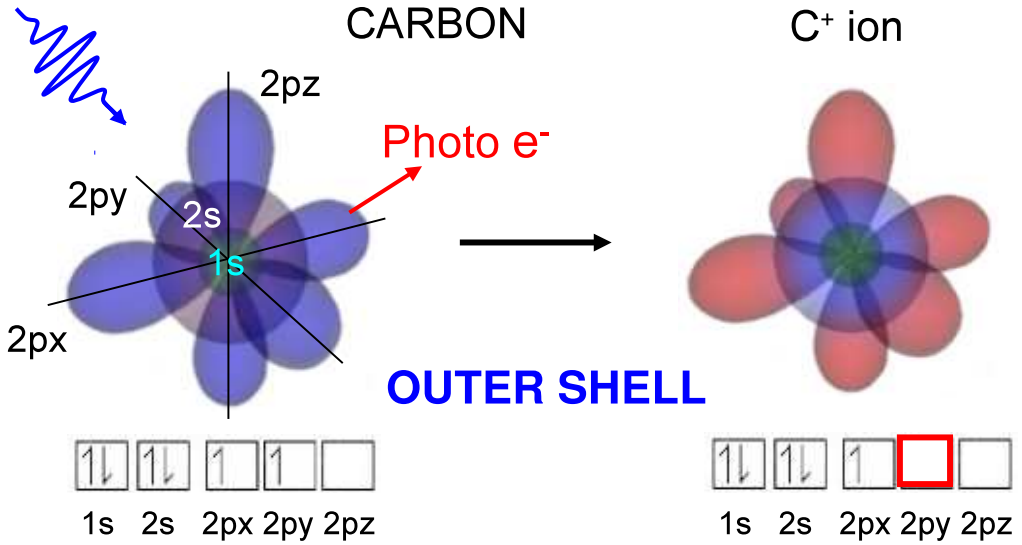

CASCADE PROCESSESS

in condensed material, 10-100 fs

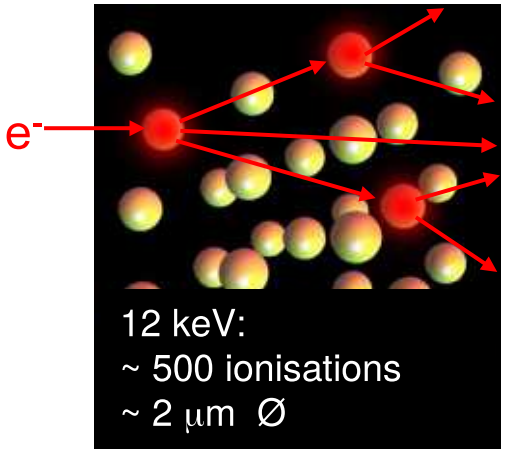

X-RAY PHOTON

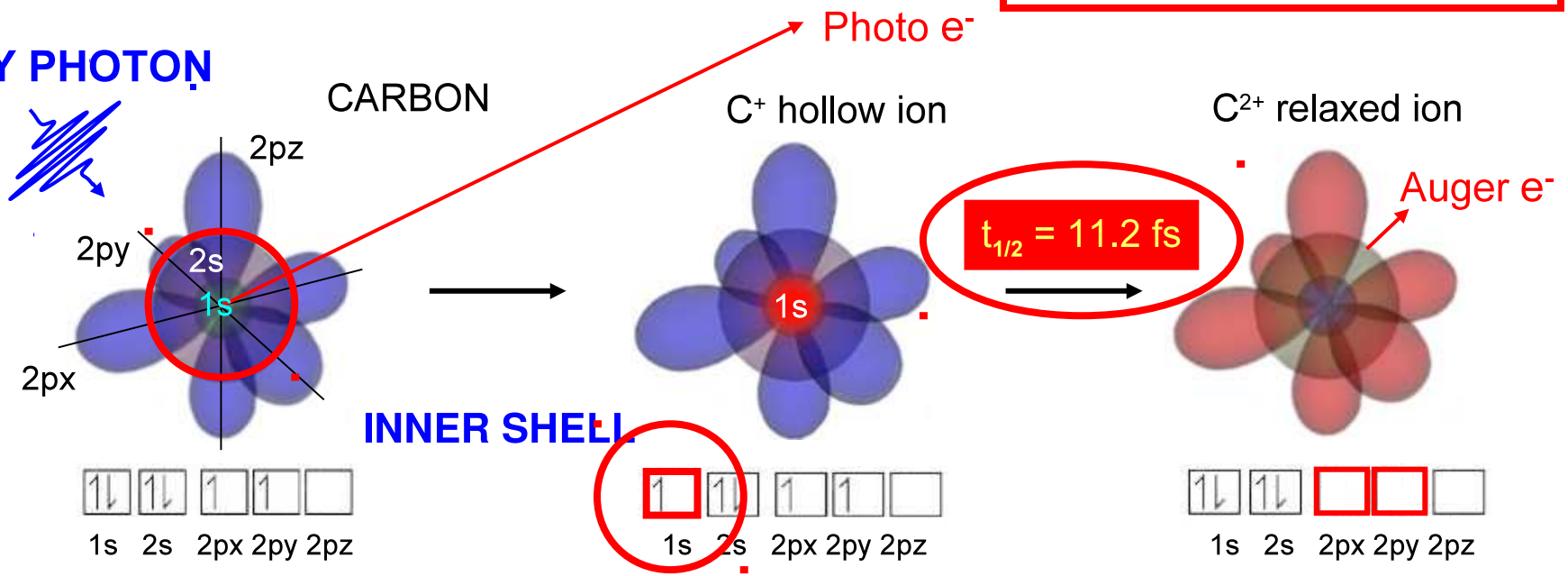

Neutze, R., Wouts, R., van der Spoel, D., Weckert, E. Hajdu, J. (2000) *Nature* 406, 752-757

REACTION SCHEME of HRP

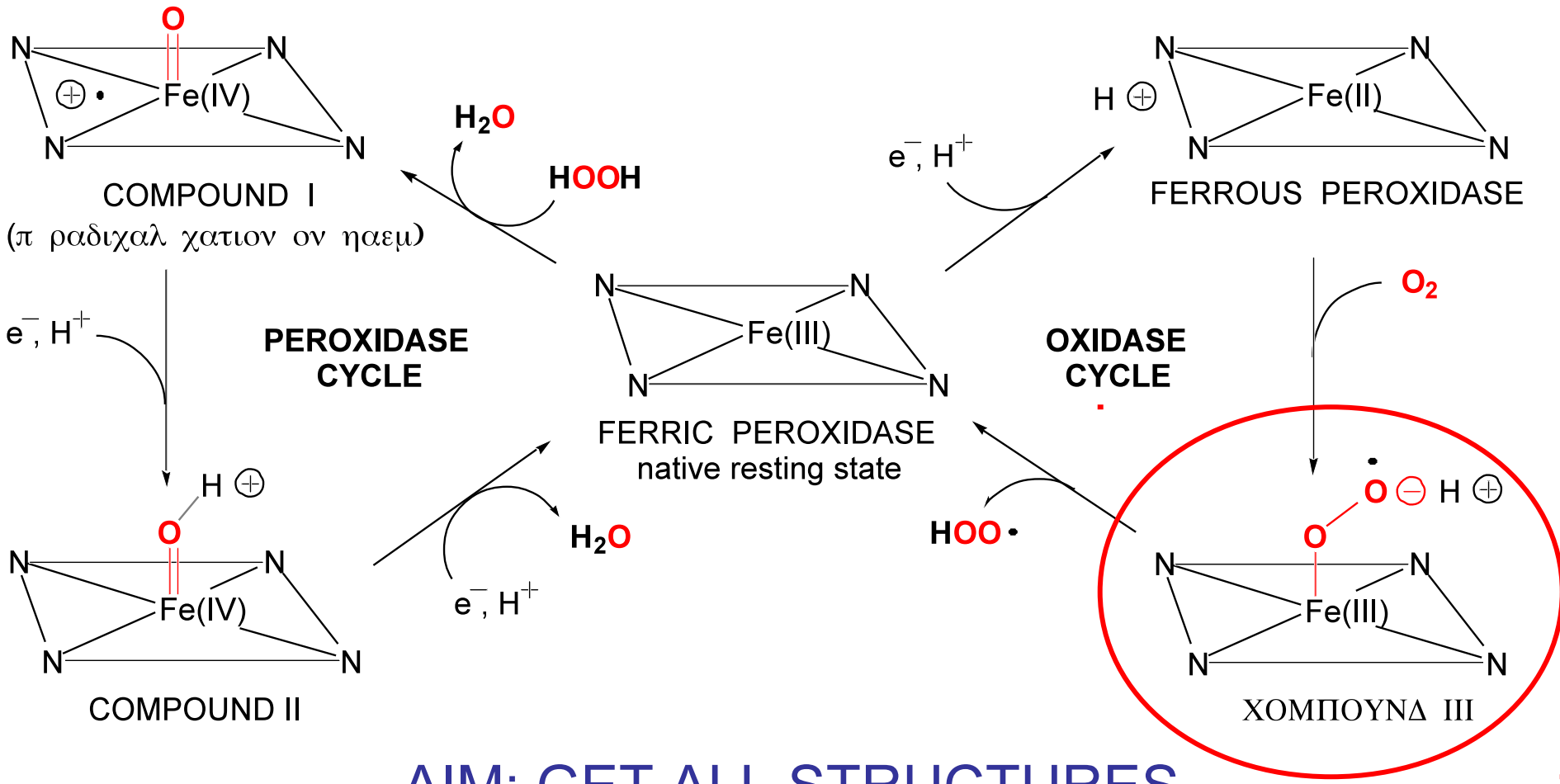

AIM: GET ALL STRUCTURES

RELEVANT TO UNDERSTANDING OXYGEN CHEMISTRY IN BIOLOGY

janos@xray.bmc.uu.se

COMPOUND III OF HRP CONTAINS A BOUND DIOXYGEN SPECIES, BUT THE X-RAY STRUCTURE SHOWS TWO WATER MOLECULES INSTEAD

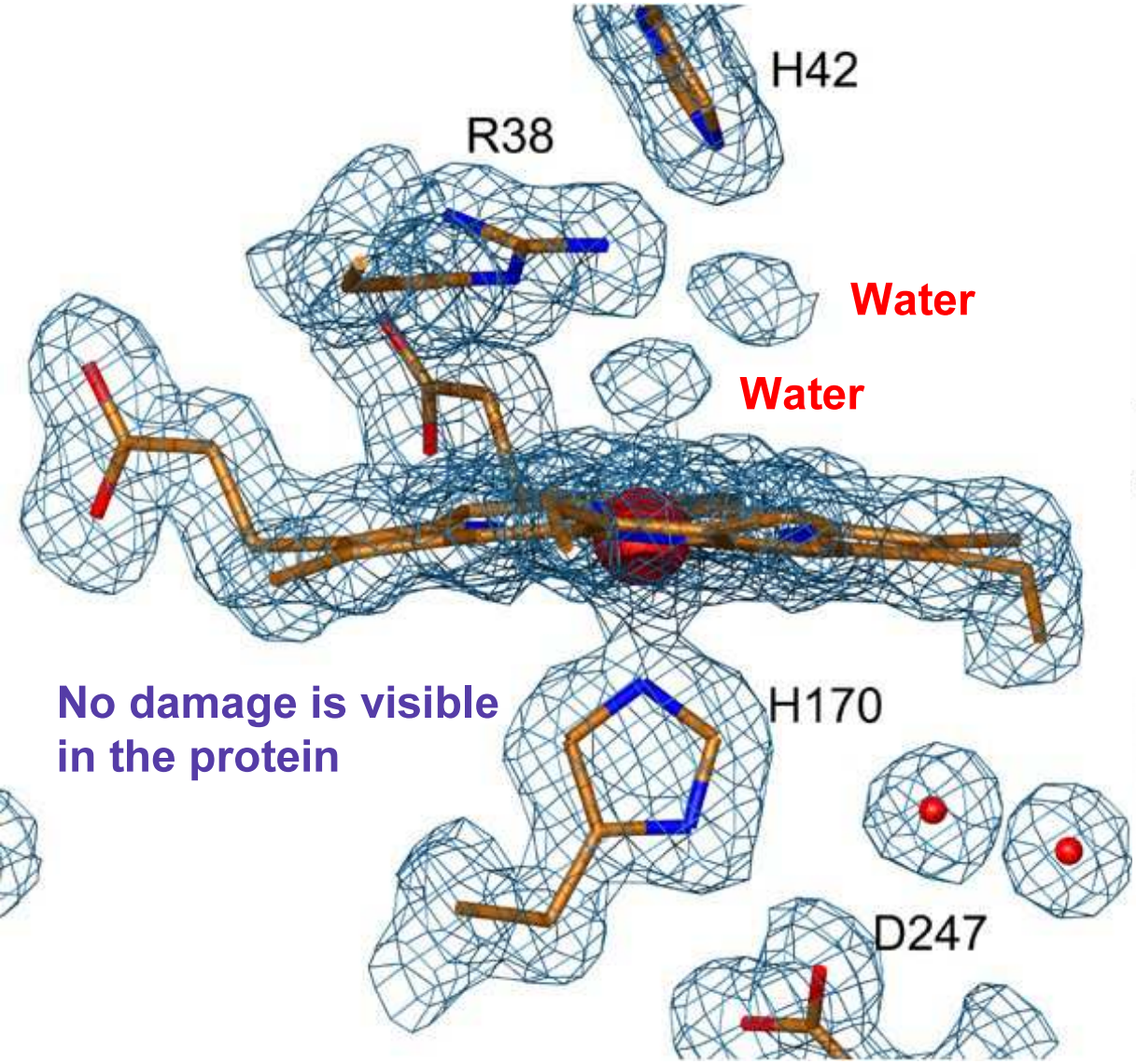

No damage is visible in the protein

SPECTRAL CHANGES INDICATE REDUCTION by X-RAYS

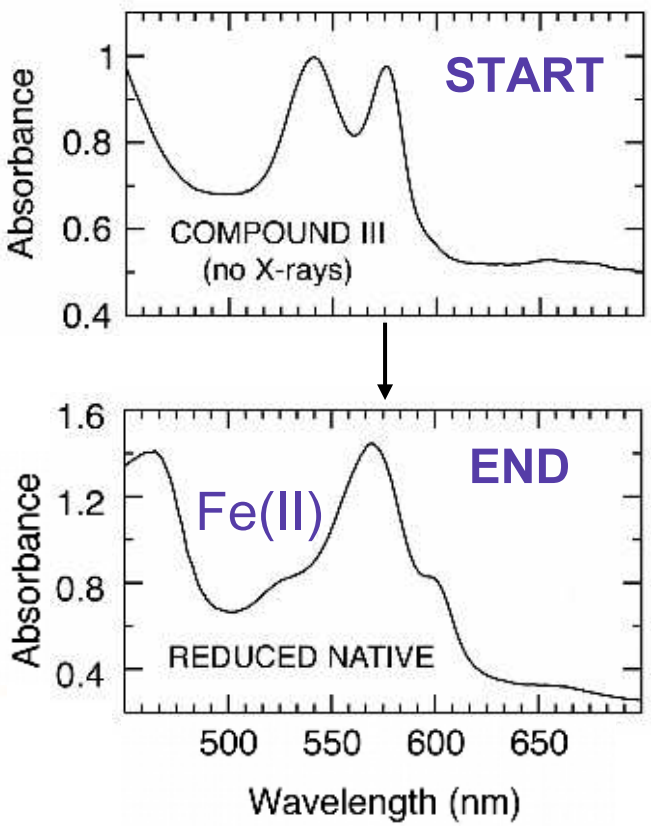

X-RAY DATA COLLECTION AS IT HAPPENS

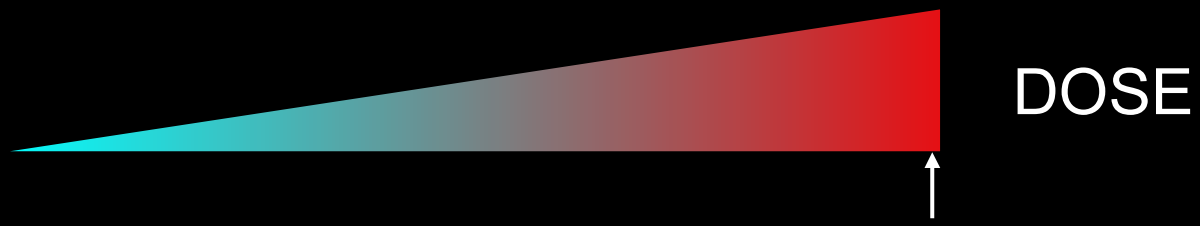

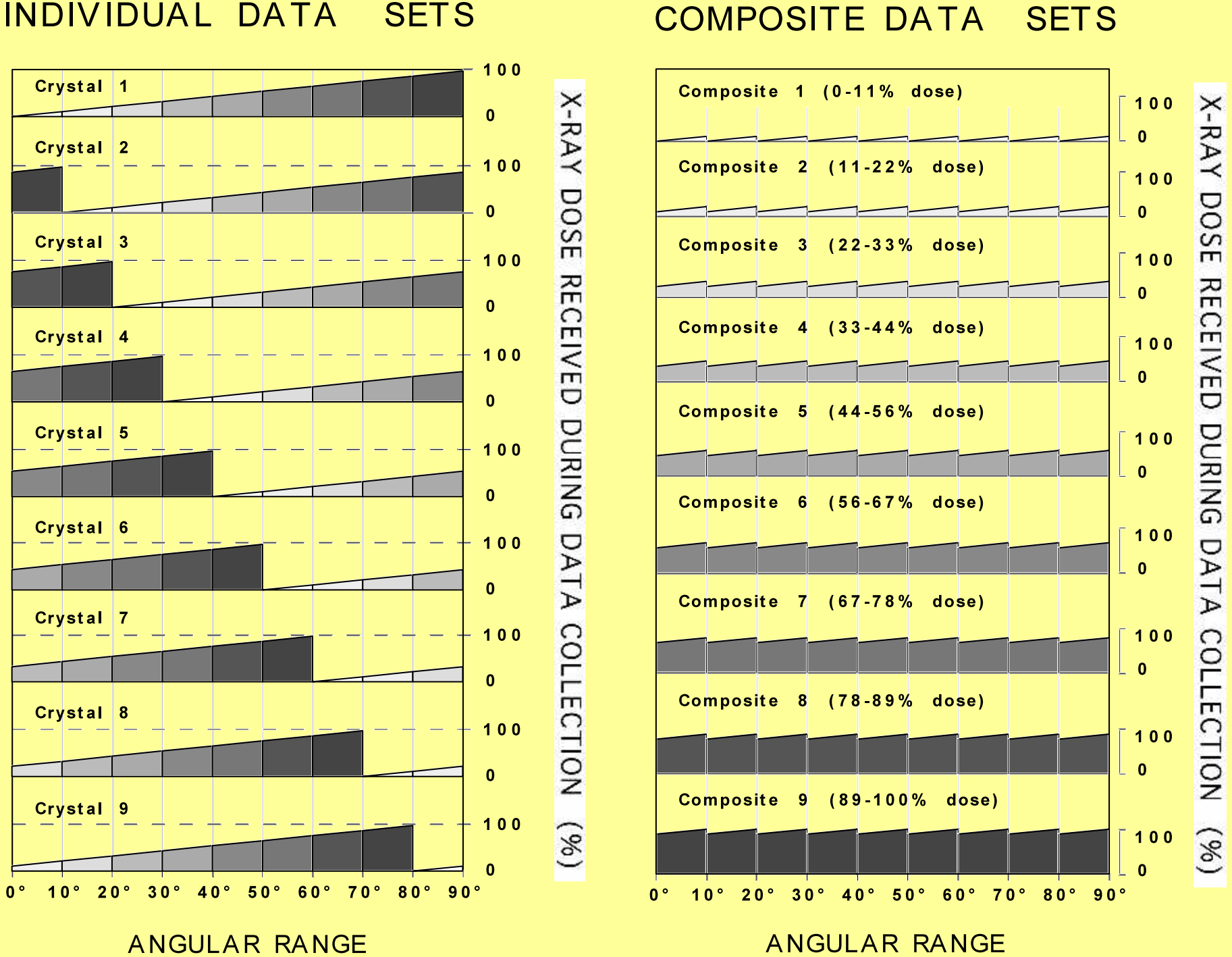
INDIVIDUAL DATA SETS
Crystal 1
Crystal 2
Crystal 3
Crystal 4
Crystal 5
Crystal 6
Crystal 7
Crystal 8
Crystal 9
100
0
0° 10° 20° 30° 40° 50° 60° 70° 80° 90°
ANGULAR RANGE
X-RAY DOSE RECEIVED DURING DATA COLLECTION (%)
COMPOSITE DATA SETS
Composite 1 (0-11% dose)
Composite 2 (11-22% dose)
Composite 3 (22-33% dose)
Composite 4 (33-44% dose)
Composite 5 (44-56% dose)
Composite 6 (56-67% dose)
Composite 7 (67-78% dose)
Composite 8 (78-89% dose)
Composite 9 (89-100% dose)
100
0
0° 10° 20° 30° 40° 50° 60° 70° 80° 90°
ANGULAR RANGE
X-RAY DOSE RECEIVED DURING DATA COLLECTION (%)

HRP WITH BOUND DIOXYGEN SPECIES ON THE HAEM

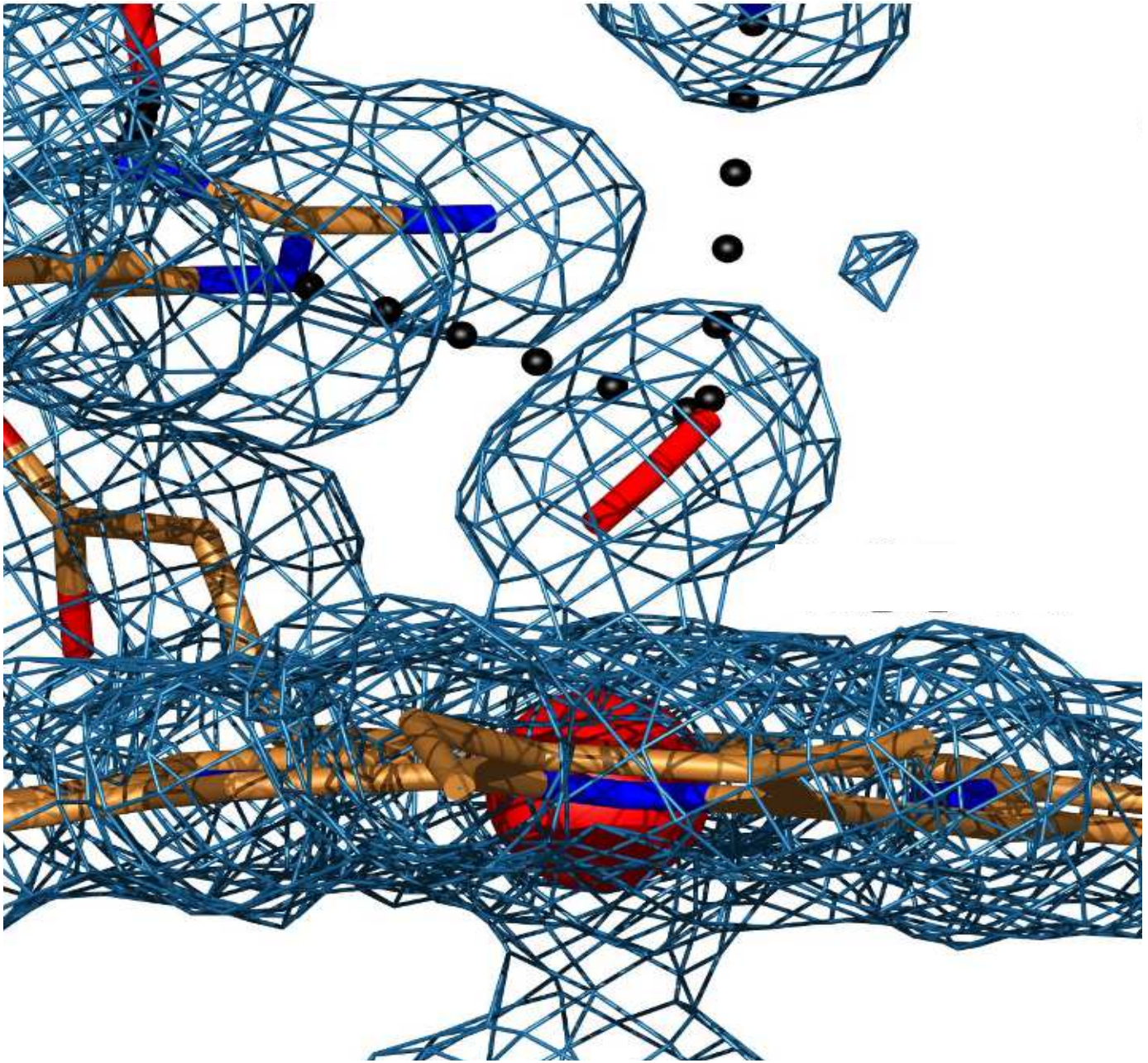

X-RAY-DRIVEN CATALYSIS: REDUCTION of O_2 to H_2O

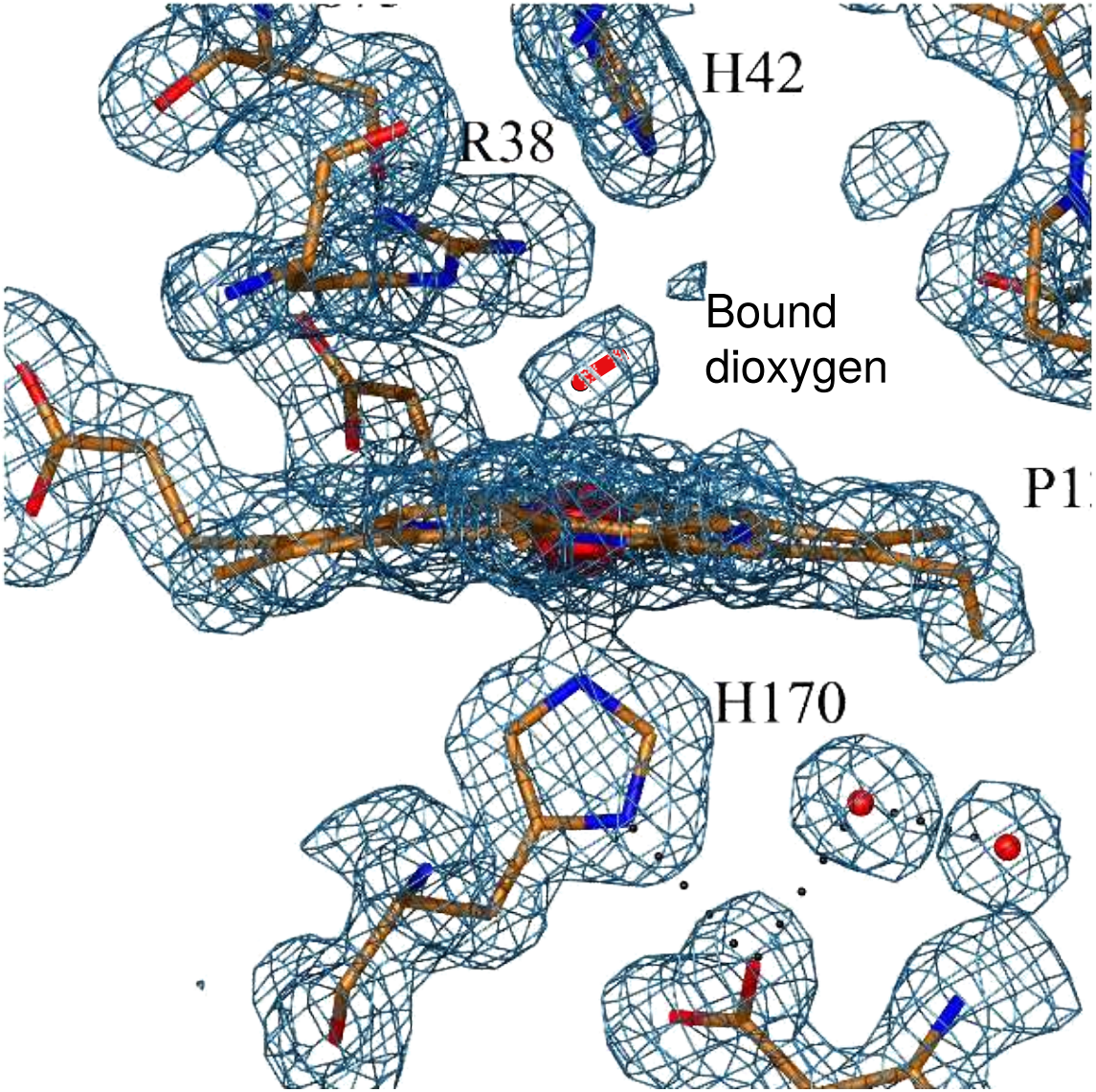

10-20º Redox enzymes evolved to channel electrons to/from the active site

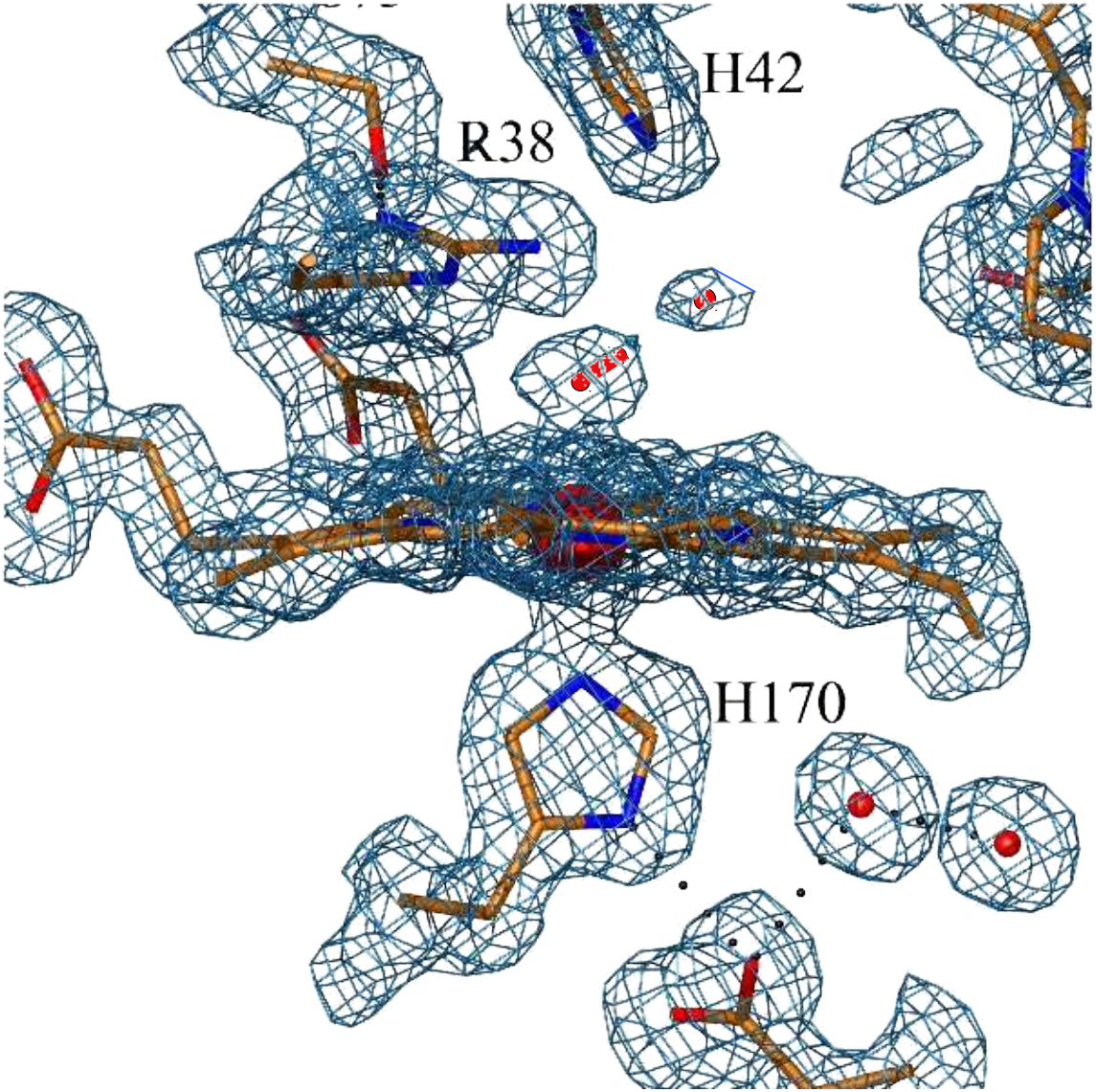

40-50º Redox enzymes evolved to channel electrons to/from the active site

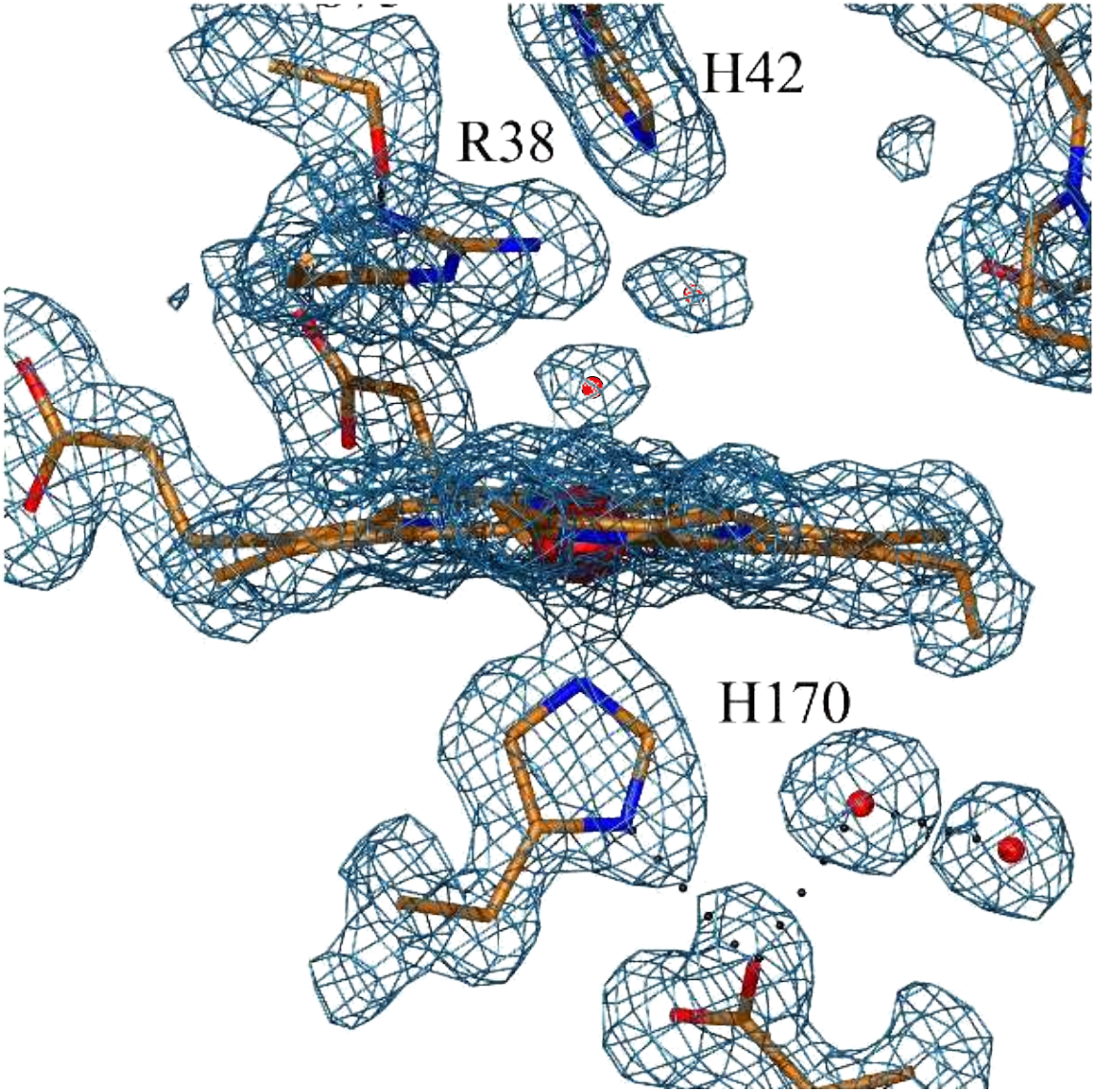

50-60º **Redox enzymes evolved to channel electrons to/from the active site**

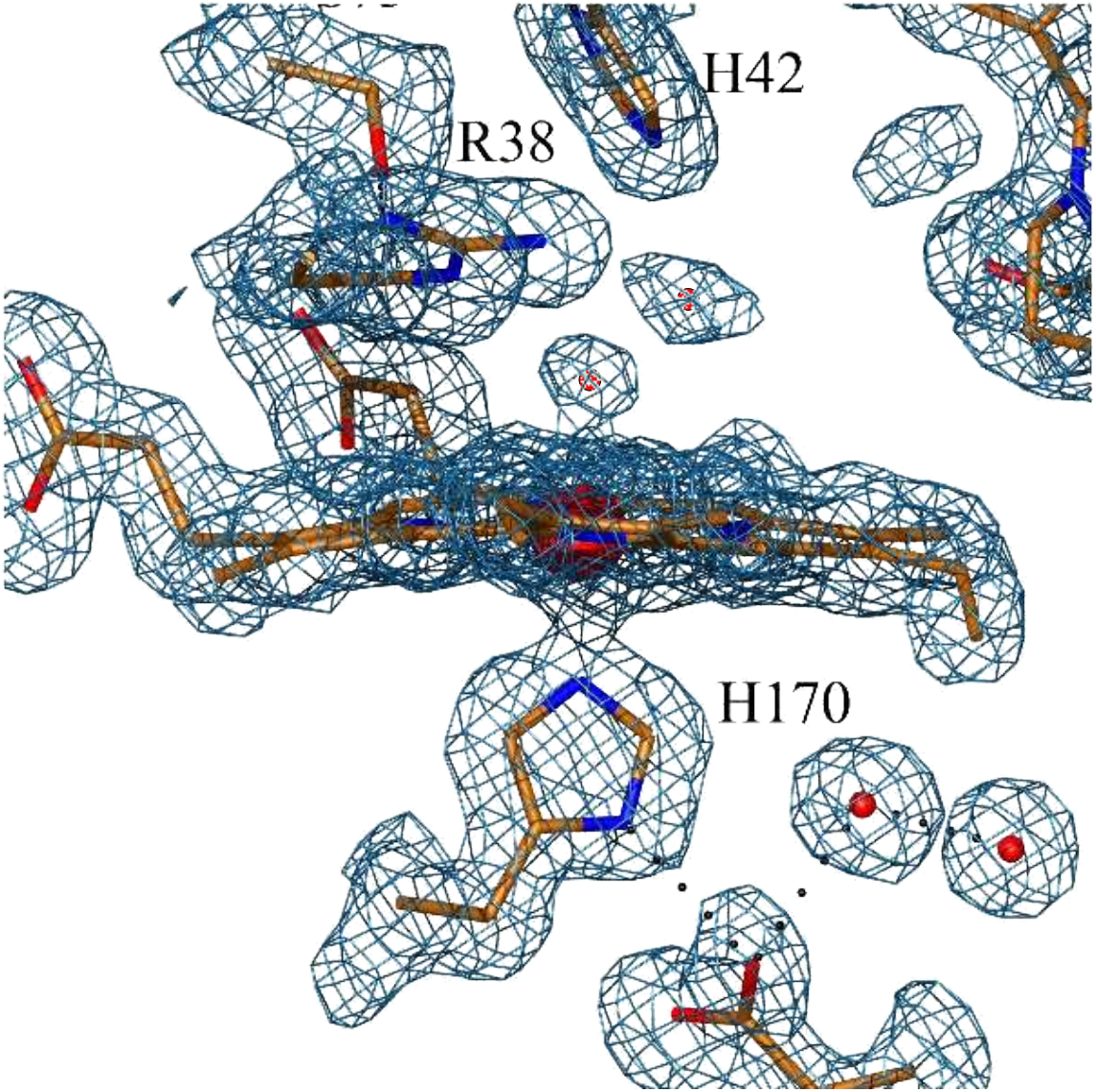

70-80º Redox enzymes evolved to channel electrons to/from the active site

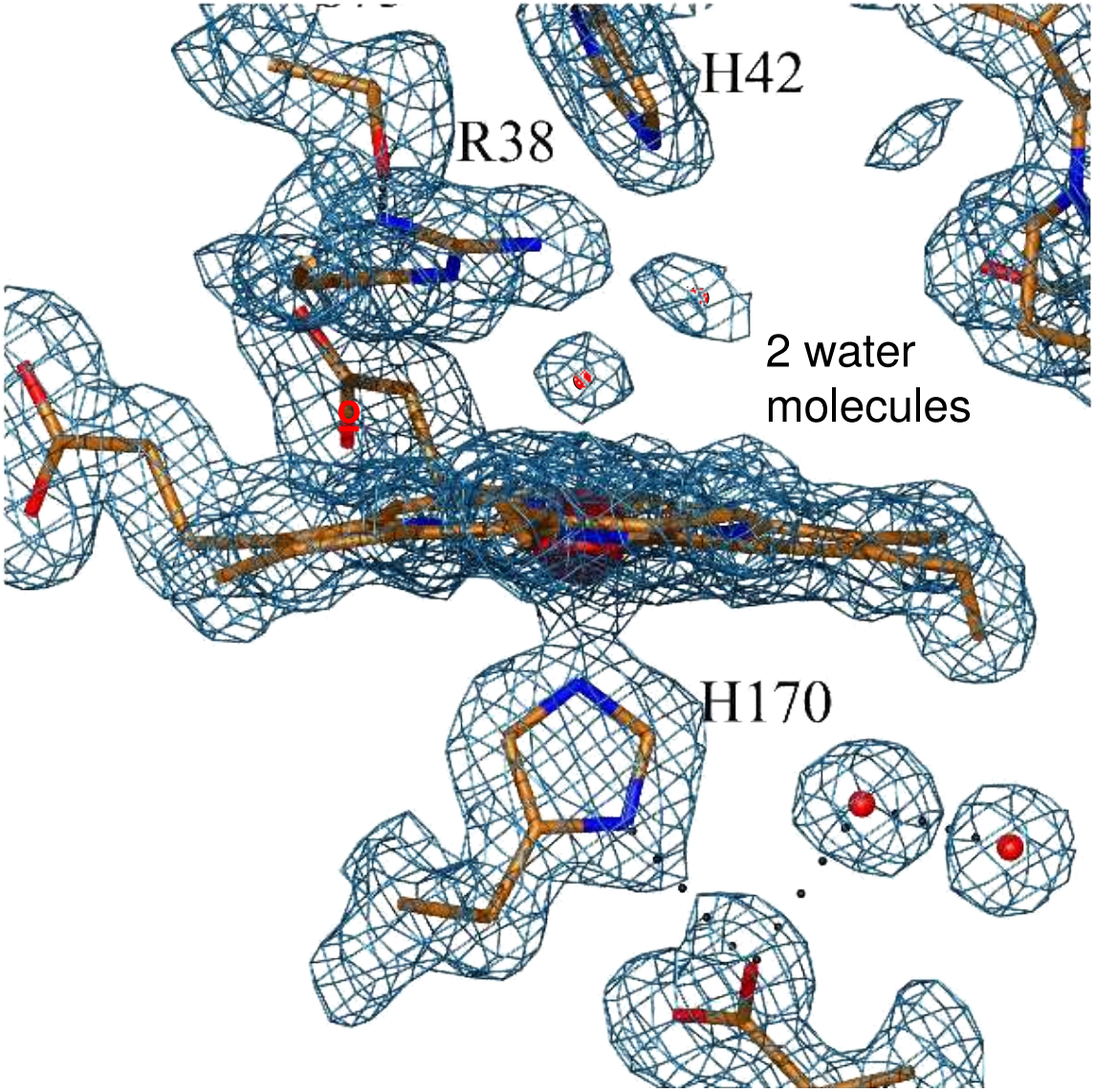

"The catalytic pathway of horseradish peroxidase at high resolution"
Berglund, G.I., Carlsson, G.H., Smith, A.T., Szoke, H., Henriksen, A. & Hajdu, J., *Nature* **417**, 463-468 (2002)

OUT-RUNNING RADIATION DAMAGE: ULTRA-FAST DIFFRACTIVE IMAGING with X-RAY LASERS

X-RAY LASERS PROVIDE A BILLION FOLD INCREASE IN PEAK BRILLIANCE RELATIVE TO SYNCHROTRONS

Such a large jump in one physical quantity is very rare, and quite remarkable

Total irradiated power = 1.74×10^{17} W

1 mm^2

The peak power of the LCLS with a 1 μm^2 focus

DEPENDING on the SPATIAL and TEMPORAL FOCUSING of the X-RAY PULSE...

Unfocused beam

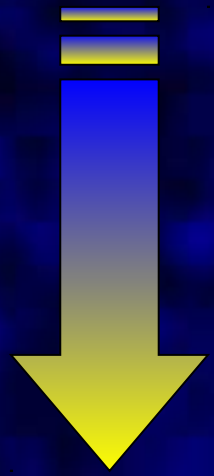

Diffraction limit

DIFFRACTION TOMOGRAPHY

FEMTOCHEMISTRY

ATOMIC PHYSICS

WARM AND HOT DENSE MATTER

STRUCTURE & FUNCTION in BIOLOGY

BOILING of VACUUM

Power densities > 10^{24} W/cm^2

VACUUM STRUCTURE WITHIN REACH?

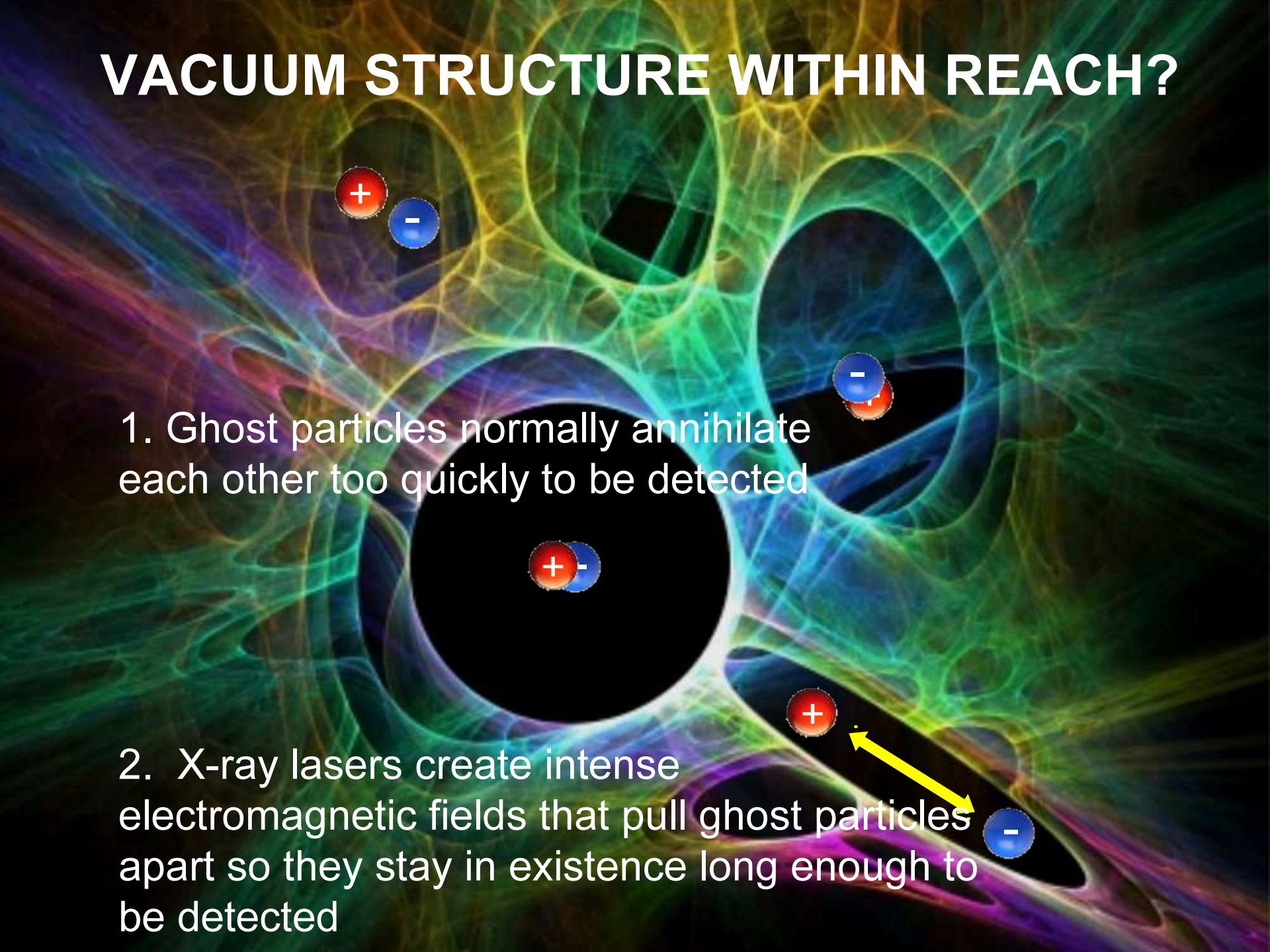

1. Ghost particles normally annihilate each other too quickly to be detected

2. X-ray lasers create intense electromagnetic fields that pull ghost particles apart so they stay in existence long enough to be detected

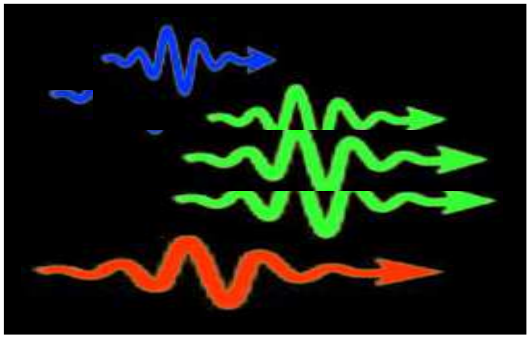

OK, but what is “light”?

We know it exhibits both wave and particle (photon) behavior, but…

Three views on the photon (quantum) character of “light”:

Einstein:

“I spent my life to find out what a photon is and I still don't know.”

Dirac:

“Each photon interferes only with itself.
Interference between different photons never occurs.”

Feynman:

Photon interference *“has in it the heart of quantum mechanics. In reality it contains the only mystery.”*

The weird quantum (photon) behavior of light

Screen with 2 slits

Detector

Diffraction image is assembled one-photon-at-a-time

Light source

photons of same energy

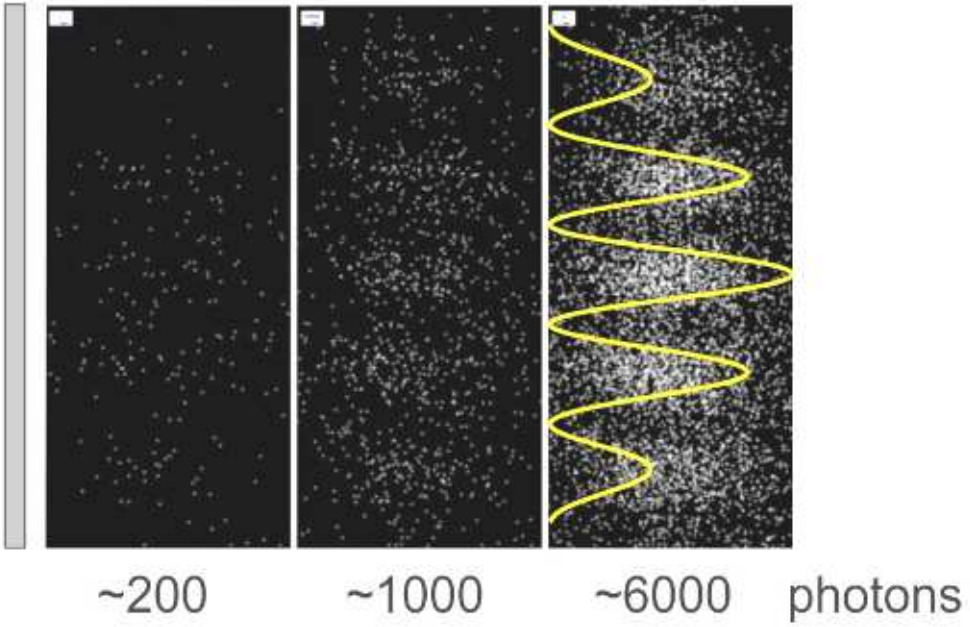

Light is "birthed" on an atom as photon

Light propagates & interacts like wave

Wave collapses into photon which is detected through photoelectric effect

Birth volume = λ^3

Diffraction pattern assembles one photon at a time

Consistent with Dirac's bold statement: "each photon (field) interferes only with itself"

Brightness and photon degeneracy parameter

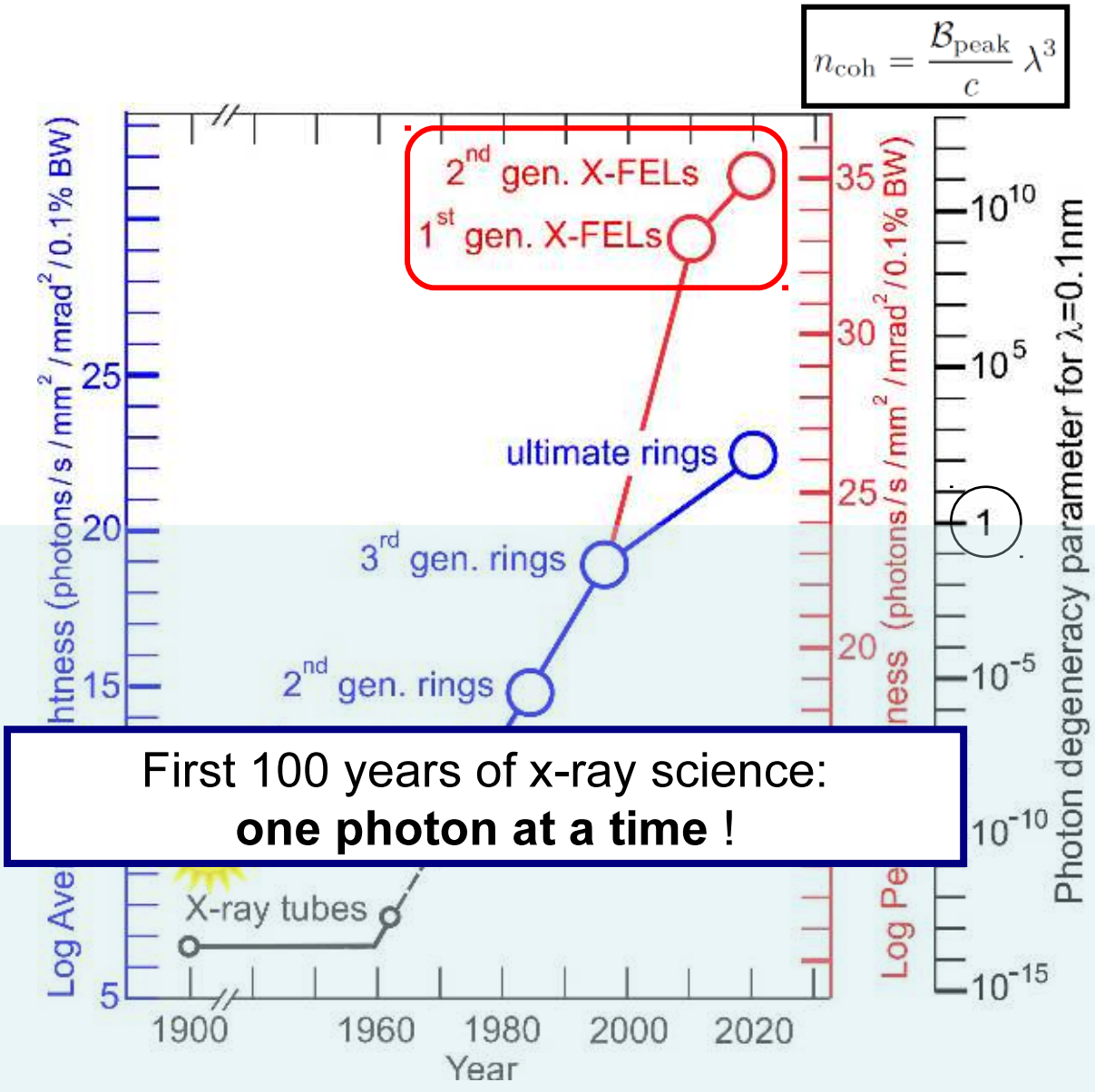

First 100 years of x-ray science:
one photon at a time !

THE HISTORY OF X-RAY LASERS IS SHORT

First lasing: 10 April 2009 (LCLS, Stanford)

”There is a steep “learning curve” to climb, for experiments and also for theory, in order to exploit these potentials” Massimo Altarelli, from yesterday

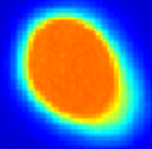

1.5×10^{12} photons @ 8.2 keV (1.5 Å)
Electron bunch length: ~78 fs FWHM
Photon pulse length: ~60 fs FWHM
Photon spike length: ~100 as FWHM
Gain coefficient: 2.9/m

Emma, P. et al. *Nature Photonics* **4**, 641-647 (2010).

A FREE-ELECTRON LASER IS A PARAMETRIC AMPLIFIER

A PARAMETRIC AMPLIFIER OPERATES BY TRANSFERRING ENERGY TO THE OUTPUT SIGNAL (the photon pulse) FROM AN OSCILLATOR (here a bunch of free electrons flying through an undulator magnet)

The relativistic bunch of free electrons interacts with its own photon field

Wonderful chaos - Just like synchrotron radiation

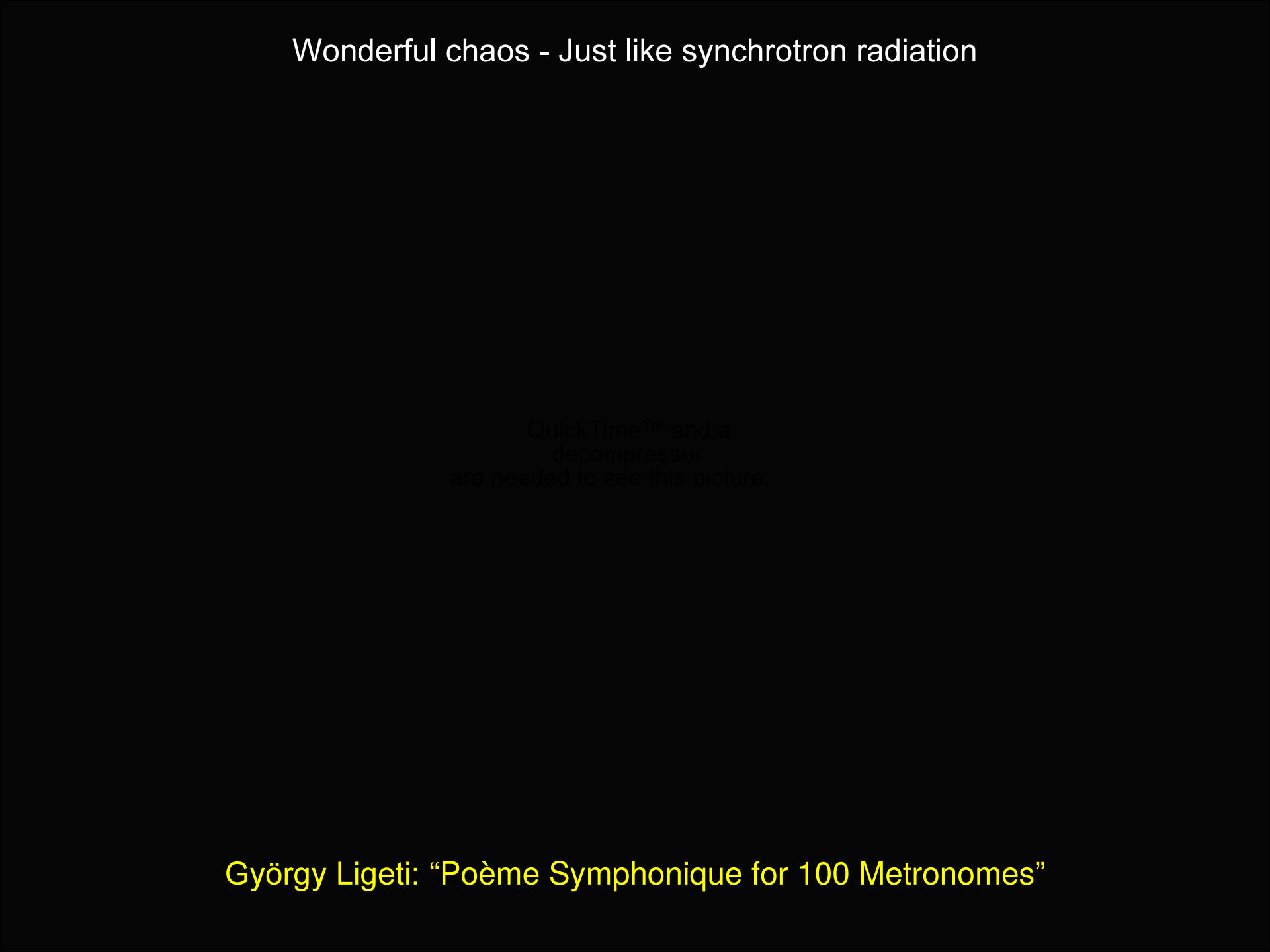

György Ligeti: “Poème Symphonique for 100 Metronomes”

ORDER FROM CHAOS: ATTOSECOND ELECTRON BUNCHING

Electrons in random distribution

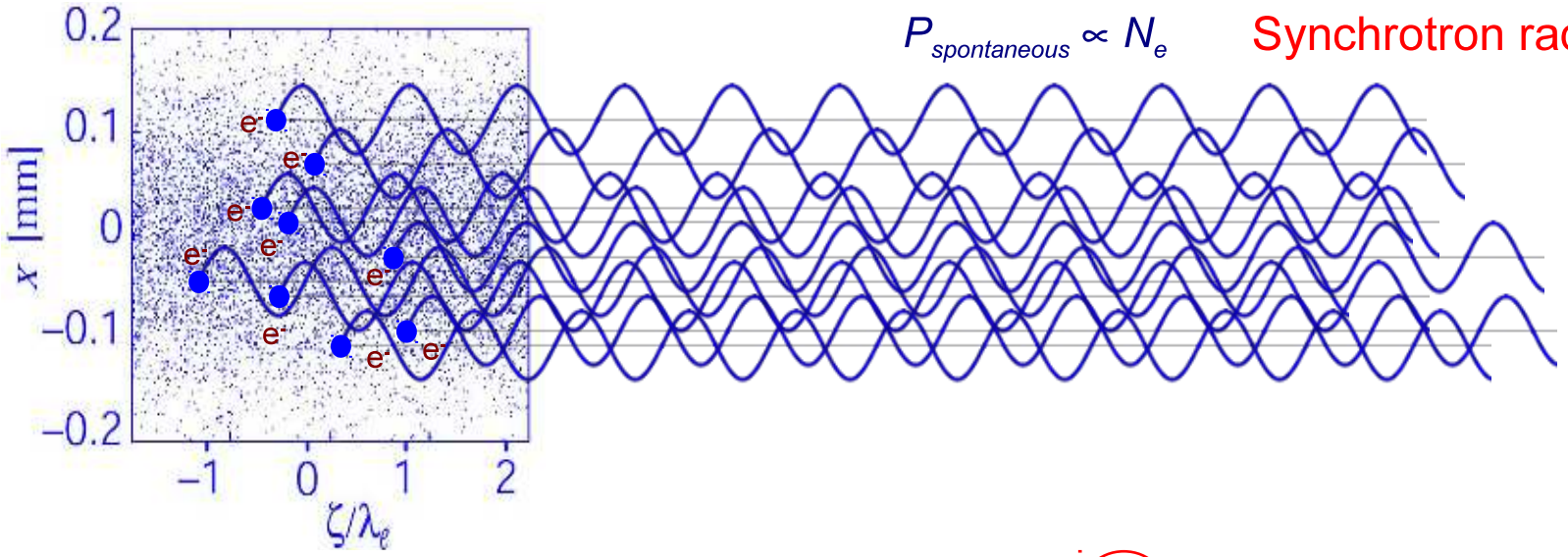

$P_{spontaneous} \propto N_e$ Synchrotron radiation

Electrons in microbunches (pancakes)

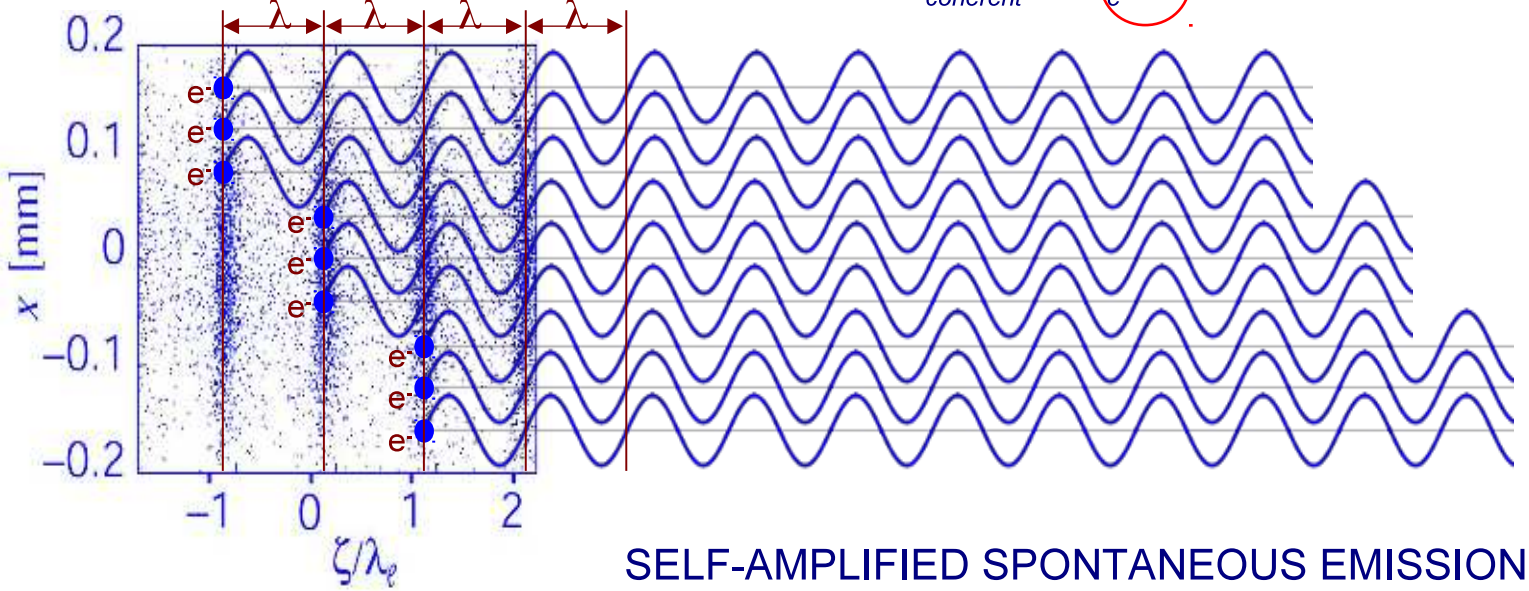

$P_{coherent} \propto N_e^2$ FEL radiation

SELF-AMPLIFIED SPONTANEOUS EMISSION (SASE)

ORDER FROM CHAOS - NOW FOR REAL

Starts like Ligeti's "Poème Symphonique for 100 Metronomes"

QuickTime™ and a
decompressor
are needed to see this picture.

S.H. Strogatz & I. Stewart: Coupled Oscillators and Biological Synchronization. Scientific American 269, 102-109 (1993).

ORDER FROM CHAOS: ATTOSECOND ELECTRON BUNCHING

Electrons in microbunches (pancakes)

$P_{coherent} \propto N_e^2$

FEL radiation

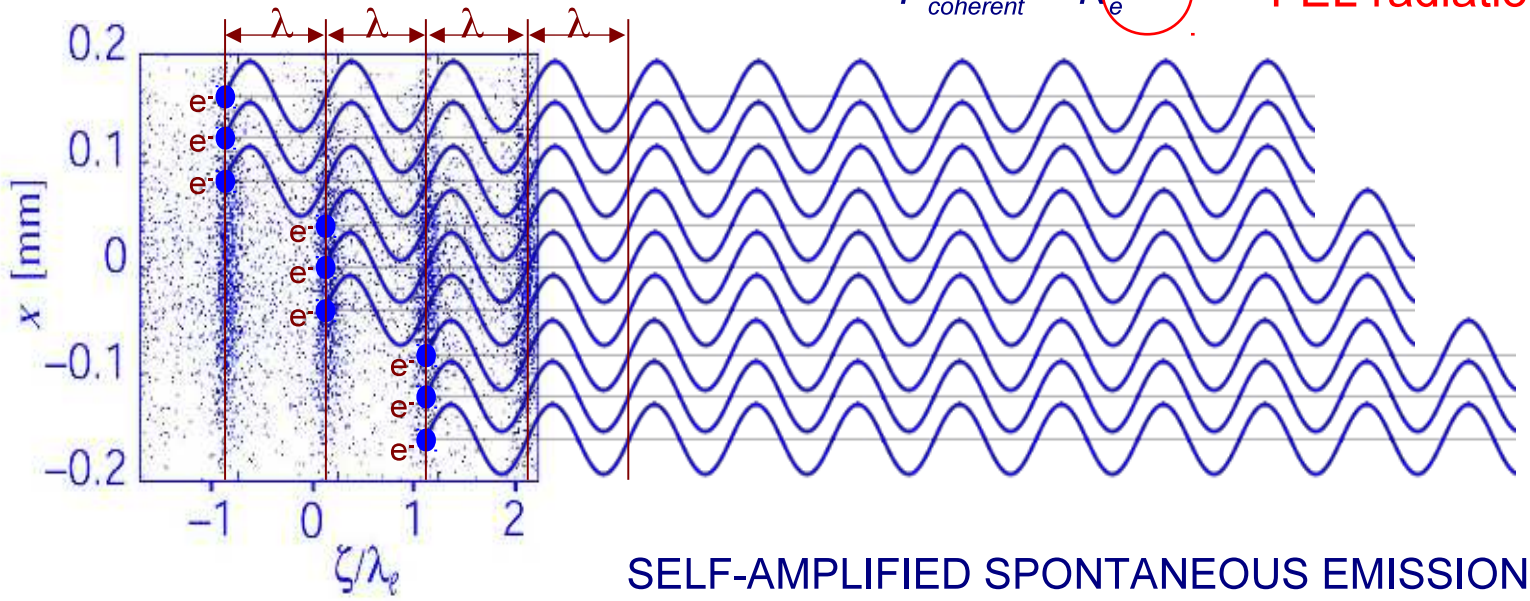

SELF-AMPLIFIED SPONTANEOUS EMISSION (SASE)

$$P = \frac{2\ a^2 q^2}{3\ c^3}$$

Larmor's equation

P = total emitted power
a = acceleration
q = charge
c = speed of light

100,000 electrons packed closely together will radiate **10,000,000,000** times more than a single electron

Tightly packed electrons behave like one giant particle with "n" charges, and emit light coherently *as a "unified whole"*

COHERENCE

Definition from the Oxford English Dictionary: *The quality of being logical and consistent, forming a unified whole.*

COHERENCE OF WAVES = CONSTANT PHASE RELATIONSHIP

A measure of coherence can be given by **correlation functions**:

The **COHERENCE FUNCTION** between signals $x(t)$ and $y(t)$ is defined as

$$\gamma_{xy}^2(f) = \frac{|S_{xy}(f)|^2}{S_{xx}(f)S_{yy}(f)}$$

$$0 \leqslant \gamma_{xy}^2(f) \leqslant 1$$

Cross-spectral density - the FT of the CROSS-CORRELATION FUNCTION

IN SPACE: similarity of the signals at different positions.
IN TIME: similarity of the signals after different time lags.

Power-spectral density - the FT of the AUTO-CORRELATION FUNCTIONS

IN SPACE: similarity of each signal with itself at a given separation distance.
IN TIME: similarity of each signal with itself at various times.

We will consider
SPATIAL or TRANSVERSE coherence
and
TEMPORAL or LONGITUDINAL coherence

TRANSVERSE (OR SPATIAL) COHERENCE refers to the continuity and uniformity of a wave in a direction perpendicular to the direction of propagation

LONGITUDINAL (OR TEMPORAL) COHERENCE can be characterised by
(i) the distance over which the phase in a beam of light remains correlated (*coherence length*)
(ii) the longest time interval over which the phase in a beam of light remains correlated (*coherence time*)

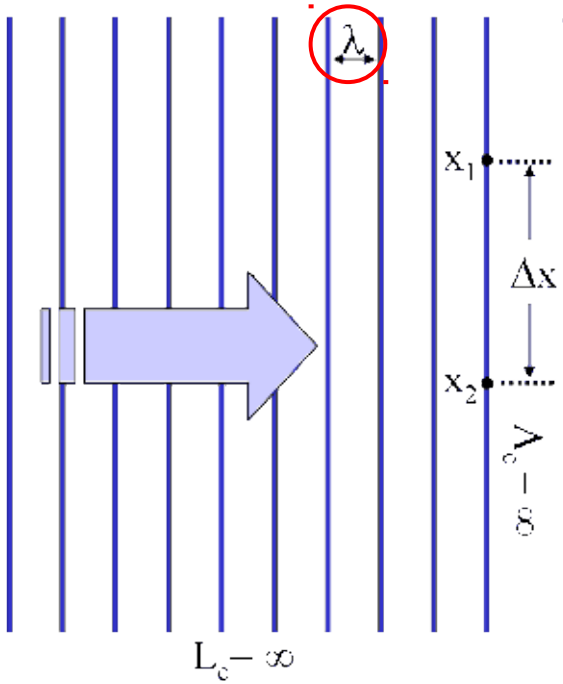

Plane wave with **infinite** coherence length

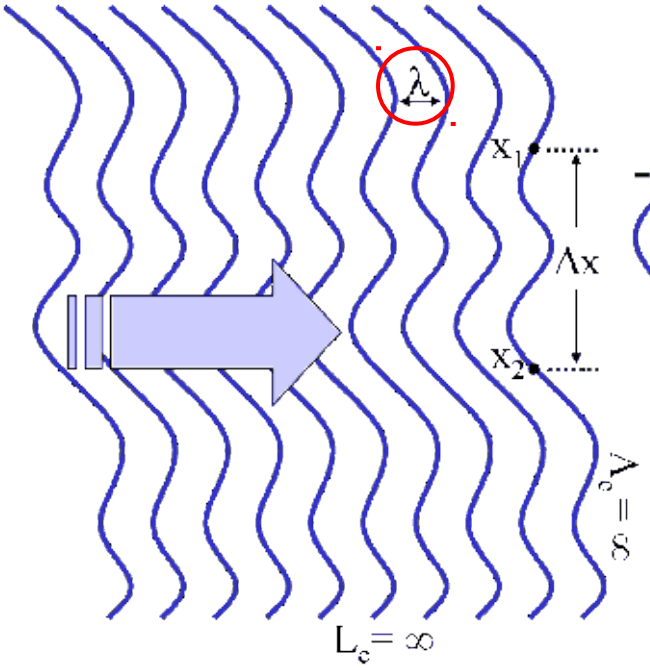

Varying wavefront with **infinite** coherence length

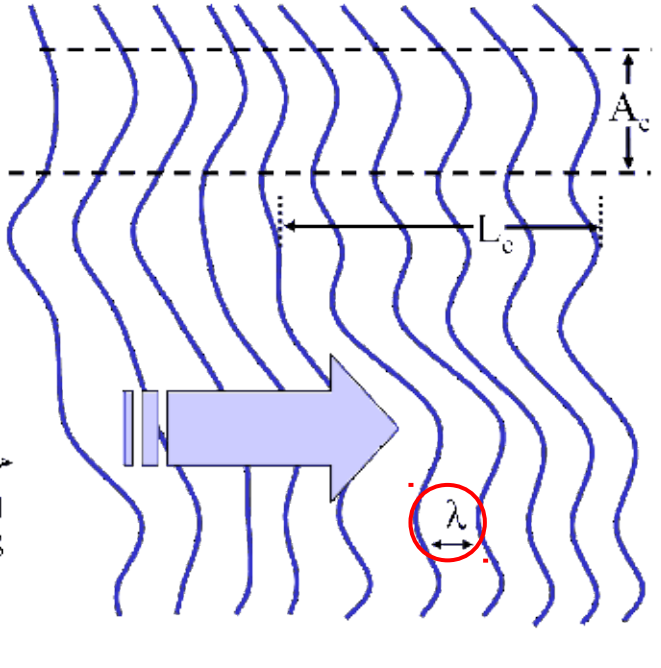

Varying wavefront with **finite** coherence length in space and time

INCOHERENT, PARTIALLY COHERENT, COHERENT

Coherence between waves can be described by correlation functions

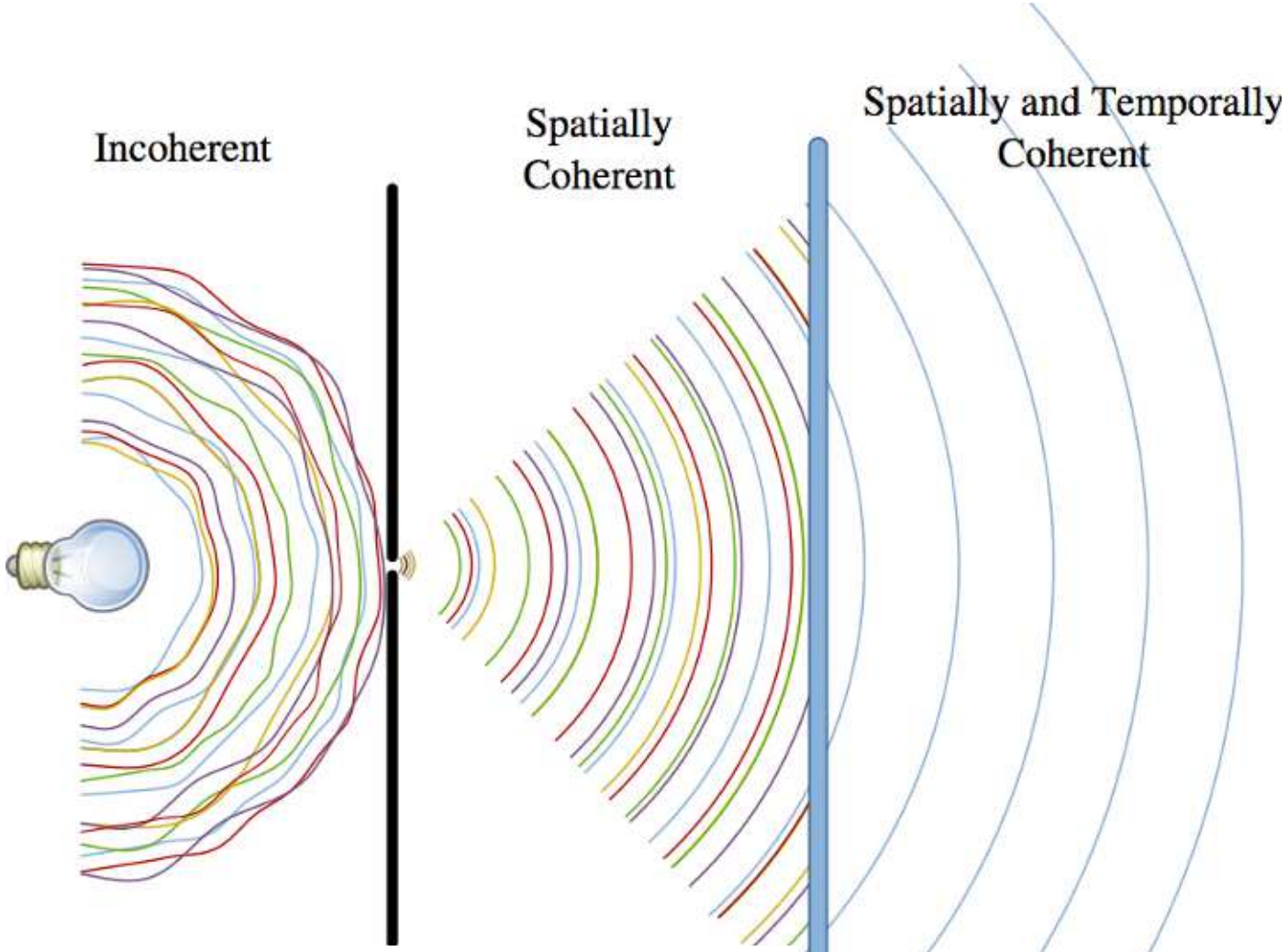

PINHOLE INTRODUCES **SPATIAL** (TRANSVERSE) COHERENCE

MONOCHROMATIC FILTER INTRODUCES **TEMPORAL** (LONGITUDINAL) COHERENCE

(perfectly monochromatic light has infinite longitudinal coherence)

Drawing by Filipe Maia, Uppsala

Why is Coherence Important for Imaging?

Coherence is an ideal property of waves that enables stationary (i.e. temporally and spatially constant) interference between waves.

Coherence is strongly related to the **sharpness of interference fringes**. We expect sharp fringes when the degree of coherence is high and no fringes at all in the absence of coherence

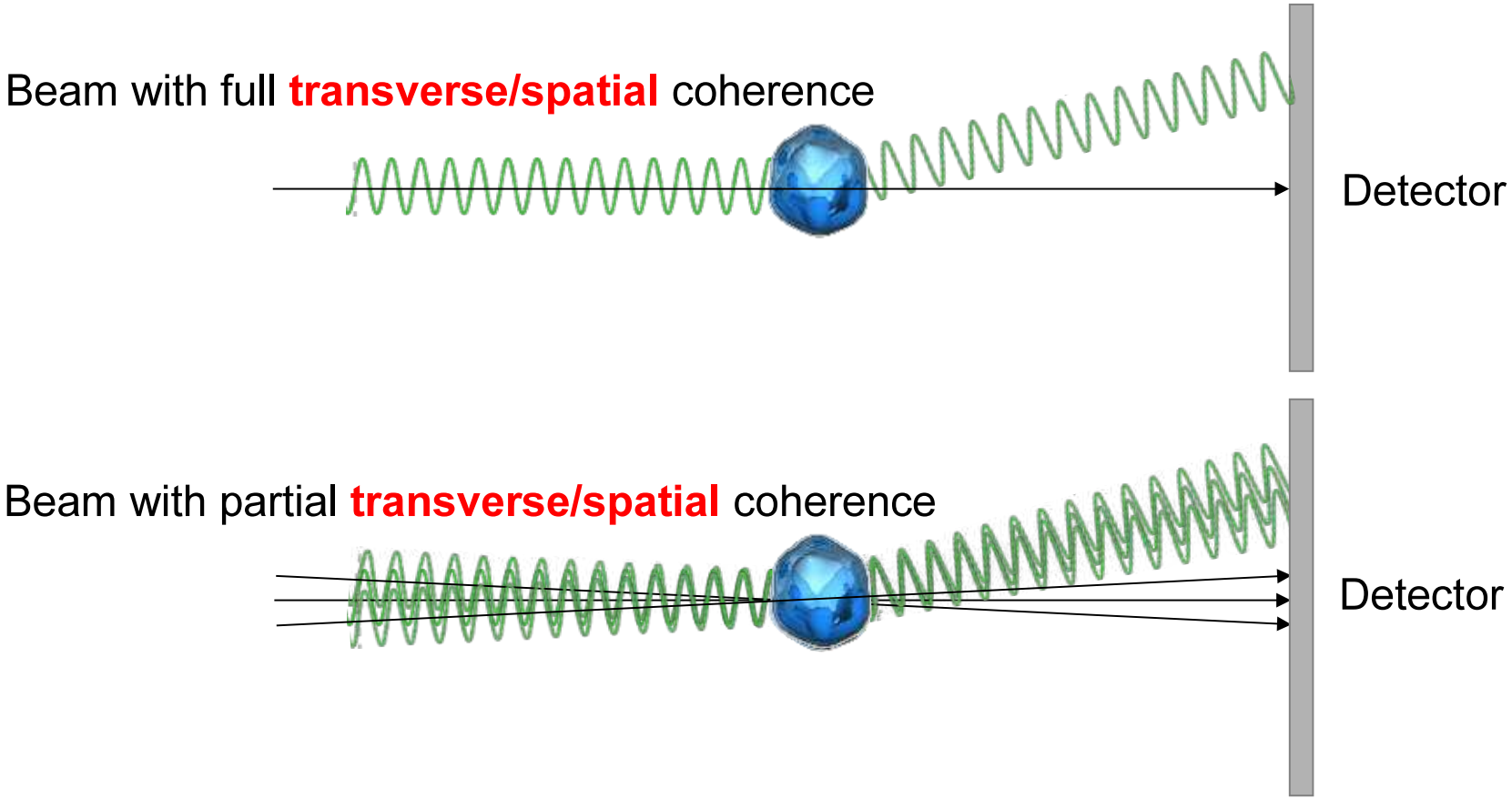

Why is Coherence Important for Imaging?

Coherence is an ideal property of waves that enables stationary (i.e. temporally and spatially constant) interference between waves.

Coherence is strongly related to the **sharpness of interference fringes**. We expect sharp fringes when the degree of coherence is high and no fringes at all in the absence of coherence

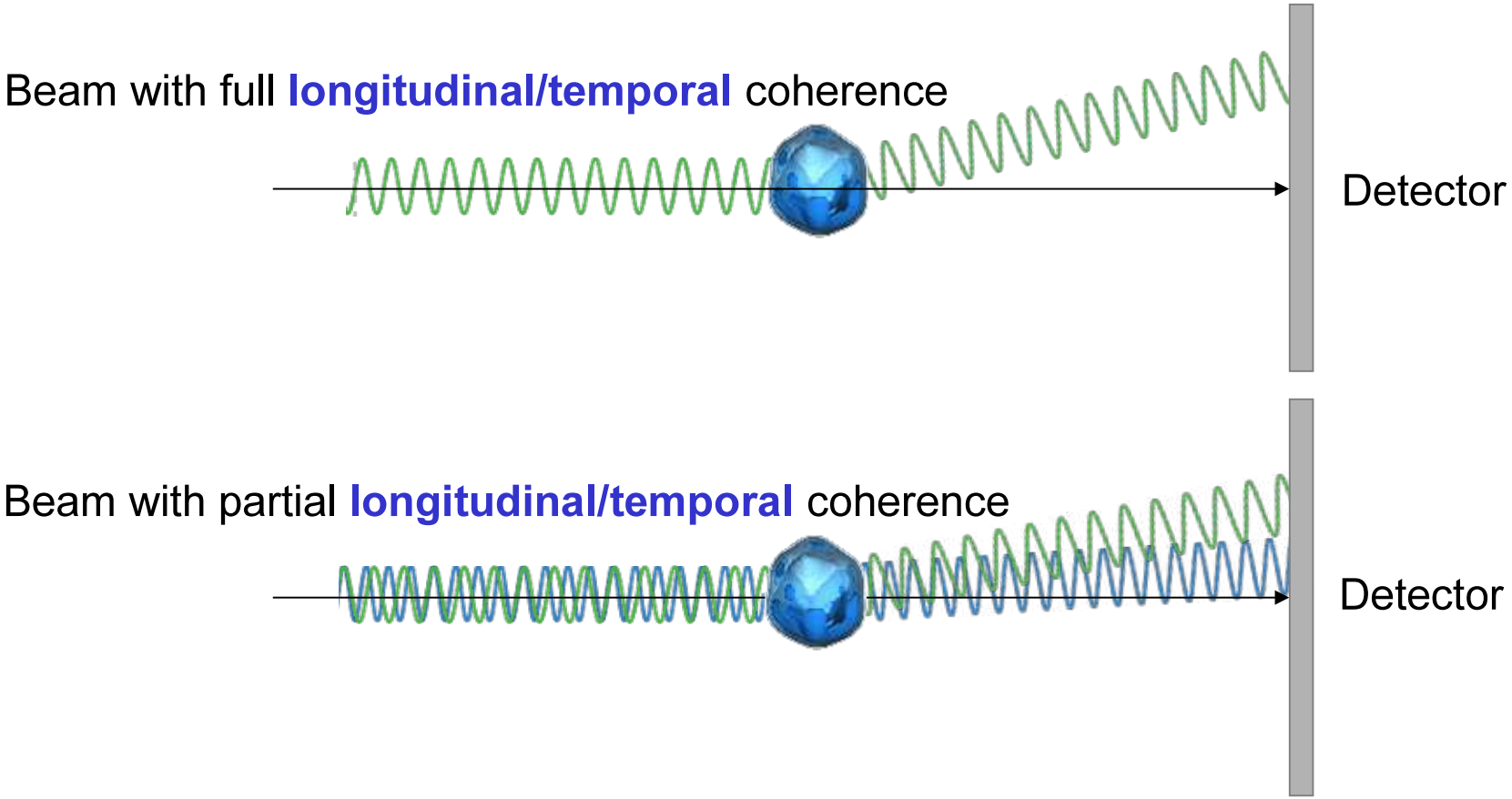

Spectral bandwidth and longitudinal coherence length

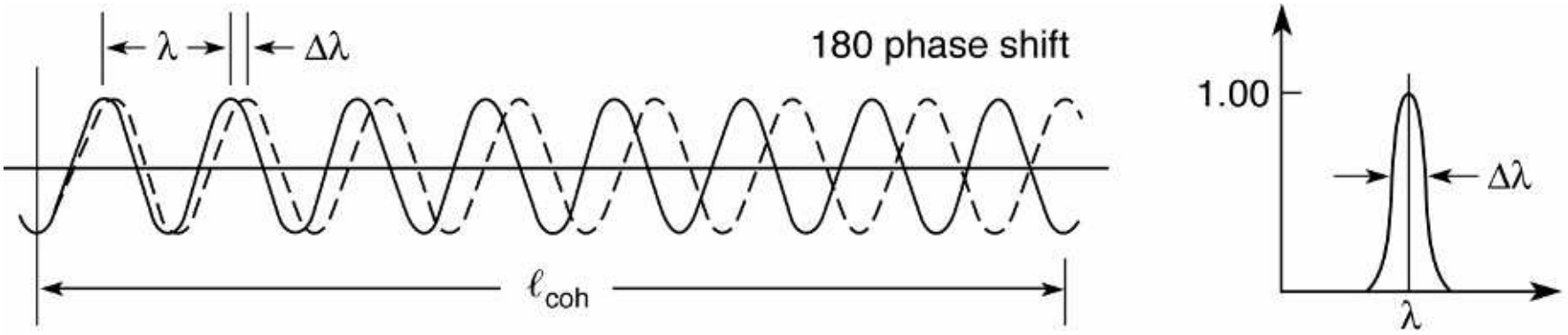

Define a coherence length ℓ_{coh} as the distance of propagation over which radiation of spectral width $\Delta\lambda$ becomes 180° out of phase. For a wavelength λ propagating through N cycles

$$\ell_{coh} = N\lambda$$

and for a wavelength $\lambda + \Delta\lambda$, a half cycle less $(N - \frac{1}{2})$

$$\ell_{coh} = (N - \tfrac{1}{2})\,(\lambda + \Delta\lambda)$$

Equating the two

$$N = \lambda/2\Delta\lambda$$

so that

$$\boxed{\ell_{coh} = \frac{\lambda^2}{2\,\Delta\lambda}} \qquad (8.3)$$

Ch08_F03.ai

The importance of coherence

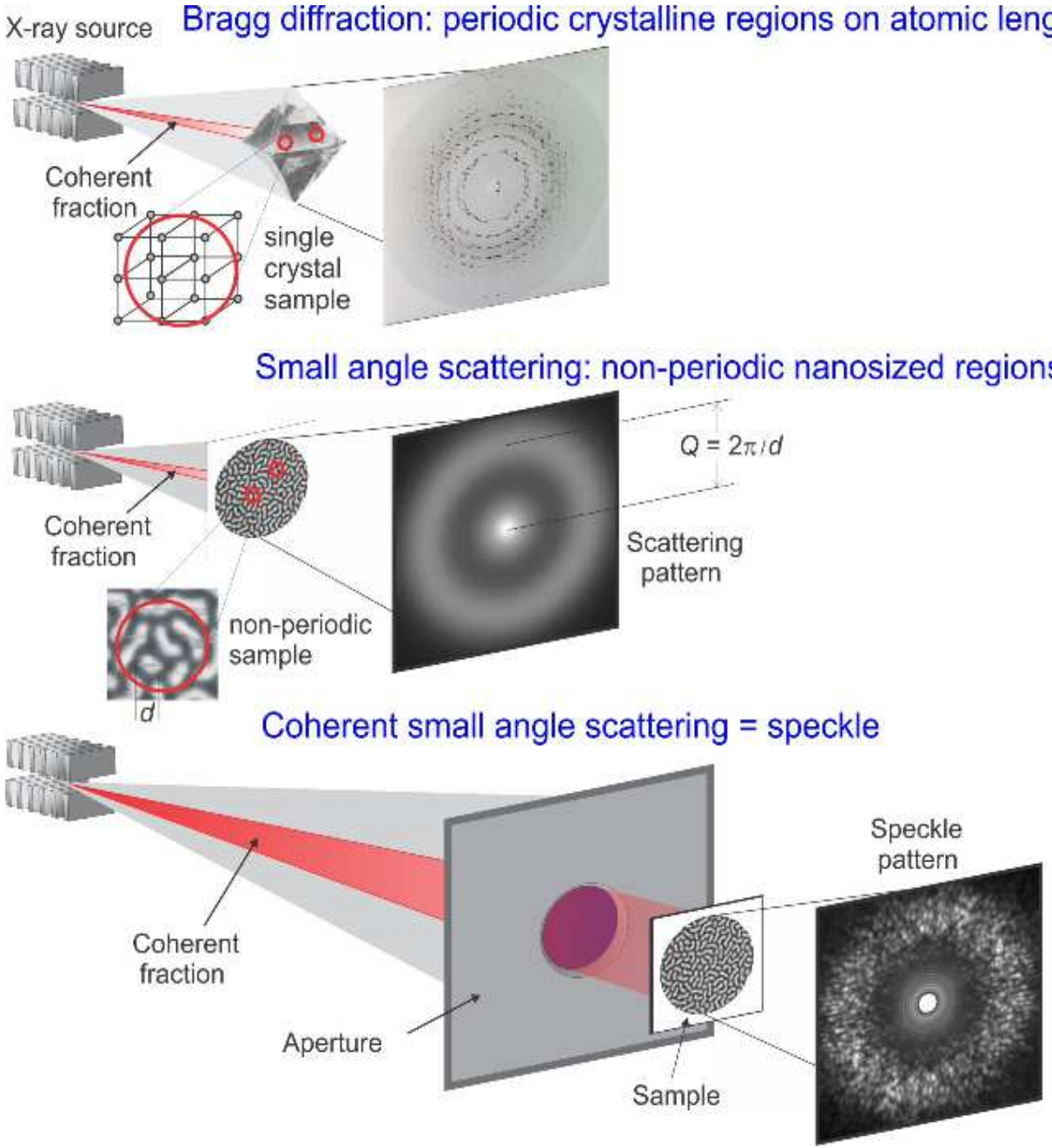

Jo Stohr, SLAC

A thermal light source *vs.* a laser light source

Ordinary thermal light source, atoms radiate independently

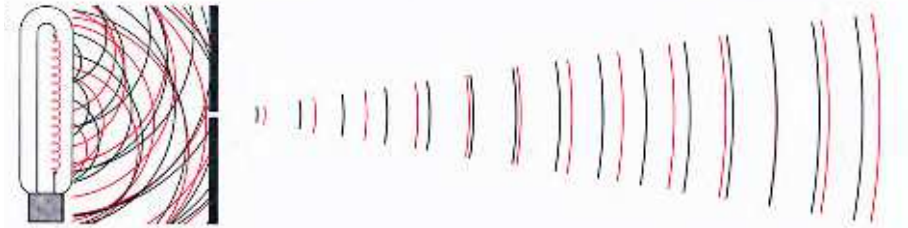

A pinhole can be used to obtain spatially coherent light, but at a great loss of power

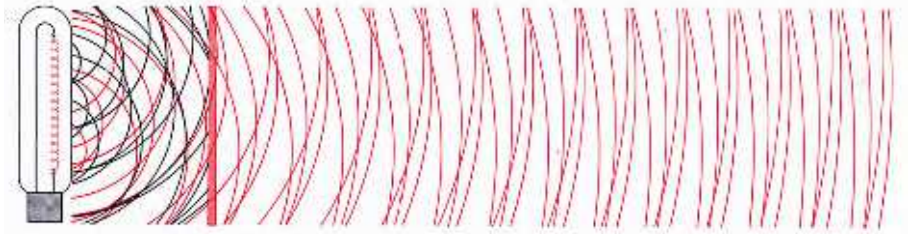

A color filter (or monochromator) can be used to obtain temporally coherent light, also at a great loss of power

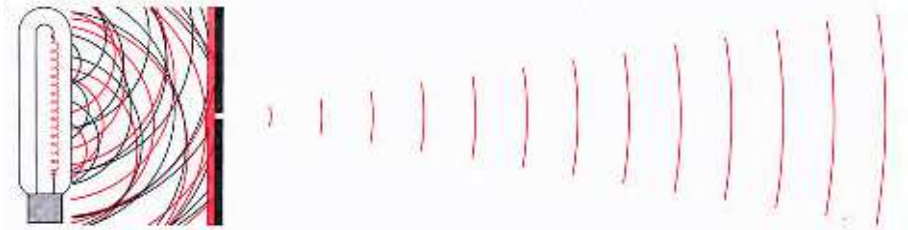

Pinhole and spectral filtering can be used to obtain light which is both spatially and temporally coherent but the power will be very small

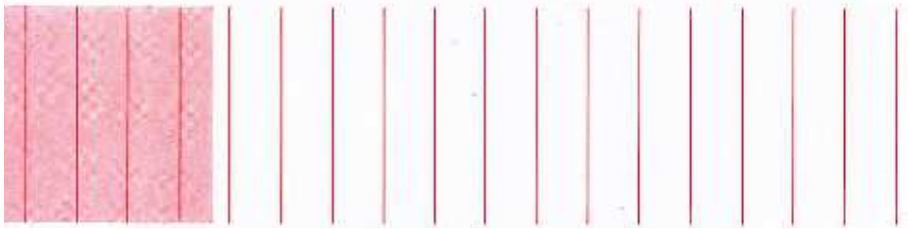

All of the laser light is both spatially and temporally coherent

A. Schawlow, "Laser Light", Sci. Amer. 219, 120 (Sept. 1968)

DIFFRACTION FROM A CRYSTAL AND FROM A SINGLE MOLECULE

X-RAY DIFFRACTION FROM A CRYSTAL AND FROM A SINGLE MACROMOLECULE

CRYSTAL

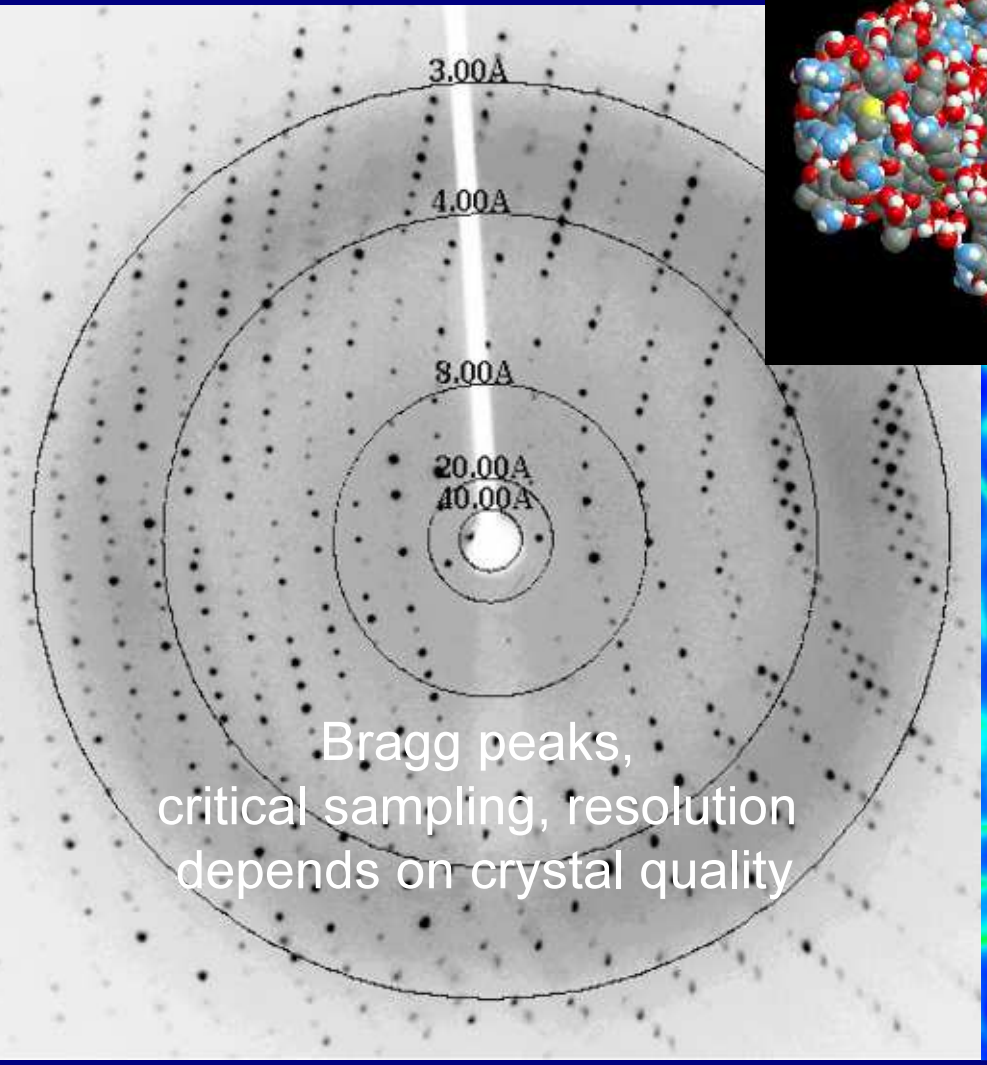

Bragg peaks,
critical sampling, resolution
depends on crystal quality

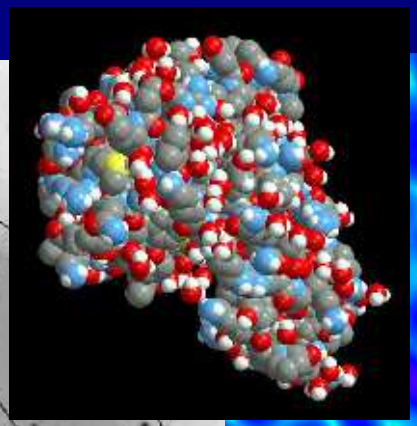

SINGLE MOLECULE

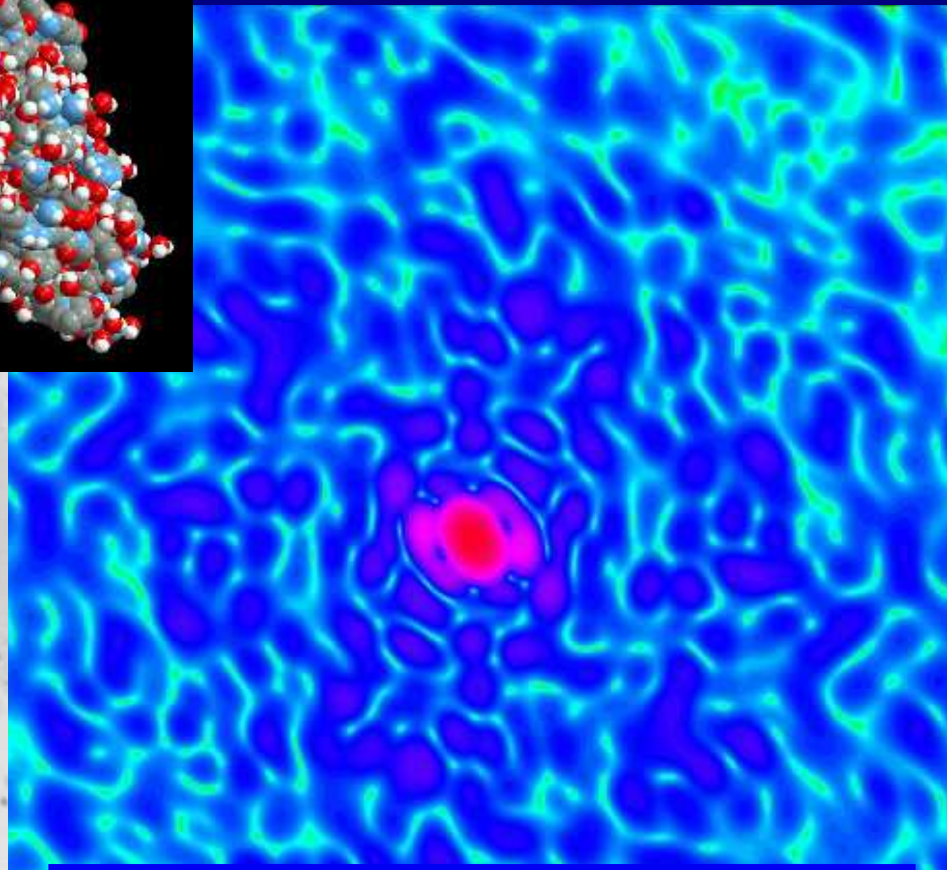

No crystal, no Bragg peaks,
continuous patterns, resolution
does not depend on sample quality

RADIATION DAMAGE KILLS

The more detail we want to see, the less is left from the sample

THERE IS A TIME COMPONENT IN DAMAGE FORMATION

Neutze, R., Wouts, R., van der Spoel, D., Weckert, E. Hajdu, J. (2000) *Nature* 406, 752-757

CRYSTAL STRUCTURE
DISTRIBUTED DAMAGE

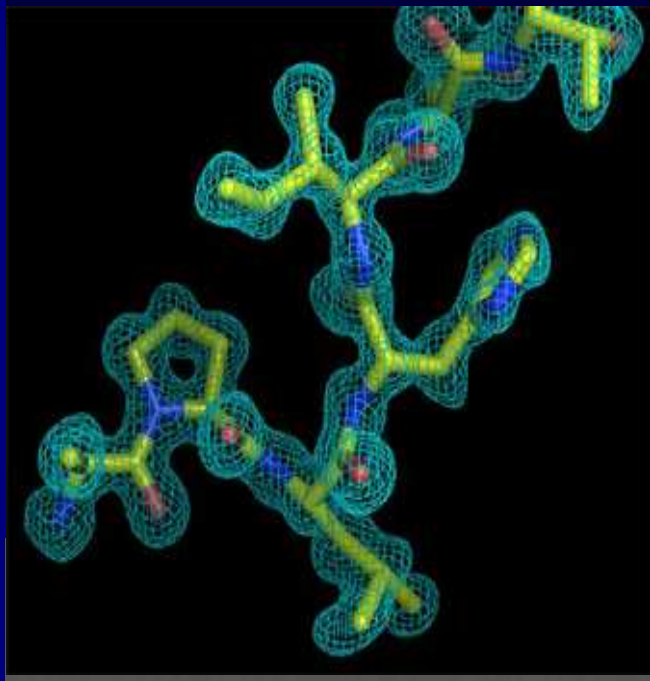

CONCENTRATED DAMAGE NO
IDENTICAL COPIES

THIS DIFFRACTION PATTERN WILL BE MODIFIED BY RADIATION-INDUCED CHANGES IN THE SAMPLE

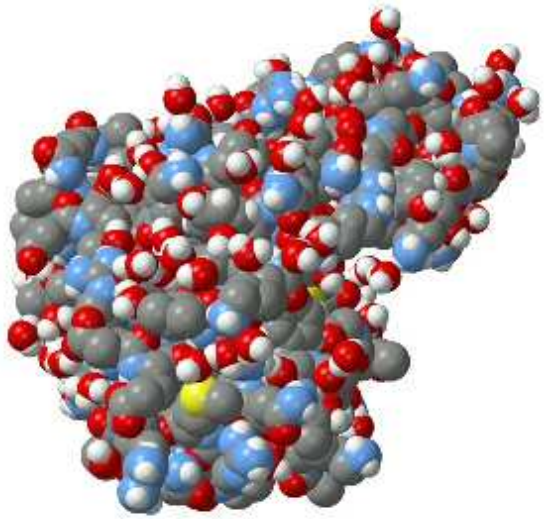

Protein molecule
(lysozyme)

Continuous
diffraction
pattern

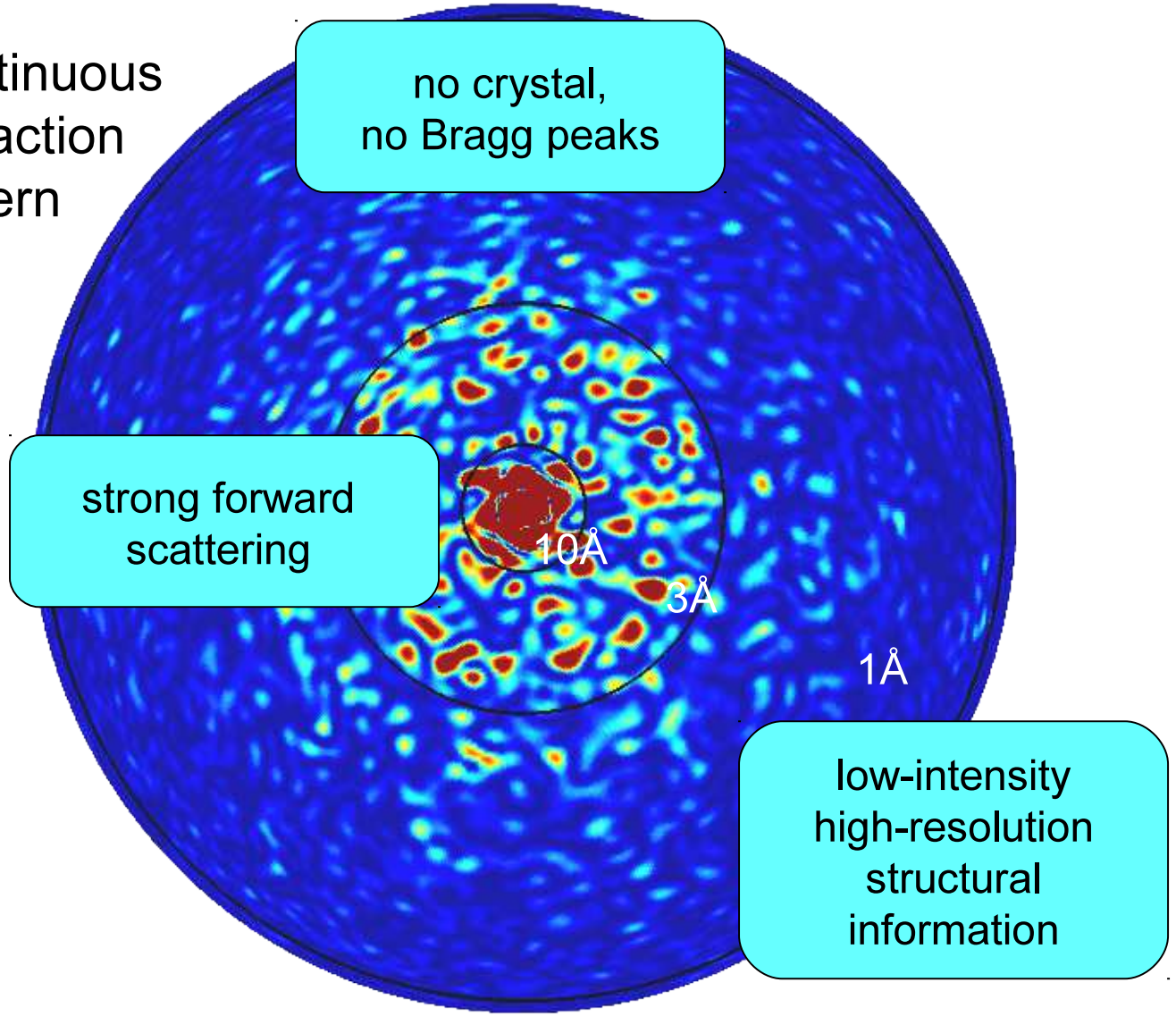

A spherical slice through the 3D reciprocal space – the Ewald sphere

Scattering and damage by X-rays

(12 keV photons, biological samples: C, N, O, H, S, P)

X-RAYS INTERACT WITH MATTER THROUGH ABSORPTION AND SCATTERING:

(1) PHOTOELECTRIC EFFECT (~90%) followed by Auger emission, shake-up excitations, and secondary electron cascades (large samples)

(2) ELASTIC SCATTERING (~7-10%)

(3) INELASTIC SCATTERING (~3%)

(4) Cascade processes in condensed materials

We compute the effect of ionisation, changing scattering factors, and sample explosion on the diffraction pattern

Compute time-integrated diffraction intensity:

$$I(\mathbf{q}) = \Omega r_e^2 \int_{-\infty}^{\infty} I(t) \left| \sum_j f_j(\mathbf{q},t) \exp\{i\mathbf{q} \cdot \mathbf{x}_j(t)\} \right|^2 dt$$

Radiation damage interferes with atomic scattering factors $f_j(\mathbf{q},t)$ and atomic positions $\mathbf{x}_j(t)$

Calculate "degradation (R) factor" to see how the explosion degrades the image

$$R = \sum_u \left| \frac{K^{-1}\sqrt{I_{real}(u)} - \sqrt{I_{ideal}(u)}}{\sum_{u'} \sqrt{I_{ideal}(u')}} \right| \qquad K = \frac{\sum_u \sqrt{I_{real}(u)}}{\sum_u \sqrt{I_{ideal}(u)}}$$

- R = 0 is ideal; larger R means larger error
- For two totally random arrays: R ~ 0.67
- Typical R -values in Protein Database: 0.20

Landscape of damage tolerance from our model

Neutze et al. (2000) *Nature* 406, 752-757

Ionisation and subsequent sample explosion cause diffraction intensities to change →

Damage-Induced Error

$$R = \frac{\left| \sqrt{I(t)} - \sqrt{I_o} \right|}{\sqrt{I_o}}$$

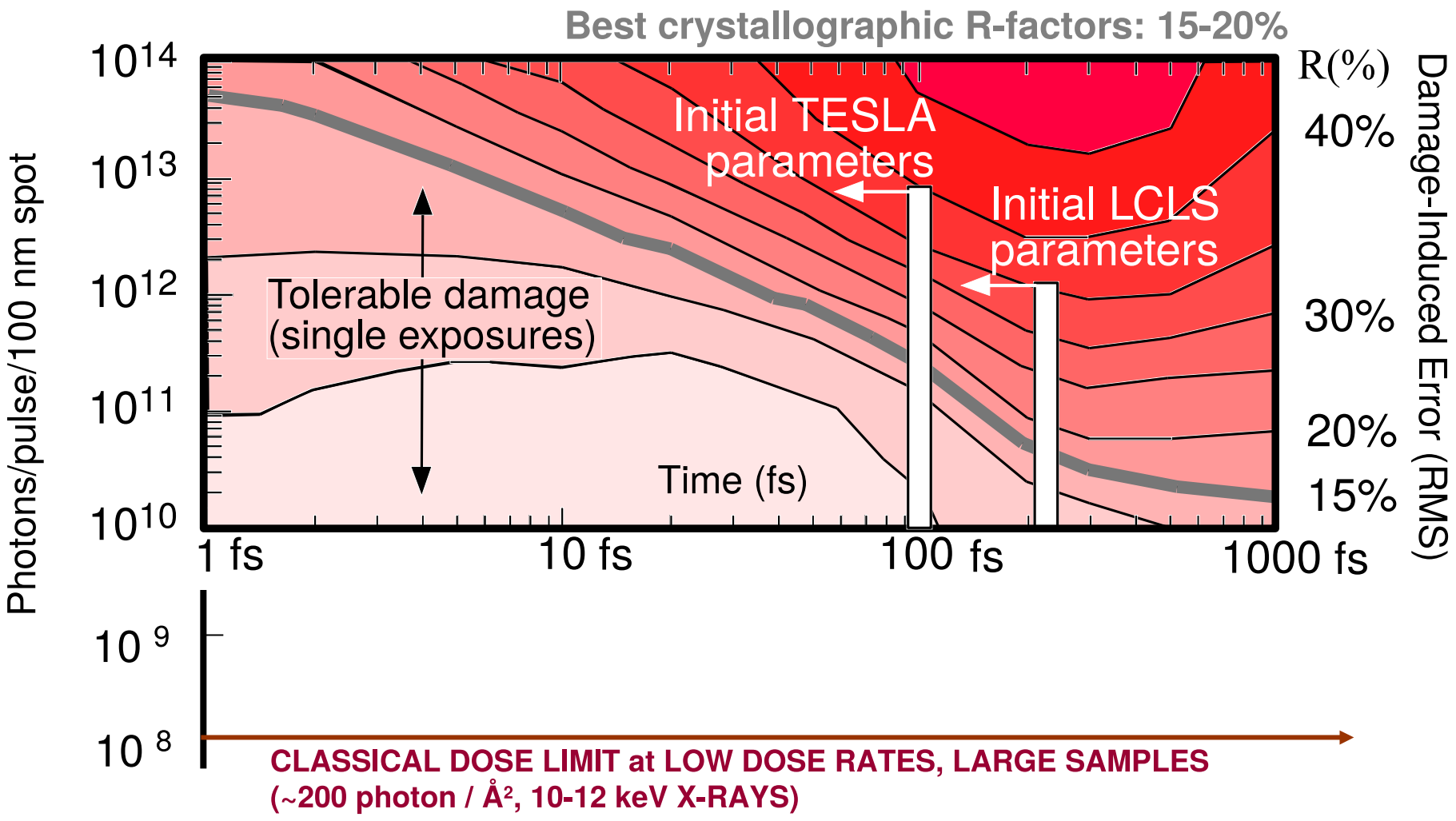

Ultrashort and very intense X-ray pulses offer the possibility to outrun key damage processes

Neutze, R., Wouts, R., van der Spoel, D., Weckert, E., Hajdu, J., *Nature* 406, 752-757, (2000).

3.8 x 10^{12} X-ray photons, 12 keV, 100 nm focus

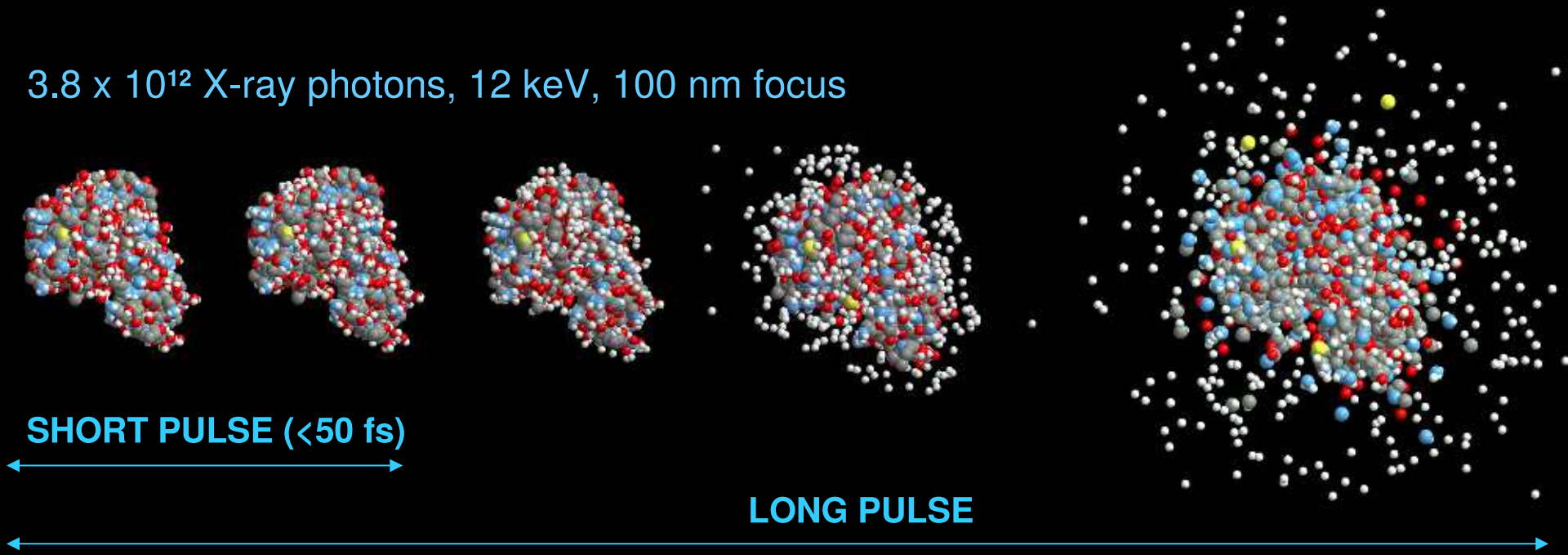

SHORT PULSE (<50 fs)

LONG PULSE

SPEED OF LIGHT *vs.*
SPEED OF A SHOCK WAVE

DIFFRACTION BEFORE DESTRUCTION:
Capture an image before the sample has time to respond

Potential for biomolecular imaging with femtosecond X-ray pulses

Richard Neutze*, Remco Wouts*, David van der Spoel*, Edgar Weckert†‡ & Janos Hajdu*

* *Department of Biochemistry, Biomedical Centre, Box 576, Uppsala University, S-75123 Uppsala, Sweden*
† *Institut für Kristallographie, Universität Karlsruhe, Kaiserstrasse 12, D-76128, Germany*

Sample damage by X-rays and other radiation limits the resolution of structural studies on non-repetitive and non-reproducible structures such as individual biomolecules or cells[1]. Cooling can slow sample deterioration, but cannot eliminate damage-induced sample movement duri… measurements[1,2]. Analys… tion[3–5] suggest that the c… X-ray photons per Å² … wavelength²) may be ext… short exposure times. He… investigate the structural information that can be recovered from the scattering of intense femtosecond X-ray pulses by single protein molecules and small assemblies. Estimations of radiation damage as a function of photon energy, pulse length, integrated pulse intensity and sample size show that experiments using very …ort exposures may provide useful …radiation damage destroys the …ultrashort, high-intensity X-ray …[7] that are currently under devel… …container-free sample handling …echniques, will provide a new …ations with X-rays.

X-ray photons depositing energy …avelength, the photoelectric cross… …s higher than its elastic-scattering …lectric effect the primary source of …t is a resonance phenomenon in …n electron ejected[8], usually from a …ut 95% of the photoelectric events

Nature **406**, 752-757 (2000)

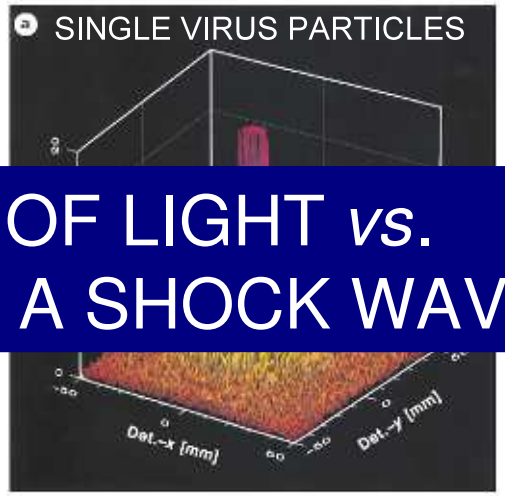

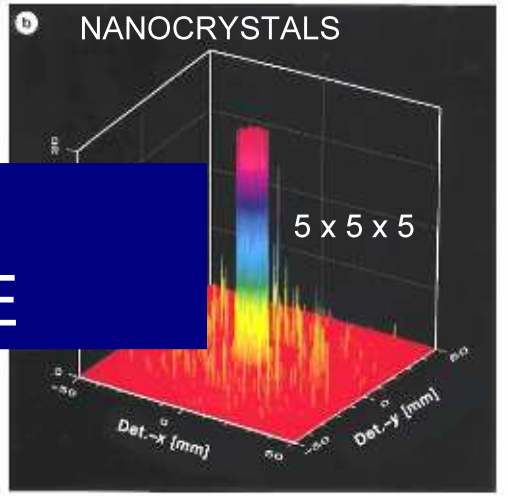

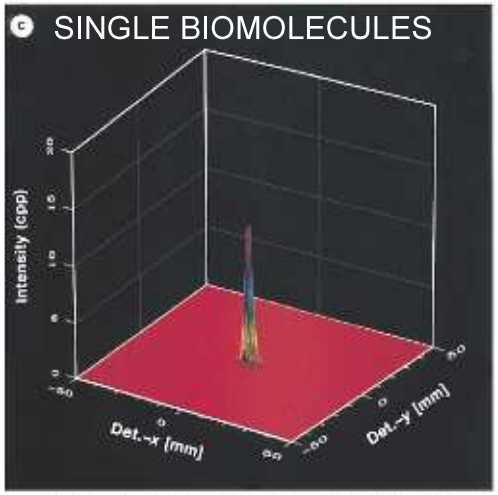

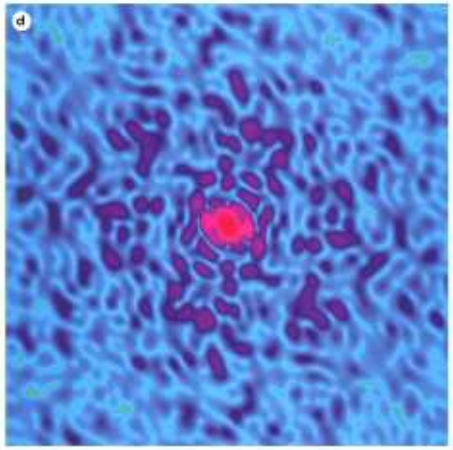

SPEED OF LIGHT *vs.*
SPEED OF A SHOCK WAVE

Figure 3 Elastic scattering from a variety of samples. a–c, Simulated diffraction images … of 0.2 Å to model an imperfect lattice. e, Scattering from a single molecule of lysozyme. d,

AIMING THE BIG GUNS

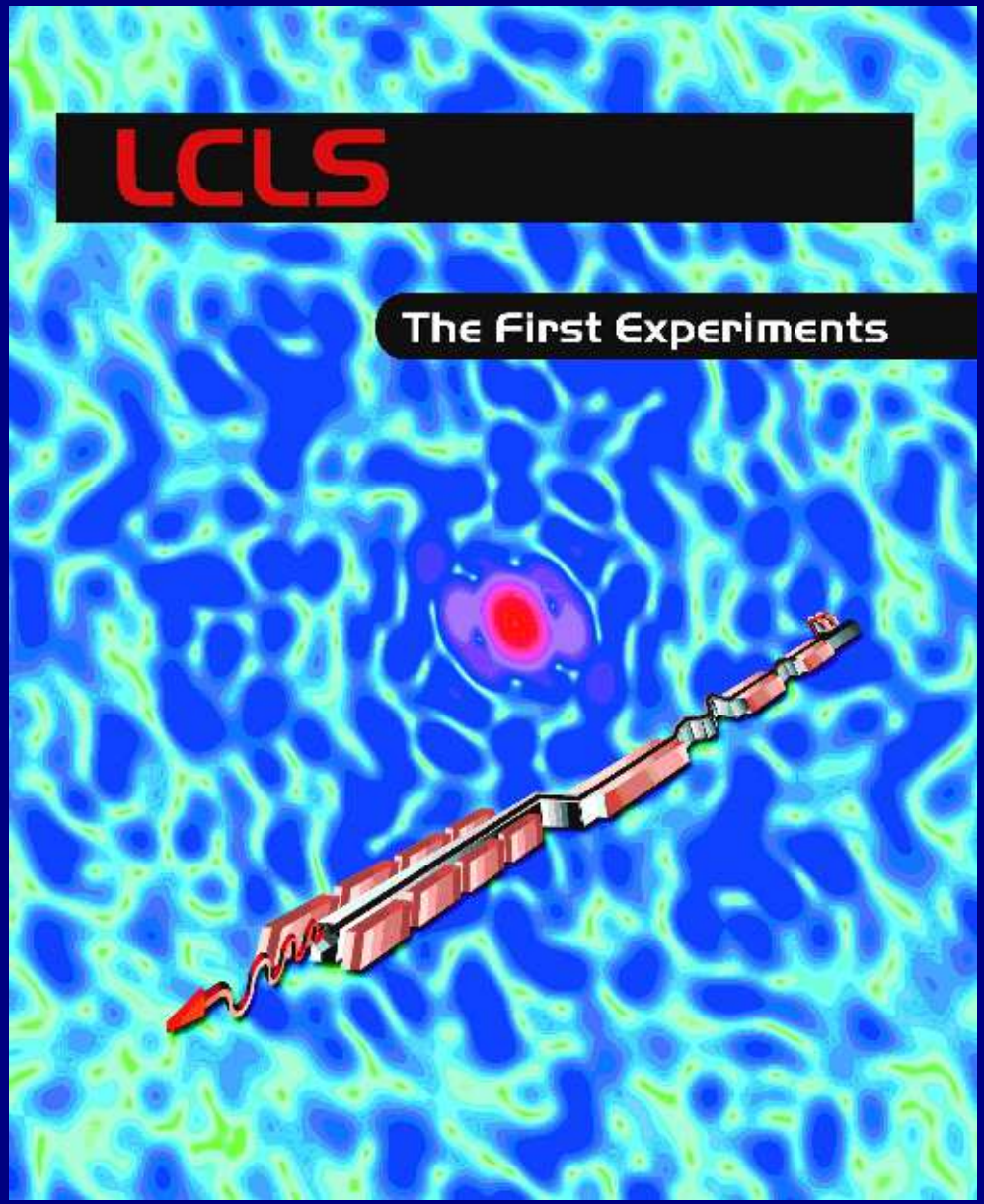

September 2000

October 2002

2002: Livermore joins our SciFi project

PROOF OF PRINCIPLE
1 February 2006

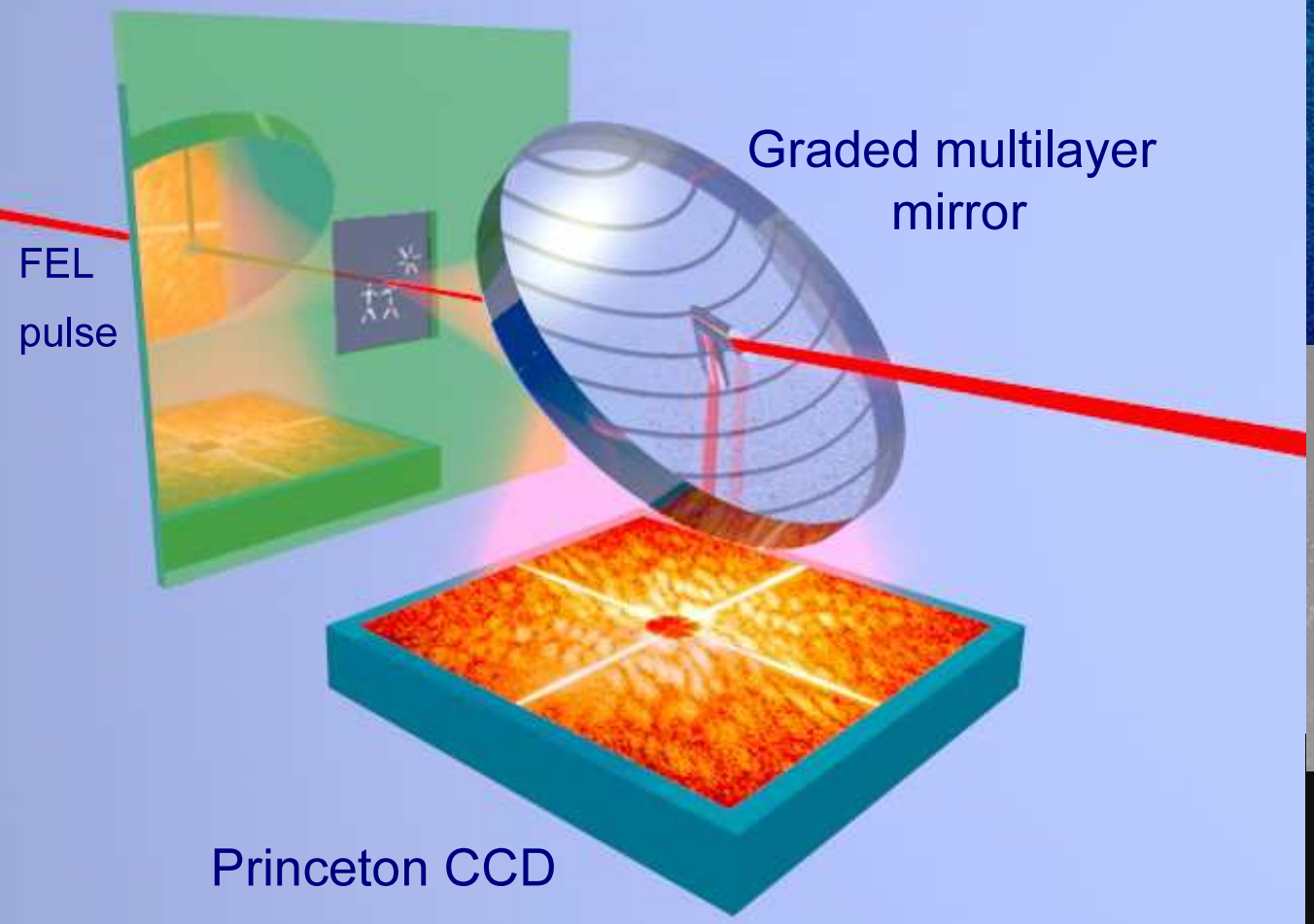

Nature Physics **2**, 839-843 (Dec. 2006)

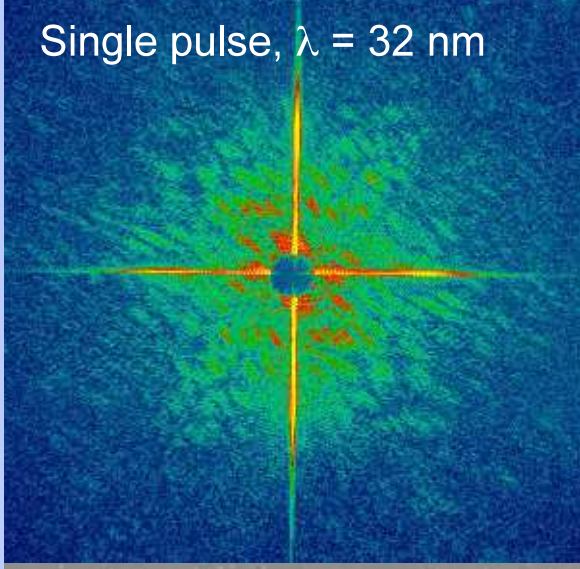

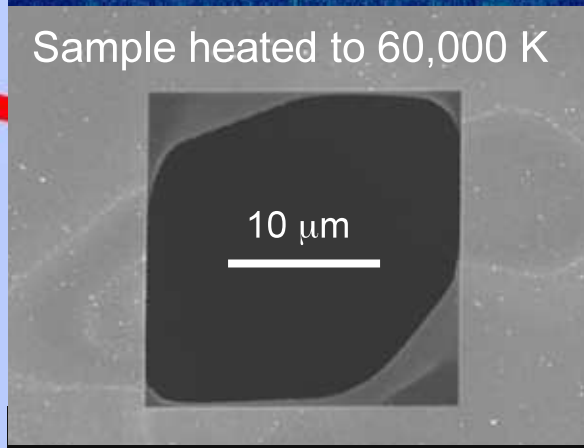

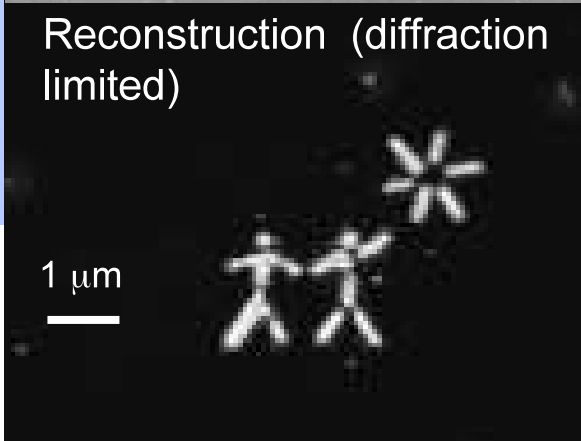

First flash diffraction experiment at the VUV-FEL

Reconstruction from the over-sampled diffraction pattern

Based on the *Gerchberg-Saxton* error reduction algorithm

- ***Hybrid Input Output* as implemented in *Shrinkwrap / Hawk***
- Uses a dynamic instead of a static support.
- Uses a low resolution version of the current guess as new support.

Filipe Maia (Uppsala University)

Crystallography needs crystals AND phases (either from an experiment or a model).

Diffraction imaging appears to require neither.

Where does that come from?

A trip through the early literature of oversampling and direct methods (P. M. Coleman and J. Hajdu)

Bernal, J.D. & Crowfoot, D. "X-ray Photographs of Crystalline Pepsin" *Nature* **133**, 794-795 (1934)

"Four weeks ago, Dr. G. Millikan brought us some crystals of pepsin prepared by Dr. Philpot in the laboratory of Prof. The Svedberg, Uppsala…"

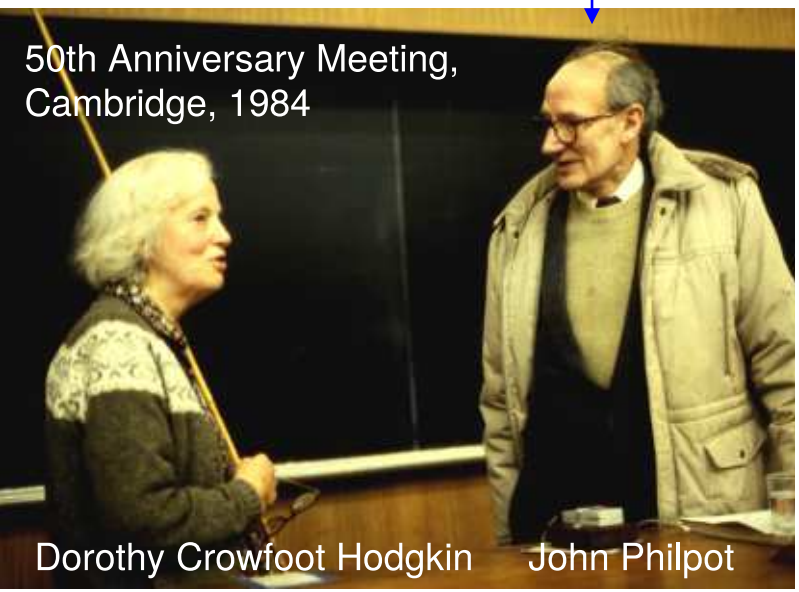

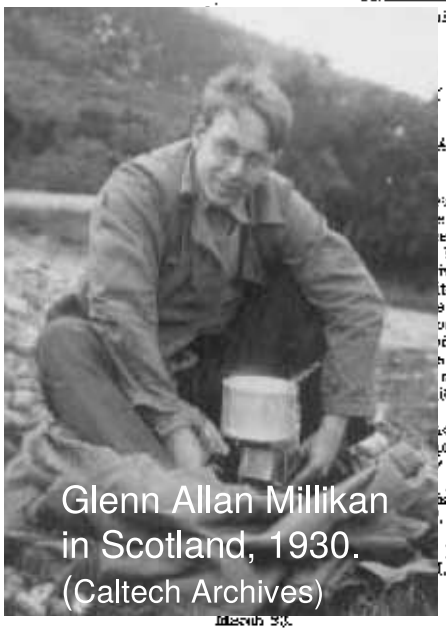
Glenn Allan Millikan in Scotland, 1930. (Caltech Archives)

NATURE MAY 29, 1934

X-Ray Photographs of Crystalline Pepsin

Four weeks ago, Dr. G. Millikan brought us some crystals of pepsin prepared by Dr. Philpot in the laboratory of Prof. The Svedberg, Uppsala. They were in the form of perfect hexagonal bipyramids up to 2 mm. in length, of axial ratio $c/a = 0{\cdot}8 = 0{\cdot}1$. When examined in their mother liquor, they appear moderately birefringent and positively uniaxial, showing a good interference figure. On exposure to air, however, the birefringence rapidly diminishes. X-ray photographs taken of the crystals in the usual way showed nothing but a vague blackening. This indicates complete alteration of the crystal and explains why previous workers have obtained negative results with proteins, so far as crystalline pattern is concerned[1]. W. T. Astbury has, however, shown that the allered pepsin is a protein of the elastin type like myosin or keratin giving an amorphous or fibrous pattern.

It was clearly necessary to avoid alteration of the crystals, and this was effected by drawing them with their mother liquor and without exposure to air into thin capillary tubes of Lindemann glass. The first photograph taken in this way showed that we were dealing with an unaltered crystal. From oscillation photographs with copper $K\alpha$-radiation, the dimensions

J. D. BERNAL,
D. CROWFOOT.

Department of Mineralogy and Petrology,
Cambridge.
May 19.

1938

Bernal, J.D., Fankuchen, I., Perutz, M.F. “An X-Ray Study of Chymotrypsin and Haemoglobin” *Nature* **141**, 523-524 (1938).

Unit cell dimensions change, and reflections move upon hydration/dehydration.

“Studies of these changes provide an opportunity of separating the effects of inter- and intra-molecular scattering. This may make possible the direct Fourier analysis of the molecular structure once complete sets of reflexions are available in different states of hydration. “

This is called “over-sampling” today.

Biochemistry, Oxford, and is similar to those of other seed globulins, excelsin and edestin given by Svedberg as about 300,000. The X-ray measurements provide some additional evidence to show that the units present in these proteins are of very considerable size, although at this stage we cannot exclude the possibility that the true chemical molecular weight of the tobacco seed globulin is a sub-multiple of 326,000.

AN X-RAY STUDY OF CHYMOTRYPSIN AND HÆMOGLOBIN

By Prof. J. D. Bernal, F.R.S., Dr. I. Fankuchen and Max Perutz, Crystallographic Laboratory, Cambridge

We have recently been fortunate in obtaining well-developed crystals of two proteins—chymotrypsin and haemoglobin. The former were prepared for us by Dr. Northrop of Princeton and the latter—methaemoglobin of horse—by Dr. Adair at the Physiological Laboratories, Cambridge. In both cases the crystals were well formed and large (½ mm.) and well suited for X-ray analysis.

Chymotrypsin crystallizes in thick diamond-shaped plates at first thought to be orthorhombic but afterwards discovered to be monoclinic twins. It was examined both in the native state in its mother liquor and dried. The cell dimensions are $a = 40{\cdot}6$ A., $b = 87{\cdot}8$ A., $c = 68{\cdot}6$ A., $\beta = 102°$ for the wet crystals, and $a = 45$ A., $b = 82{\cdot}5$ A., $c = 57{\cdot}5$ A., $\beta = 112°$ for the dry. The space group in both cases is probably $P2_1$. The cell volumes are 219,000 and 151,000 A.^{3} respectively. It is evident that very considerable shrinkage takes place on drying, nearly all of which is in the direction of the c axis. The density of the wet crystals could be measured by the methods of Adair and was found to be 1·277. If we assumed four molecules per cell this would give a molecular weight including water of crystallization of 42,800. In the case of the dry crystals it was unfortunately impossible to measure the density on account of the difficulty of removing crystallized salts. Assuming the density of the dried protein to be the same as that of dry insulin, namely, 1·31, the molecular weight is 32,000. This value for the molecular weight of a protein seems rather lower than is usually obtained by the centrifuge method, which, however, has not as yet been applied to chymotrypsin. It is difficult without a deeper analysis to say much about the inner structure of the crystals, but the extreme strength of (001) indicates a layer structure, while the weakness of $(h0l)$ when h is odd points to a pseudo-glide plane parallel to (010).

The haemoglobin crystals were found to be monoclinic and usually twinned, corresponding very closely to the description given by Reinhert and Brewer. The dimensions are $a = 108$ A., $b = 63{\cdot}2$ A., $c = 54{\cdot}2$ A., $\beta = 113°$ for the wet crystals and $a = 102$ A., $b = 56$ A., $c = 49$ A., $\beta = 134°$ for the dry. The space group in both cases is $C2$ with a face-centred pseudo-hexagonal cell. The cell volumes are 348,000 and 202,000 respectively. Here the shrinkage takes place apparently more by the increase of the β angle rather than by the shortening of cell edges. The

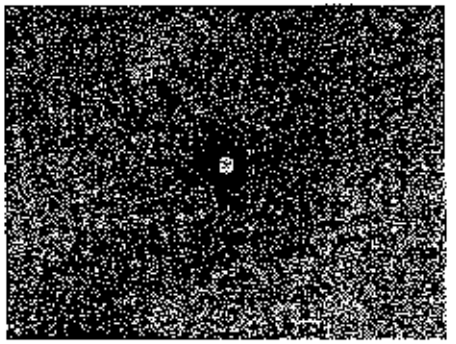

Fig. 1.

WET HÆMOGLOBIN CRYSTAL; 5° OSCILLATION ABOUT b-AXIS SHOWING (hol) ZONE AT CENTRE OF PHOTOGRAPH. NOTE THE PSEUDO-HEXAGONAL CHARACTER OF THE PATTERN AND THE INTENSITY OF THE REFLEXIONS AT HIGH ANGLES.

of 1·26 based on that measured by Chick and Martin[2] for the closely similar equine albumin, the molecular weight is 77,000. The air-dried crystals still contain water. Taking the amount estimated by Haurowitz[3] as 9·6 per cent, the molecular weight of the dry protein becomes 69,000, which agrees excellently with the 67,000 found by chemical methods.

The molecular arrangement appears to be based on a layer lattice with a puckered pseudo-hexagonal network. In the dry crystals it is possible to arrive at a structure which accounts qualitatively for the

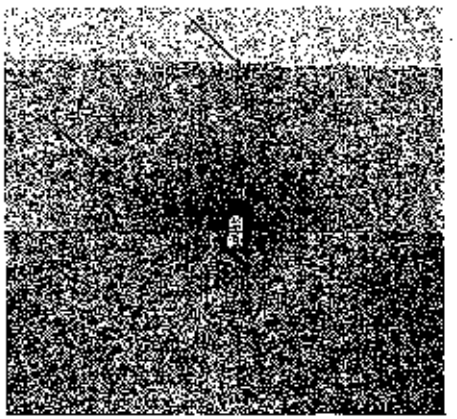

Fig. 2.

COMPARISON PHOTOGRAPH OF CHYMOTRYPSIN: WET BELOW AND DRY ABOVE; 5° OSCILLATION ABOUT b-AXIS SHOWING AT CENTRE OF PHOTOGRAPH THE (hol)-ZONE. NOTE LARGE DIFFERENCE OF SPACING OF (001)-REFLEXIONS ($l = 1$) AND COMPARATIVELY SMALL DIFFERENCE OF [illegible] SEPARATION. THE [illegible] CRYSTAL WAS A [illegible] IN THE DRY

1949

Shannon, C. E. “Communications in the Presence of Noise” *Proceedings of the Institute of Radio Engineers* **37**, 10-21 (1949).

“If a function f(t) contains no frequencies higher than W cps, it is completely determined by giving its ordinates at a series of points spaced 1/2W seconds apart”

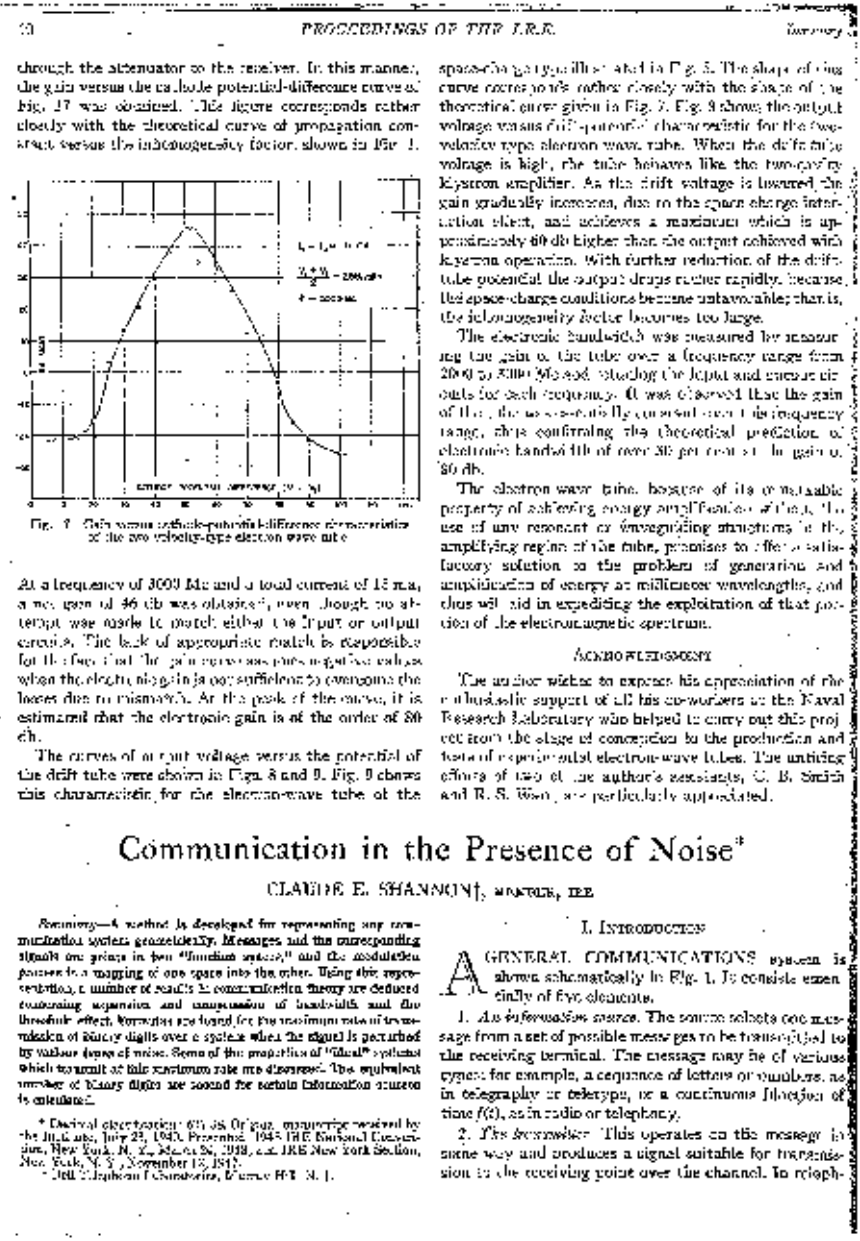

PROCEEDINGS OF THE I.R.E.

through the attenuator to the receiver. In this manner, the gain versus the cathode potential-difference curve of Fig. 17 was obtained. This figure corresponds rather closely with the theoretical curve of propagation constant versus the inhomogeneity factor, shown in Fig. 1.

Fig. 7—Gain versus cathode-potential-difference characteristic of the two velocity-type electron wave tube

At a frequency of 3000 Mc and a total current of 15 ma, a net gain of 46 db was obtained, even though no attempt was made to match either the input or output circuits. The lack of appropriate match is responsible for the fact that the gain curves pass negative values when the electronic gain is not sufficient to overcome the losses due to mismatch. At the peak of the curve, it is estimated that the electronic gain is of the order of 80 db.

The curves of output voltage versus the potential of the drift tube were shown in Figs. 8 and 9. Fig. 9 shows this characteristic for the electron-wave tube of the space-charge grating kind, and in Fig. 8, the shape of this curve corresponds rather closely with the shape of the theoretical curve given in Fig. 7. Fig. 9 shows the output voltage versus drift-potential characteristic for the two-velocity type electron wave tube. When the drift tube voltage is high, the tube behaves like the two-cavity Klystron amplifier. As the drift voltage is lowered, the gain gradually increases, due to the space charge interaction effect, and achieves a maximum which is approximately 40 db higher than the output achieved with klystron operation. With further reduction of the drift-tube potential the output drops rather rapidly, because the space-charge conditions become unfavorable; that is, the inhomogeneity factor becomes too large.

The electronic bandwidth was measured by measuring the gain of the tube over a frequency range from 2000 to 3000 Mc/sec, reading the input and output circuits for each frequency. It was observed that the gain of the tube was essentially constant over the frequency range, this confirming the theoretical prediction of electronic bandwidth of over 30 per cent for a gain of 30 db.

The electron wave tube, because of its remarkable property of achieving energy amplification [illegible], the use of any resonant or waveguiding structures in the amplifying region of the tube, promises to offer a satisfactory solution to the problem of generation and amplification of energy at millimeter wavelengths, and thus will aid in expediting the exploitation of that portion of the electromagnetic spectrum.

ACKNOWLEDGMENT

The author wishes to express his appreciation of the enthusiastic support of all his co-workers at the Naval Research Laboratory who helped to carry out this project from the stage of conception to the production and test of experimental electron-wave tubes. The untiring efforts of two of the author's assistants, C. B. Smith and R. S. Weis, are particularly appreciated.

Communication in the Presence of Noise*

CLAUDE E. SHANNON†, MEMBER, IRE

Summary—A method is developed for representing any communication system geometrically. Messages and the corresponding signals are points in two "function spaces," and the modulation process is a mapping of one space into the other. Using this representation, a number of results in communication theory are deduced concerning expansion and compression of bandwidth and the threshold effect. Formulas are found for the maximum rate of transmission of binary digits over a system when the signal is perturbed by various types of noise. Some of the properties of "ideal" systems which transmit at this maximum rate are discussed. The equivalent number of binary digits are assigned for certain information sources of interest.

* Decimal classification: 621.38. Original manuscript received by the Institute, July 23, 1940. Presented, 1948 IRE National Convention, New York, N. Y., March 25, 1948, and IRE New York Section, New York, N. Y., November 19, 1947.

† Bell Telephone Laboratories, Murray Hill, N. J.

I. Introduction

A GENERAL COMMUNICATIONS system is shown schematically in Fig. 1. It consists essentially of five elements.

1. *An information source.* The source selects one message from a set of possible messages to be transmitted to the receiving terminal. The message may be of various types: for example, a sequence of letters or numbers, as in telegraphy or teletype, or a continuous function of time $f(t)$, as in radio or telephony.

2. *The transmitter.* This operates on the message in some way and produces a signal suitable for transmission to the receiving point over the channel. In teleph-

What Sayre realised later was the fact that crystal lattices provide “critical sampling”

February 1952

Bragg, L. and Perutz, F.M. “The structure of haemoglobin” *Proc. R. Soc. London* **A213**, 425-435 (1952)
Received: 20 February 1952

“This paper describes the first steps in an attempt to solve the structure of a haemoglobin molecule by X-ray analysis, using a direct method. It is based on an extensive series of absolute measurements of the diffraction by various shrinkage stages of a haemoglobin crystal, and estimates based on many crystalline forms of the general dimensions of the haemoglobin molecule.”

See also “*What Mad Pursuit* ” by F.H.C. Crick.

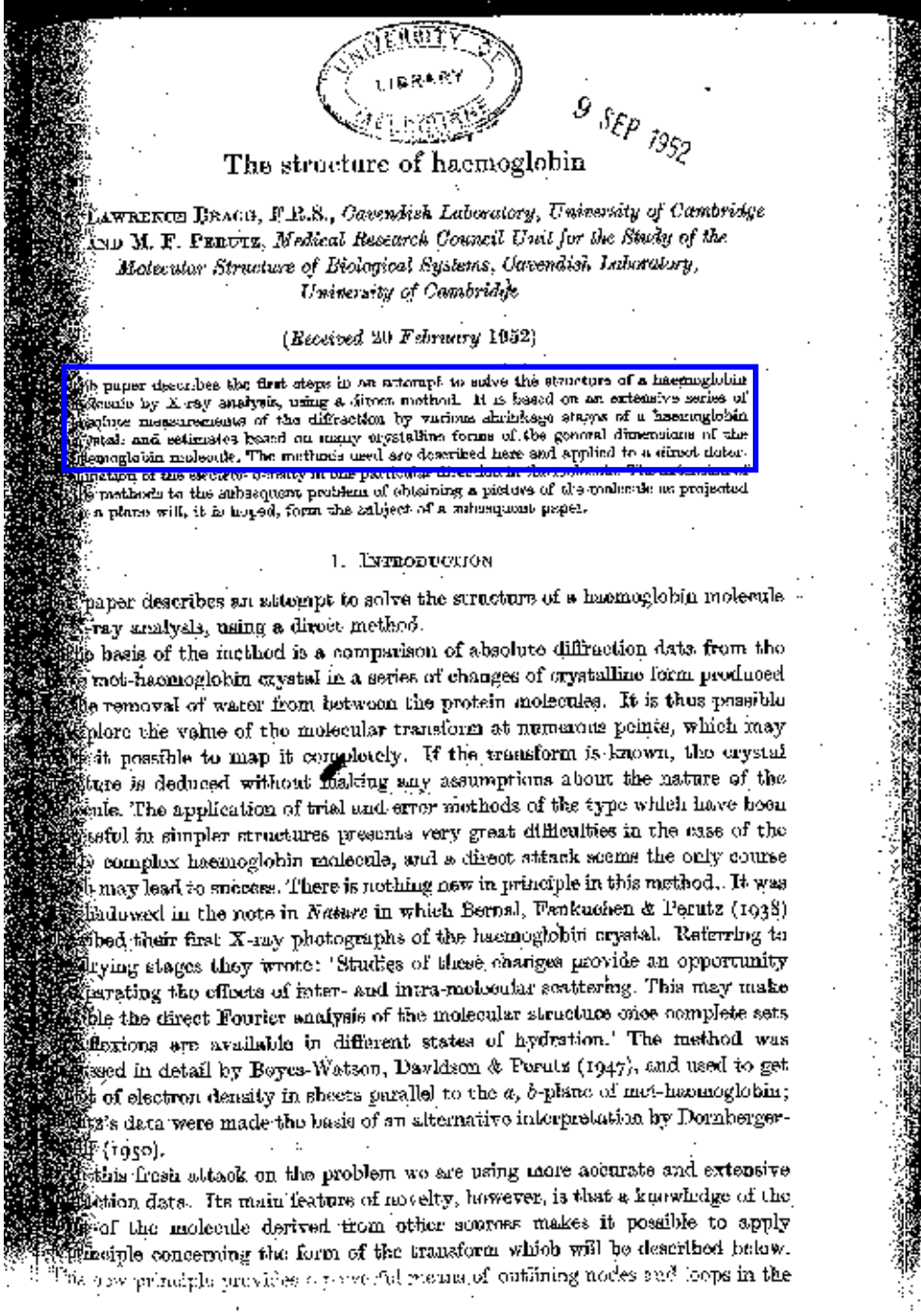

The structure of haemoglobin

LAWRENCE BRAGG, F.R.S., *Cavendish Laboratory, University of Cambridge*
AND M. F. PERUTZ, *Medical Research Council Unit for the Study of the Molecular Structure of Biological Systems, Cavendish Laboratory, University of Cambridge*

(*Received* 20 *February* 1952)

This paper describes the first steps in an attempt to solve the structure of a haemoglobin molecule by X-ray analysis, using a direct method. It is based on an extensive series of absolute measurements of the diffraction by various shrinkage stages of a haemoglobin crystal and estimates based on many crystalline forms of the general dimensions of the haemoglobin molecule. The methods used are described here and applied to a first determination of the electron-density in one particular direction in the crystal. The application of these methods to the subsequent problem of obtaining a picture of the molecule as projected on a plane will, it is hoped, form the subject of a subsequent paper.

1. Introduction

paper describes an attempt to solve the structure of a haemoglobin molecule -ray analysis, using a direct method.

basis of the method is a comparison of absolute diffraction data from the met-haemoglobin crystal in a series of changes of crystalline form produced removal of water from between the protein molecules. It is thus possible plore the value of the molecular transform at numerous points, which may it possible to map it completely. If the transform is known, the crystal ture is deduced without making any assumptions about the nature of the ule. The application of trial and error methods of the type which have been ful in simpler structures presents very great difficulties in the case of the complex haemoglobin molecule, and a direct attack seems the only course may lead to success. There is nothing new in principle in this method. It was adowed in the note in *Nature* in which Bernal, Fankuchen & Perutz (1938) bed their first X-ray photographs of the haemoglobin crystal. Referring to rying stages they wrote: 'Studies of these changes provide an opportunity arating the effects of inter- and intra-molecular scattering. This may make ble the direct Fourier analysis of the molecular structure once complete sets flexions are available in different states of hydration.' The method was ssed in detail by Boyes-Watson, Davidson & Perutz (1947), and used to get of electron density in sheets parallel to the *a*, *b*-plane of met-haemoglobin; ta's data were made the basis of an alternative interpretation by Dornberger-F (1950).

this fresh attack on the problem we are using more accurate and extensive tion data. Its main feature of novelty, however, is that a knowledge of the of the molecule derived from other sources makes it possible to apply principle concerning the form of the transform which will be described below. The new principle provides a powerful means of outlining nodes and loops in the

July 1952

Sayre, D. “Some implications of a theorem due to Shannon”
Acta Cryst. **5**, 843 (1952)
Received 3 July 1952

“Direct structure determination, for centrosymmetrie structures, could be accomplished as well by finding the sizes of the $|F|^2$ at half-integral h as by the usual procedure of finding the signs of the F's at integral h.”

contraction of 2% is largely in a direction normal to the shearing movement:

Parameter of γ: $a = 3{\cdot}585$ Å;
whence $\frac{1}{2}a_\gamma\sqrt{2} = 2{\cdot}535$ Å, $\frac{2}{3}a_\gamma\sqrt{3} = 4{\cdot}140$ Å.
Parameters of ε: $a = 2{\cdot}528$ Å, $c = 4{\cdot}080$ Å.

The mechanism is of the type which produces a 'Widmanstätten' pattern of strain bands; and the contraction associated with the transformation limits the growth of ε around each nucleus. A photomicrograph (Fig. 2) confirms both the strain pattern and the absence of massive precipitate, although individual phases cannot be distinguished.

References

Barrett, C. S., Geisler, H. & Mehl, R. F. (1941). *Trans. Amer. Inst. Min. (Metall.) Engrs.* **100**, 228.
Barrett, C. S., Geisler, A. H. & Mehl, R. F. (1943). *Trans. Amer. Inst. Min. (Metall.) Engrs.* **152**, 201.
Jones, F. W. & Pumphrey, W. I. (1949). *J. Iron Steel Inst.* **163**, 121.
Nishiyama, Z. (1936). *Kinzoku no Kenkyu*, **13**, 300.
Parr, J. G. (1952). *J. Iron Steel Inst.* **171**, 137.
Schmidt, W. (1929–30). *Arch. Eisenhüttenw.* **3**, 292.
Troiano, A. R. & McGuire, F. T. (1943). *Trans. Amer. Soc. Met.* **31**, 340.

Acta Cryst. (1952). **5**, 843

Some implications of a theorem due to Shannon.

By D. Sayre, *Johnson Foundation for Medical Physics, University of Pennsylvania, Philadelphia 4, Pennsylvania, U. S. A.*

(*Received 3 July 1952*)

Shannon (1949), in the field of communication theory, has given the following theorem: If a function $d(x)$ is known to vanish outside the points $x = \pm a/2$, then its Fourier transform $F(X)$ is completely specified by the values which it assumes at the points $X = 0, \pm 1/a, \pm 2/a, \ldots$. In fact, the continuous $F(X)$ may be filled in merely by laying down the function $\sin \pi aX/\pi aX$ at each of the above points, with weight equal to the value of $F(X)$ at that point, and adding.

Now the electron-density function $d(x)$ describing a single unit cell of a crystal vanishes outside the points $x = \pm a/2$, where a is the length of the cell. The reciprocal-lattice points are at $X = 0, \pm 1/a, \pm 2/a, \ldots$, and hence the experimentally observable values of $F(X)$ would suffice, by the theorem, to determine $F(X)$ everywhere, if the phases were known. (In principle, the necessary points extend indefinitely in reciprocal space, but by using, say, Gaussian atoms both $d(x)$ and $F(X)$ can be effectively confined to the unit cell and the observable region, respectively.)

For centrosymmetrical structures, to be able to fill in the $|F|^2$ function would suffice to yield the structure, for sign changes could occur only at the points where $|F|^2$ vanishes. The structure corresponding to the $|F|^2$ function is the Patterson of a single unit cell. This has twice the width of the unit cell, and hence to fill in the $|F|^2$ function would require knowledge of $|F|^2$ at the half-integral, as well as the integral h's. This is equivalent to a statement made by Gay (1951).

I think the conclusions which may be stated at this point are:

1. Direct structure determination, for centrosymmetrie structures, could be accomplished as well by finding the sizes of the $|F|^2$ at half-integral h as by the usual procedure of finding the signs of the F's at integral h.

2. In work like that of Boyes-Watson, Davidson & Perutz (1947) on haemoglobin, where $|F|^2$ was observed at non-integral h, it would suffice to have only the values at half-integral h.

The extension to three dimensions is obvious.

References

Boyes-Watson, J., Davidson, E. & Perutz, M. F. (1947). *Proc. Roy. Soc.* A, **191**, 83.
Gay, R. (1951). Paper presented at the Second International Congress of Crystallography, Stockholm.
Shannon, C. E. (1949). *Proc. Inst. Radio Engrs., N.Y.* **37**, 10.

Acta Cryst. (1952). **5**, 843

Unit-cell dimensions and space groups of synthetic peptides. I. Glycyl-L-tyrosine, glycyl-L-tyrosine hydrochloride, glycyl-DL-serine and glycyl-DL-leucine.

By T. C. Tranter, *Wool Industries Research Association, 'Torridon', Headingley, Leeds 6, England*

(*Received 5 June 1952*)

1963: Rossmann and Blow

Connects non-crystallographic symmetry to Shannon and Sayre.

First attempt to write down relationships between structure factors.

...gr. (1963). 16, 39

...ermination of Phases by the Conditions of Non-Crystallographic symmetry

MICHAEL G. ROSSMANN AND D. M. BLOW

M.R.C. Laboratory of Molecular Biology, University Postgraduate Medical School, Hills Road, Cambridge, England

(*Received 2 February 1962*)

If a molecule is either repeated more than once within the same crystallographic asymmetric unit, or if more than one crystal form is available, then the phase problem can be reduced to finding the set of unknown phases (α's) which gives the largest value of R in the expression

$$R = \sum_i \sum_j A_{ij} \cos(\alpha_i - \alpha_j + \varphi_{ij})$$

The coefficients A_{ij} and angles φ_{ij} are simple functions of the structure amplitudes and overall dimensions of the molecule relative to a chosen origin. The matrix $[A_{ij}]$ is populated mainly along its diagonal. A general technique for finding the phases from the expression R is given. It is applied to a two-dimensional case where there are two identical five-atom molecules in plane group $p1$.

1. Introduction

(1952) has given the crystallographic inter-...ion of a theorem of Shannon (1949), which ...en considered from a more general standpoint ...llouin (1956). The theorem indicates that if the ...ties $|F|^2$ could be measured at points corres-...ng to the reciprocal lattice of the doubled cell, ...structure determination could be accomplished. ...tion approaching this arises when two identical ...les (or 'sub-units') are contained in the crys-...phic asymmetric unit; and a similar situation ...when the identical structure may be crystallized ... different unit cells. In each case, for the ...sition of a structure of given volume, the ... of observable intensities is doubled.

...n earlier paper (Rossmann & Blow, 1962, ...d to as R. & B.) we have described how the ... angular orientations of the sub-units may be ...ined. We now wish to show how the condition ...he sub-units shall have identical structure ...es information about the phases. The method ... illustrated by a two-dimensional example in ...two sub-units of five atoms exist in a unit cell ...e group $p1$ (Fig. 1).

...ive atom structure showing two identical five atom ...ities contained within the 12 Å radius circles and ...d by a rotation of $-140°$.

In order to solve this problem, it is necessary to ...e able to define the operation which, by rotation and translation, brings one sub-unit into coincidence with the other, and to have a rough idea of how the sub-units are arranged in the unit cell. The rotational parameters can be derived by the methods of R. & B. In some ways the translational parameters can then be found by comparing the original and rotated Patterson functions, (this has been done successfully for insulin, unpublished), while, for instance, in plane group $p1$ the translation is trivial, since the origin may be chosen to lie on the rotation axis. Whether the arrangement of sub units is then uniquely determined will depend on the physical information available about their size and shape. For the purposes of this communication, we shall assume that this problem can be solved.

The 'rotation function' described in R. & B. was applied to a model structure, with the result shown

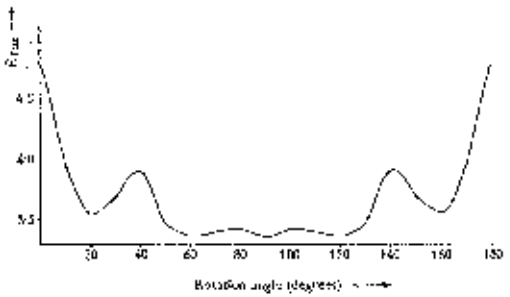

Fig. 2. *Rotation function (2 Å resolution), R_{max}, which measures the different overlap of the Patterson with a rotated version of itself. The relative orientation of the two five atom molecules is shown to be $-140°$, $-40°$, $+40°$ or $+140°$. The calculation was done by Mr D. Davies, to whom we are indebted.*)

1964: Rossmann and Blow

Another formulation of the phase equations

data published for the pure metals, calibration of the X-ray camera for the measurements on the alloys was not considered necessary.

The room temperature lattice constants obtained by Hultgren & Zapffe and by Kondrashev *et al.* are compared with the values obtained in this investigation in Fig. 1. The data of this investigation are in excellent agreement with those obtained by Hultgren & Zapffe. In contrast to the observations of Kondrashev *et al.*, whose alloys were obviously not in equilibrium, the cell constants follow a smooth curve with a considerable positive deviation from Vegard's law. The molar volumes (V) and the relative integral molar volumes (ΔV^M, volumes of mixing), calculated from the relation

$$\Delta V^M = V - (N_{\mathrm{Ni}} V_{\mathrm{Ni}} + N_{\mathrm{Pd}} V_{\mathrm{Pd}}),$$

where N_i and V_i are respectively the mole fraction and molar volume of pure component i, are also shown in Table 1. In many respects the volume of mixing presents a more realistic picture of the effects of alloying than do the cell constants, since a solution which obeys Vegard's law represents a negative deviation from the rule of mixtures in a volume sense.

In view of the recent suggestions, e.g. Myasnikova-Yevstigneyeva (1959) and Pecherskaya (1961), that a superstructure exists at about 75 at.% Pd, the cell constants of the 77·7 at.% Pd alloy were determined as a function of time at 700 (7 days) and 510 °C (14 days). It was expected that if the system tended toward long-range order, the ordering reaction would be accompanied by an increase in volume as in the similar Fe–Pd system which forms a superlattice below 800 °C (Hultgren & Zapffe, 1959). However, within the precision of the measurements, the cell dimensions remained constant at 3·963 (0) and 3·858 (4) Å respectively.

The authors would like to thank the Battelle Memorial Institute for performing the chemical analyses and the International Nickel Company for furnishing the high-purity Ni and Pd used in the investigation.

References

Bennett, L. R. & Speiser, R. (1964). To be published.

Fraenkel, W. & Sauer, A. (1937). *Z. anorg. Chem.* **166**, 161.

Hultgren, R. & Zapffe, C. (1939). *Trans. Amer. Inst. Min. (metall.) Engrs.* **135**, 56.

Kondrashev, Yu. D., Tyapunova, I. P. & Vant, Z. L. (1951). *Doklady Akad. Nauk SSSR*, **78**, 709.

Myasnikova, G. (1959). *Issled. oblasti Nauk Fiziken. SSR*, No. 1, 104.

Nelson, J. B. & Riley, D. P. (1946). *Proc. Phys. Soc. Lond.* **57**, 160.

Nishi, N. (1961). *J. Phys. Soc. Japan*, **16**, 338.

Pecherskaya, M. K. (1951). *Issled. Akad. Nauk Fiziken. SSR, Ser. Fiz.-Tekh., Khim. i Geol. Nauk*, No. 4, 35.

Swanson, H. E. & Tatge, E. (1951). *J. C. Pd. Papers, N. B. S.*

Swanson, H. E. & Tatge, E. (1953). *N. B. S. Circular* 539, I, 21.

Acta Cryst. (1964). **17**, 1471

Solution of the phase equations representing non-crystallographic symmetry.

By Michael G. Rossmann, *Department of Biological Sciences, Purdue University, Lafayette, Indiana, U.S.A.* and D. M. Blow, *M.R.C. Laboratory of Molecular Biology, Hills Road, Cambridge, England*

(*Received* 22 *May* 1964)

A set of phase relationships must be satisfied whenever the asymmetric unit contains some non-crystallographic symmetry. For instance if there are two molecules or subunits in the asymmetric unit which are related by a local twofold axis, as is the case for a chymotrypsin (Blow, Rossmann & Jeffery, 1964), there are conditions which the phase angles must fulfil if the electron density distributions of the two subunits are to be equal. The derivation of the necessary conditions has been given by Rossmann & Blow (1962) (equations (7) and (8)). These two equations may be combined to give an equation of the form

$$\sum_j A_{ij} \exp[i(\alpha_i + \alpha_j + \varphi_{ij})] = S_i \qquad (1)$$

for each reflection. Here i and j identify the individual reflections, and the quantities A_{ij}, ξ_{ij} and φ_{ij} can be calculated from a knowledge of the structure amplitudes and the rotational and translational relationship between the two independent molecules. α_i and α_j are the phases of the ith and jth structure factor. In any one equation there are few terms with significantly large magnitudes A_{ij}.

Since writing the previous paper (Rossmann & Blow, 1962) we have found an alternative procedure leading towards a solution of these equations which we believe to be superior, as it considers the interdependence of each of the terms in a single equation instead of treating them independently. Also, the amount of computation involved is greatly reduced.

Let us write (1) as

$$\exp(i\alpha_i) \sum_j A_{ij} \exp[i(\alpha_j + \varphi_{ij})] = S_i \qquad (2)$$

or

$$T_i \exp(i\alpha_i + \Phi_i) + A_{ii} \exp[i(2\alpha_i + \varphi_{ii})] = S_i \qquad (3)$$

where

$$T_i \exp(i\Phi_i) = \sum_{j \neq i} A_{ij} \exp[i(\alpha_j + \varphi_{ij})]. \qquad (4)$$

At any stage of the refinement we have an estimate of the phase angle α_i from previous results. The precision of this estimate can be expressed in terms of a figure of merit m_i (Dickerson, Kendrew & Strandberg, 1961) which varies from unity for complete certainty down to the phase angle to zero when there is no phase information. We propose to replace (4) by the following expression for actual calculation:

1966: Main and Rossmann

The generalised convolution formula appears

BUSING, W. R., MARTIN, K. O. & LEVY, H. A. (1962). *ORFLS, A Fortran Crystallographic Least-squares Program*. Oak Ridge National Laboratory, Oak Ridge, Tennessee, U.S.A.
DAUBEN, C. H. & TEMPLETON, D. H. (1955). *Acta Cryst.* **8**, 841.
KUTSCHABSKY, A. D. (1957). *J. Gen. Chem. U.S.S.R.* (Eng. transl.), **23**, 321.
MACDONALD, A. C. & TROTTER, J. (1965). *Acta Cryst.* **18**, 243.
MIJIMA, R. & MORIO, S. (1931). *Proc. Imp. Acad. Tokyo*, **7**, 351.
MIJIMA, R. & MORIO, S. (1932). *Ber. dtsch. chem. Ges.* **65**, 539.
OKAMOTO, T., NAKAMURA, M., IITAKA, Y., YOSHINO, A. & ARIWA, T. (1965). *Chem. Pharm. Bull. (Japan)*, **13**, 1279.
PRZYBYLSKA, M. (1961). *Acta Cryst.* **14**, 624.
PRZYBYLSKA, M. (1961). *Acta Cryst.* **14**, 129.
PRZYBYLSKA, M. (1963). *Acta Cryst.* **16**, 87.
SHIGASAWA, T. (1951). *Chem. Pharm. Bull. (Japan)*, **4**, 6.
SOBIKOSHI, H., ARIWA, T. & SHIMA, T. (1959). *Bull. Chem. Soc. Japan*, **32**, 824.
THOMAS, L. H. & UMEDA, K. (1957). *J. Chem. Phys.* **26**, 293.
WEISSNER, K., ITO, S. & VALENTA, Z. (1958). *Experientia*, **14**, 167.
YUDNOV, S. (1948). *J. Gen. Chem. U.S.S.R.* (Eng. transl.), **18**, 531

(1969). 25, 61

Relationships among Structure Factors due to Identical Molecules in Different Crystallographic Environments

PETER MAIN AND MICHAEL G. ROSSMANN

Department of Biological Sciences, Purdue University, Lafayette, Indiana, U.S.A.

(*Received* 13 *July* 1965 *and in revised form* 23 *December* 1965)

ostraints on phases are imposed when a molecule crystallizes in different crystal forms or occurs ore than once per asymmetric unit. These restrictions are expressed by the equations

$$|F_h| \exp\{i\alpha_h\} = \frac{1}{r} \sum_{m=1}^{+r} |F_k| \exp\{i\alpha_k + i \sum_{n=1}^{N} G_{hmn} \exp(i\varphi_{mn})\}.$$

ere $|F_h|$, α_h, $|F_k|$, and α_k are the structure factors and their phases at the reciprocal lattice points and k in either the same or different crystals. G_{hmn} and φ_{mn} are simple functions of the rotation and nslation parameters relating the molecules in the structures concerned. These equations have been ved in both one and three dimensions. In the one-dimensional case the same arbitrary electron ensity distribution was repeated several times at irregular intervals within the unit cell. All chosen ositions led to equations that could be solved correctly, suggesting that in general there is a unique olution. Refinement of initial approximate translation parameters during phase solution was also uccessful.

Introduction

ere are chemically identical molecules in different crystallographic environments, the phase problem be approached in three distinct stages. The first involves determining the three rotation parameters that relate any two molecules. The rotation function (Rossmann & Blow, 1962; Sasada, 1964) has proved successful for this purpose in a number of cases (Blow, Rossmann & Jeffery, 1964; Prothero & Rossmann, 1964; Dodson, Harding, Hodgkin & Rossmann, 1966; Palmer, Palmer & Dickerson, 1964). The second stage involves determining the translation parameters that relate these molecules. A method of determination of these parameters has been worked out in a special situation when the noncrystallographic molecules are within the

1967: Peter Main

..applied to a small test case

Acta Cryst. (1967). 23, 50

Phase Determination Using Non-crystallographic Symmetry

BY PETER MAIN

Department of Biological Sciences, Purdue University, Lafayette, Indiana, U.S.A.

(*Received 9 September 1966*)

A three-dimensional hypothetical structure containing four crystallographically independent but chemically identical molecules in space group $P1$ has been solved. Each molecule contained ten carbon atoms separated by distances greater than 1·2 Å. The solution of the phases required only a knowledge of the structure amplitudes and the relative orientations and positions of the molecules.

1. Introduction

In a paper by Main & Rossmann (1966) (hereafter MR) there was described a method of phase determination which depended upon having chemically identical molecules in different crystallographic environments. Equating the electron densities of such molecules places restriction on the phases which are expressed by equation (10) of MR.

$$|\mathbf{F}_\mathbf{p}| \exp(i\alpha_\mathbf{p}) = \frac{U}{V'} \sum_{h=-\infty}^{\infty} |\mathbf{F}_\mathbf{h}| \exp(i\alpha_\mathbf{h}) \sum_{n=1}^{N} G_{\mathbf{hpn}} \exp\{2\pi i(\mathbf{p} \cdot \mathbf{S}_n - \mathbf{h} \cdot \mathbf{S})\} \quad (1)$$

where $|\mathbf{F}_\mathbf{p}|$, $\alpha_\mathbf{p}$, $|\mathbf{F}_\mathbf{h}|$ and $\alpha_\mathbf{h}$ are the structure amplitudes and their phases at the reciprocal lattice points $\mathbf{p}$ and $\mathbf{h}$ in either the same or different crystals. Each molecule is enclosed in an envelope of volume U, the centres of the N molecular envelopes in the 'p' crystal being at $\mathbf{S}_n (n = 1, 2 \ldots N)$, while $\mathbf{S}$ is the centre of a molecular envelope in the 'h' crystal. The function $G_{\mathbf{hpn}}$ is the magnitude of the Fourier transform of the molecular envelope which is given both in magnitude and phase by

$$G_{\mathbf{hpn}} \{\exp i\Omega_{\mathbf{hpn}}\} = \int_U \exp\{2\pi i(\mathbf{p} \cdot [\mathbf{C}_n] \mathbf{h} - \mathbf{h} \cdot [\mathbf{C}]\mathbf{x})\} d\mathbf{x}, \quad (2)$$

where $[\mathbf{C}_n]$ is the rotation matrix describing the orientation of the nth molecule in crystal 'p' and $[\mathbf{C}]$ is the rotation matrix corresponding to the molecule centred on $\mathbf{S}$ in crystal 'h'.

MR showed that, using these equations in a one-dimensional case, the phases $\alpha_\mathbf{p}$ and $\alpha_\mathbf{h}$ could be determined with sufficient accuracy for the structure to be recognized in the resulting Fourier synthesis. This paper describes the method of phase determination used there and by MR, as well as the application of the technique to the solution of a hypothetical three-dimensional structure in the space group $P1$.

2. Method of phase determination

Because of the nature of the function $G_{\mathbf{hpn}}$ the largest terms on the right hand side of equation (1) will tend to have $|\mathbf{h}| \simeq |\mathbf{p}|$ or, more specifically, $\mathbf{h}$ and $\mathbf{p}$ will be such that the vector $(\mathbf{p} \cdot [\mathbf{C}_n] - \mathbf{h} \cdot [\mathbf{C}])$ is small. Initially the only known phase will be $\alpha_0 (= 2\pi)$, so that the first phases to be determined will be those for which $|\mathbf{p}|$ is small as these will have the largest interaction with $\mathbf{F}_0$. Next, equations with $|\mathbf{p}|$ a little larger are used since these will have large interactions with the phases previously determined. The equations are therefore arranged in increasing order of their Bragg angle and knowledge of the phases is gradually extended outwards in reciprocal space. This is similar in outline to the method of Rossmann & Blow (1963).

The actual process of phase determination is to take one new phase, $\alpha_\mathbf{p}$, on the edge of the known part of reciprocal space and find its 'best' value by a search procedure. This is done by choosing an equation with $\alpha_\mathbf{p}$ on the left hand side and summing the right hand side over all known values of $\alpha_\mathbf{h}$. Arbitrary values of $\alpha_\mathbf{p}$ at say 5° intervals are substituted into the equation and the discrepancy between the two sides is calculated for each value of $\alpha_\mathbf{p}$. This is repeated for each equation which contains $\alpha_\mathbf{p}$ explicitly on the left hand side and the sum of all the discrepancies for each angle is computed. That value of $\alpha_\mathbf{p}$ which gives the lowest total discrepancy is considered to be the best present estimate of the phase, subject to the error introduced by the lack of knowledge or inaccuracy of the phases $\alpha_\mathbf{h}$. In the event that $\mathbf{h}$ and $\mathbf{p}$ refer to the same crystal, terms involving $\alpha_\mathbf{p}$ may occur also on the right hand side, that is, those terms for which $\mathbf{h} = \pm\mathbf{p}$. This procedure is similar to that described by Rossmann & Blow (1966).

As estimates of more phases become known, phases determined earlier may now be redetermined with more accuracy. The determination of a batch of phases is therefore followed by a refinement of all known phases before further phase determination takes place. The refinement consists simply of substituting the present estimate of the phases in the right hand sides of the equations and performing the vector summation. The argument of each resultant is then taken as the new estimate of the phase angle appearing on the left hand side of the equation. Whenever the same phase appears explicitly on the left hand side of more than one equa-

1967: Crowther

A matrix algebra formulation opens possibilities to develop rapid computer algorithms.

1964), although in these two examples the reflexion already almost vanishes at the second reflexion, which is very close to the first one in angular position. The reflexion found in the present study, however, is too small to conclude therefrom the existence of solid state effects. It is also to be mentioned that the present X-ray diffraction data do not give any information about the region below $\sin\theta/\lambda = 0{\cdot}25$ Å^{-1}.

It is apparent that the contradictory results found by various authors are related to the techniques used for determining the intensity data on the absolute basis. In measurements of this kind, it is necessary to pay much attention to detailed experimental conditions. For example, we have found that an inaccuracy of $\pm 0{\cdot}2°$ (in 2θ) in the zero alignment (Batterman *et al.*, 1960) may result in an error of 1·5% in the integrated intensity when $\theta = 10°$, if the receiving slit is very narrow.

As was pointed out at the Seventh International Congress of Crystallography in Moscow 1966 (Informal Session on the Powder Intensity Project), it is very desirable to have a standard powder specimen for X-ray intensity measurements, because with such a specimen a relative measurement can readily be converted to an absolute one. In the light of our measurements, carbonyl iron seems to be suitable for the purpose. This powder is stable, and identical specimens will be available in different laboratories because of a well standardized procedure for the preparation of this substance.

References

BATTERMAN, B. W., CHIPMAN, D. R. & DEMARCO, J. J. (1960). *Phys. Rev.* 122, 68.
CHIPMAN, D. R. & PASKIN, A. (1959). *J. Appl. Phys.* 30, 1992.
COOPER, M. J. (1962). *Phil. Mag.* 7, 2059.
COOPER, M. J. (1965). *Acta Cryst.* 18, 813.
FREEMAN, A. J. & WATSON, R. E. (1961). *Acta Cryst.* 14, 231.
HARRISON, R. J. & PASKIN, A. (1964). *Acta Cryst.* 17, 325.
HOSOYA, S. (1964). *J. Phys. Soc. Japan*, 19, 235.
UDAGAWA, S. & YAMAGUCHI, T. (1966). *J. Phys. Soc. Japan*, 21, 2638.
INGHRAM, G. & SHORTLE, P. (1964). *Ann. Acad. Sciant. Fenn.* A VI, 147.
JAMES, R. W. (1962). *The Optical Principles of the Diffraction of X-rays*. London: Bell.
JAUNCEY, F. E., JR. & MUELDAWER, L. (1954). *Acta Metallurg.* 2, 513.
SHORTLE, P. & PAAKKARI, T. (1966). *Ann. Acad. Scient. Fenn.* A VI, 224.

Acta Cryst. (1967). **22**, 758

A Linear Analysis of the Non-Crystallographic Symmetry Problem

BY R. A. CROWTHER

Medical Research Council Laboratory of Molecular Biology, Hills Road, Cambridge, England

(*Received* 7 *September* 1966 *and in revised form* 24 *November* 1966)

Linear equations are derived which express constraints on the structure factors of a crystal having more than one identical molecule or subunit in the asymmetric unit. Solution of these equations leads to a series of functions having the required non-crystallographic symmetry. Any structure having the postulated symmetry can be expressed as a linear combination of these functions. This approach has the advantage that far fewer variables are needed to describe the system to a given resolution than in the conventional method using amplitudes and phases. The reduction in the number of variables is used as a measure of the information content of the equations.

Introduction

It has been shown (Rossmann & Blow, 1963; Main & Rossmann, 1966) that, when a crystal contains more than one identical molecule or subunit per asymmetric unit, equations can be set up which imply constraints on the phases of the structure factors. These equations contain certain parameters relating to the relative rotational and translational positioning of the subunits within the asymmetric unit. However, there exist methods for determining these parameters (Rossmann & Blow, 1962; Rossmann, Blow, Harding & Colter, 1964) and it is assumed in all that follows that their values are known.

Iterative methods for solution of the equations have been proposed which, for a number of simple trial structures, appear to converge to a unique answer agreeing well with the known phases (Rossmann & Blow, 1964; Main & Rossmann, 1966). Both these papers attempt to derive values for the unknown phases and in doing so formally separate the amplitudes and phases of the structure factors as they appear in the equations. This means that the equations to be solved are non-linear from the beginning of the calculation.

The methods described in this paper formally keep the amplitude and phase together as an unknown complex structure factor. The equations are now linear in

1969, Crowther

… application to a small test object

First indication that a large number of iterations would be needed to recover images de novo.

References

…E. J. & BAILAR, J. C. JR (1959). *J. Amer. Chem. Soc.* 2620.
…SHANK, D. W. J. (1956a). *Acta Cryst.* **9**, 754.
…SHANK, D. W. J. (1956b). *Acta Cryst.* **9**, 757.
…SHANK, D. W. J., PAULING, D. E., BUTCHER, A., …ELL, F. M. & TRUTER, M. R. (1961). In *Computing …thods and the Phase Problem in X-ray Crystal Anal…*, p. 32. Oxford: Pergamon Press.
…R, F. P., CARVAN, F. …. & SHULMAN, L. (1959). *J. …er. Chem. Soc.* **81**, 290.
…ational Tables for X-ray Crystallography (1959). Vol. …Birmingham: Kynoch Press.
…ational Tables for X-ray Crystallography (1962). Vol. …Birmingham: Kynoch Press.
…, F. M. (1919). *Z. Kristallogr.* **55**, 207.
…ON, R., MASON, S. F. & NORMAN, B. J. (1966). *J. …m. Soc. A*, p. 301.
MASON, S. F. & NORMAN, B. J. (1964). *Proc. Chem. Soc.* p. 339.
MASON, S. F. & NORMAN, B. J. (1965). *Chem. Comm.* p. 73.
MCCAMMAN, A. J., MASON, S. F. & NORMAN, B. J. (1966). *Chem. Comm.* p. 49.
NAKATSU, K. (1962). *Bull. Chem. Soc. Japan*, **35**, 832.
NAKATSU, K., SAITO, Y. & KUROYA, H. (1956). *Bull. Chem. Soc. Japan*, **29**, 428.
NAKATSU, K., SHIRO, M., SAITO, Y. & KUROYA, H. (1957). *Bull. Chem. Soc. Japan*, **30**, 158.
PETERSEN, B. & HOWE, J. (1965). *Acta Cryst.* **19**, 673.
PETERSON, S. W. & LEVY, H. A. (1957). *J. Chem. Phys.* **26**, 220.
PINNOCK, P. R., TAYLOR, C. A. & LIPSON, H. (1956). *Acta Cryst.* **9**, 173.
SAITO, Y., NAKATSU, K., SHIRO, M. & KUROYA, H. (1955). *Acta Cryst.* **8**, 729.
SAITO, Y., NAKATSU, K., SHIRO, M. & KUROYA, H. (1957). *Bull. Chem. Soc. Japan*, **30**, 795.
WERNER, A. (1912). *Ber. dtsch. chem. Ges.* **45**, 1228.

…Cryst. (1969). B25, 2571

The Use of Non-Crystallographic Symmetry for Phase Determination

BY R. A. CROWTHER

Medical Research Council, Laboratory of Molecular Biology, Hills Road, Cambridge, England

(*Received* 13 *January* 1969)

When a crystal contains more than one identical molecule or sub-unit in the crystallographic asymmetric unit, the structure factors must satisfy a set of complex linear equations. Given a set of structure amplitudes for a structure with the postulated non-crystallographic symmetry, the particular nature of the eigenvalue spectrum of the matrix of the equations provides a formal basis for an iterative procedure for generating the phases of the structure factors from the equations. The method has been tested on a number of model structures. An estimate is given of how strong the non-crystallographic symmetry constraints must be in order to generate a unique set of phases.

Introduction

…revious paper (Crowther, 1967) it was shown that …tructure-factor equations, which may be con…ed when a crystal contains more than one iden…molecule or sub-unit within the crystallographic …netic unit (Main & Rossmann, 1966), can be …n in the form

$$\mathbf{H}\mathbf{F}=\mathbf{F}\,. \qquad (1)$$

F is a vector whose elements are the complex …ure factors out to the resolution to which we are …ng and **H** is a hermitian matrix ($H_{rs}=H_{sr}^{*}$, where …tersk denotes complex conjugate) describing the …e geometry of the sub-units. The elements of **H** …pressed in terms of the rotations and translations …g the various sub-units, which we assume are …n, so that the elements of **H** can be evaluated …tically for any given arrangement of sub-units. …y eigenvector of the matrix **H** corresponding to …eigenvalue is a possible solution of (1) and con…y the number of independent solutions of (1) is equal to the number of unit eigenvalues of the matrix **H**. The Fourier transform of the particular set of structure factors constituting an eigenvector of **H** will be called an eigendensity. Eigenvectors and eigendensities corresponding to unit eigenvalues will be termed 'allowed'. Any structure with the postulated non-crystallographic symmetry may, to the resolution to which we are working, be expressed as a linear combination of the allowed eigendensities and correspondingly its transform may be expressed as a linear combination of the allowed eigenvectors. The allowed eigendensities form a more appropriate set of functions in which to expand a density with non-crystallographic symmetry than the more normally used Fourier terms.

Turning now to structure determination, let us take an unknown structure with known non-crystallographic symmetry. The question we pose is whether, given a set of measured structure amplitudes, it is possible to use the constraints introduced by non-crystallographic symmetry to solve the structure. For simplicity we take the space group to be $P1$ and let us suppose that $(2N+1)$ reflexions are to be included,

Single-Molecule X-ray Imaging - Containerless sample handling

One pulse, one measurement

3. Nanoscale manipulation

Biomolecule/particle injection

4. Data collection

2. X-ray Laser Development

Noisy diffraction patterns

X-ray laser pulse

Combine many measurements

1. Theories of damage in ultra-fast imaging

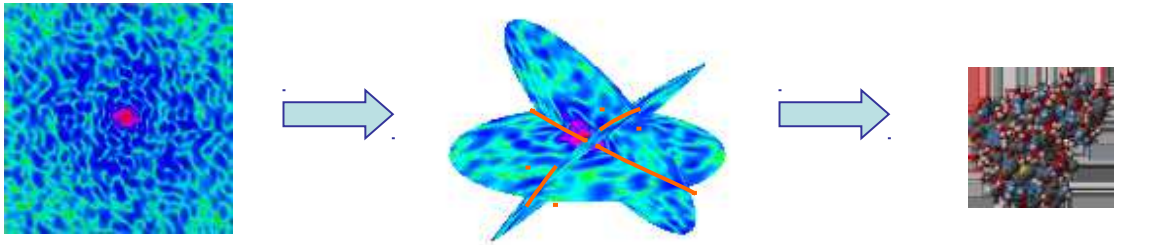

Data frames

Combined data set

Reconstruction

5. Data processing, phasing & reconstruction

BIOLOGY IN THE GAS PHASE?

Many infectious diseases are transmitted via aerosols

Ocean sprays put out 10^{13} kg aerosol per year from droplets formed when bubbles burst

Metabolically active cells have been captured at altidudes of 20-70 km

The Telegraph

HOME » SCIENCE » SPACE

Sea plankton 'found living outside International Space Station'

Russian cosmonauts claim to have discovered tiny marine creatures thriving in zero-gravity on the outside of the International Space Station

Russian cosmonauts claim to have found marine creatures living on the outside of the International Space Station where conditions for life are believed to be impossible

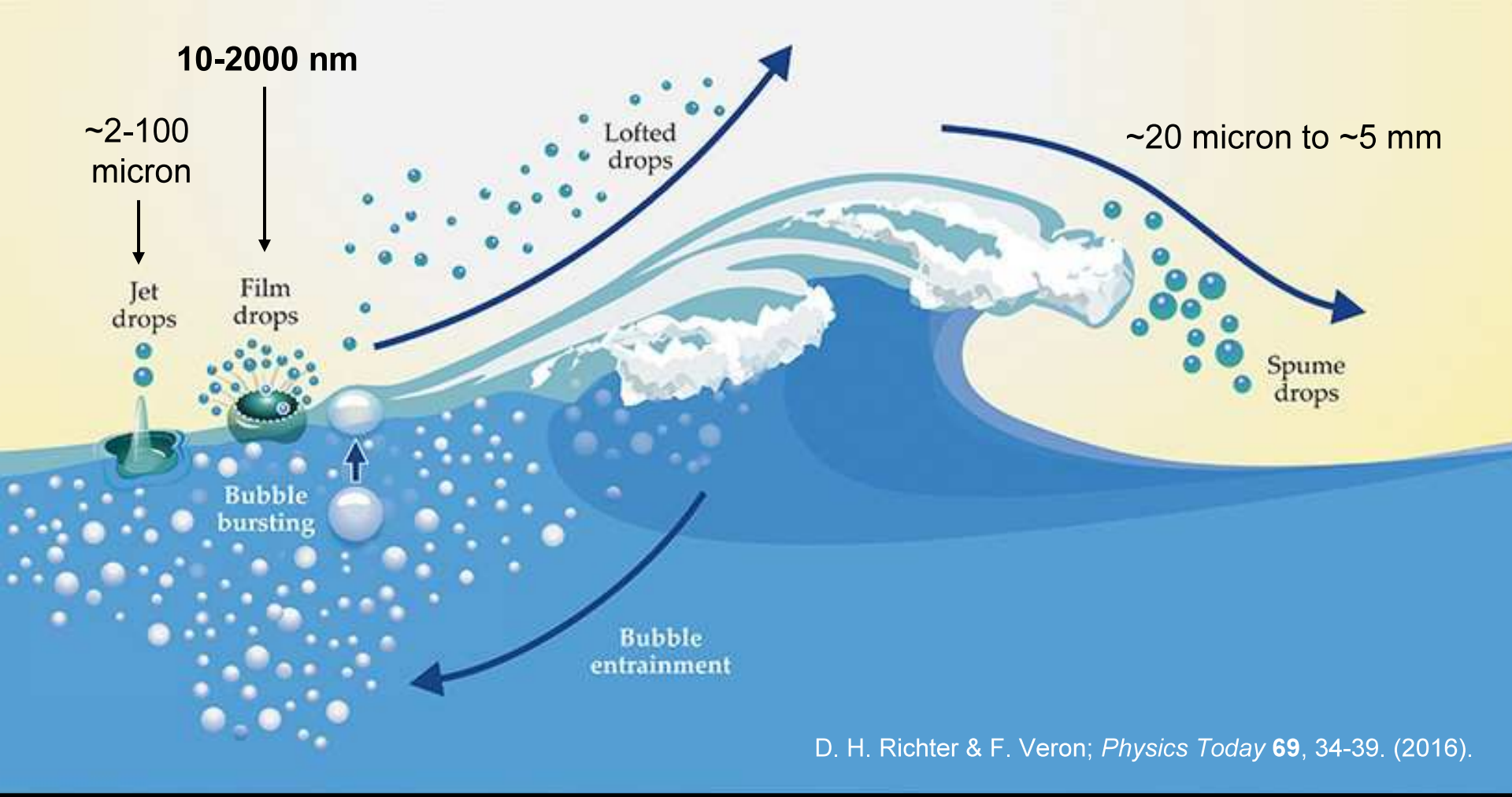

D. H. Richter & F. Veron; *Physics Today* **69**, 34-39. (2016).

THE EXPERIMENTAL SET UP

Random hits in random orientations

$$\nu_{hit} = \frac{F d_{x-ray}^2}{v_p d_p}$$

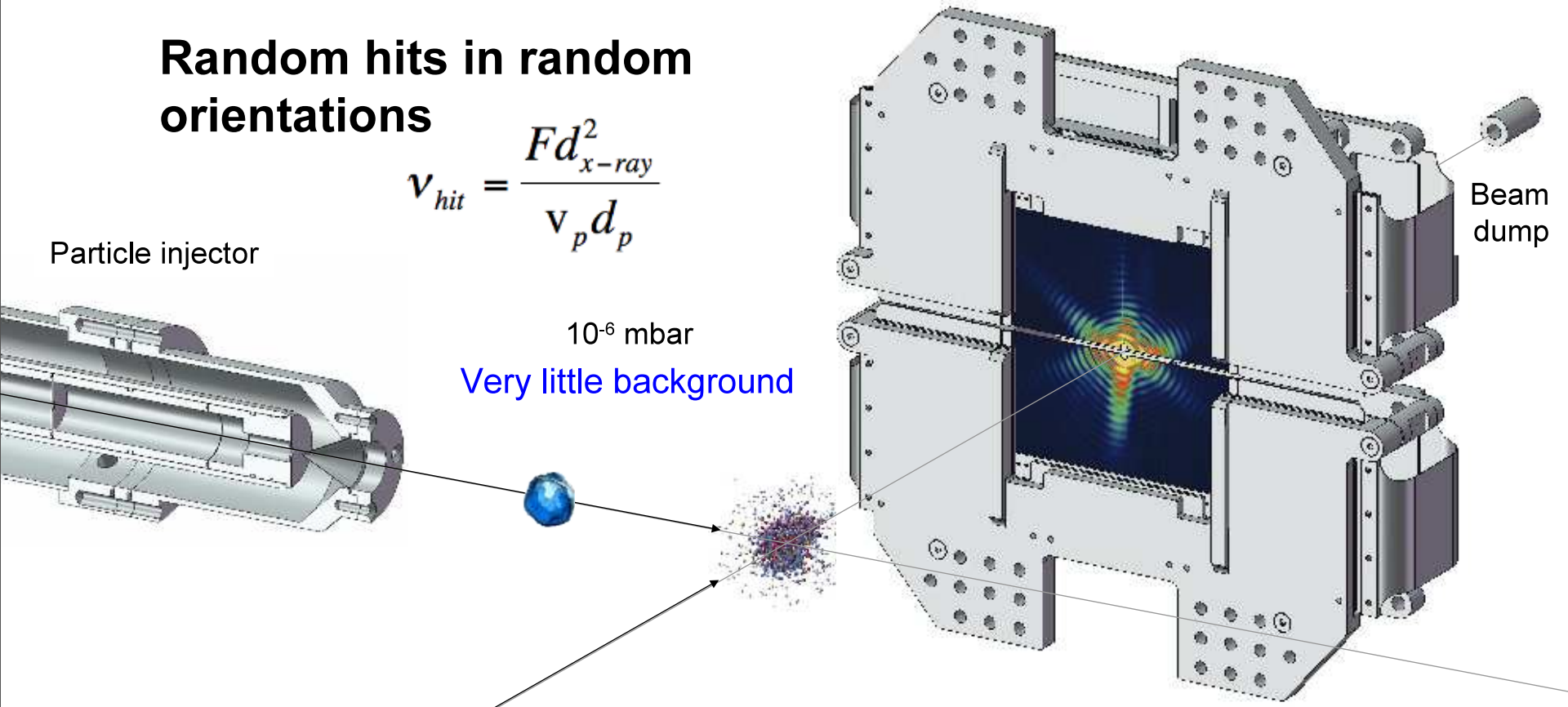

One pulse, one measurement

AEROSOL SAMPLE INJECTION

AEROSOLISATION, EQUILIBRATION

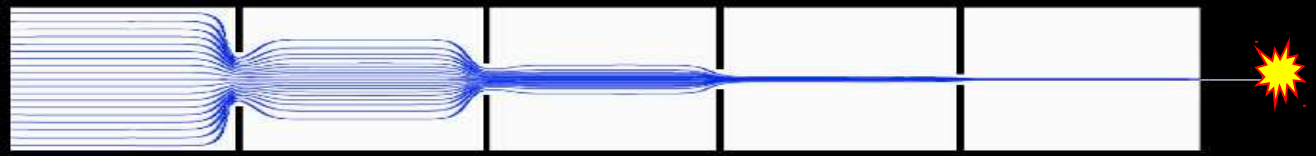

AERODYNAMIC FOCUSING: W.K. Murphy and G.W. Sears, "Production of Particulate Beams" *J. Appl. Phys.* **35**, 1986–1987 (1964).

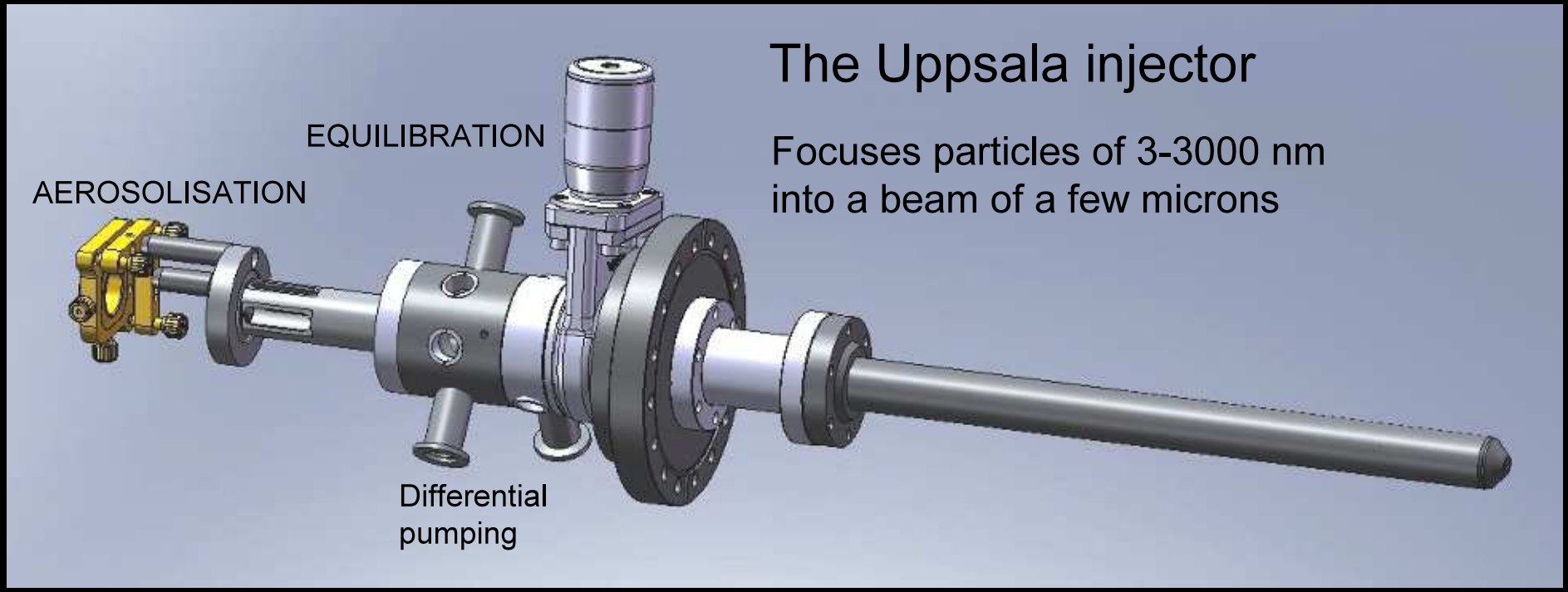

AEROSOLISATION

FLOW FOCUSSING:
Gas dynamic virtual nozzle (GDVN)

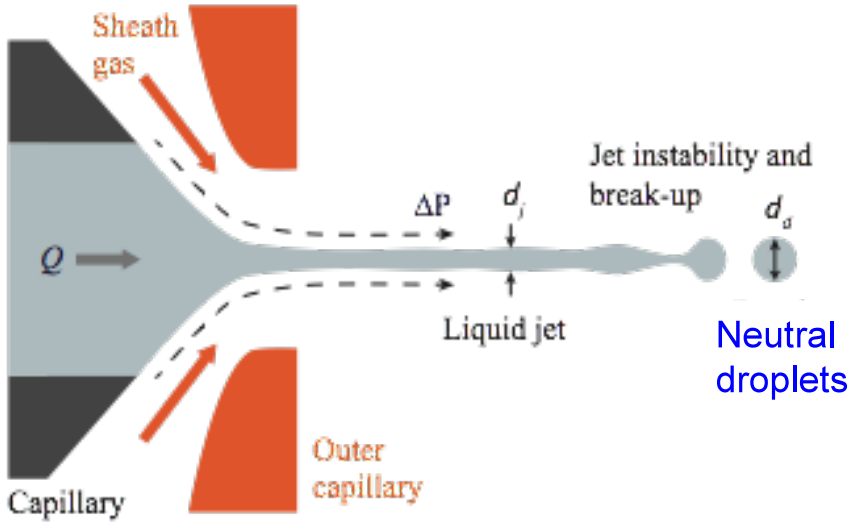

FIELD FOCUSSING:
Cone-jet electrospray (ESI)

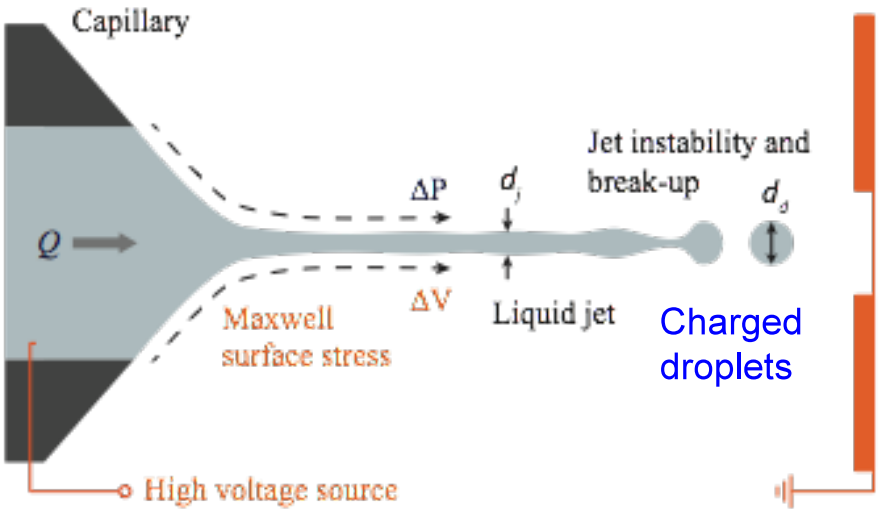

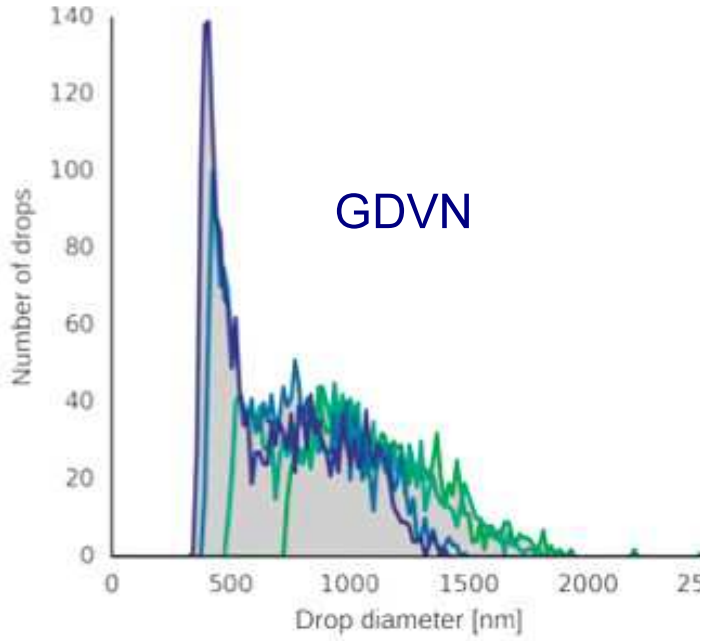

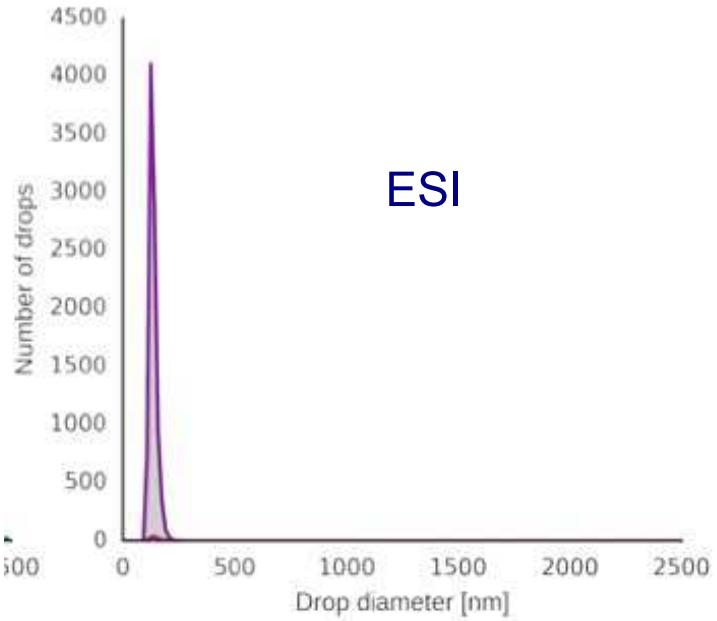

THE SMALLER THE DROPLETS THE LESS THE CONTAMINATION ON THE SAMPLE

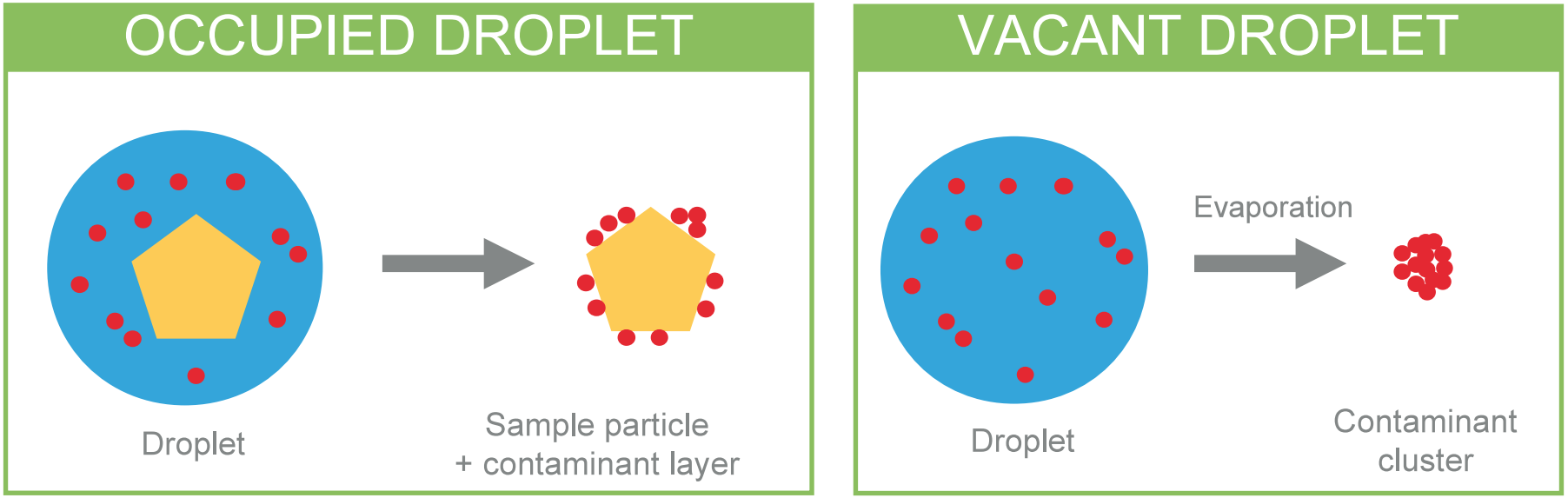

Reducing droplet size is sort of “sample purification”

GENTLE VAPOURISATION with a GAS DYNAMIC VIRTUAL NOZZLE

DePonte, D.P. et al.. J. Phys. D 41, 195505 (2008).

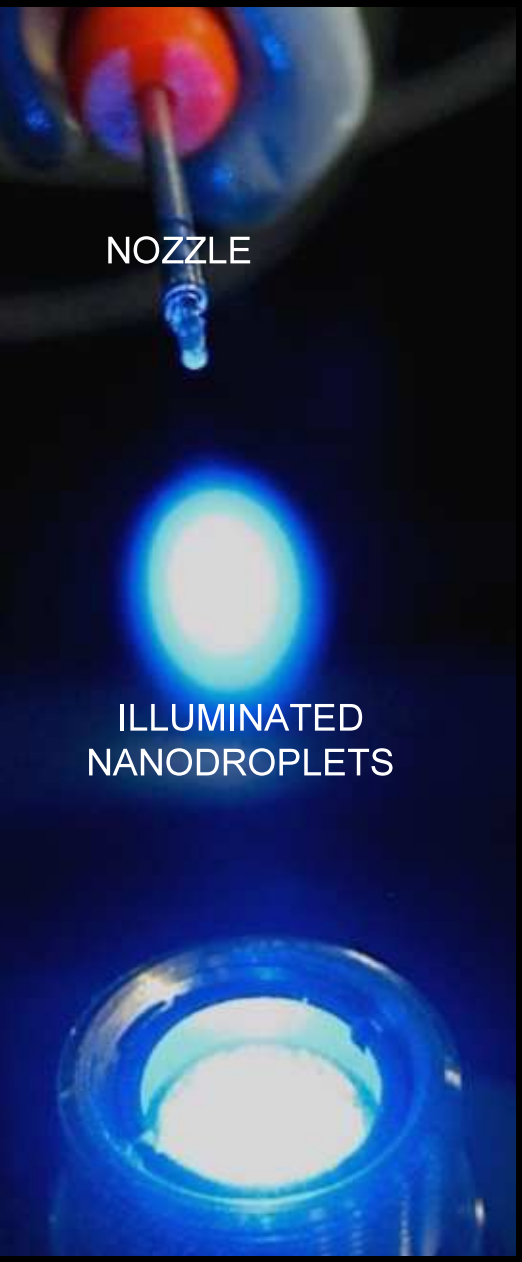

20 μm Ø

LIQUID FLOWS
at 0.06 m/s

THE GAS EXERTS A
"FLEXIBLE SQUEEZE"
ON THE JET

HELIUM

HELIUM

Acceleration
zone ~100 μm

The fluid is moving ~1 m/s faster in front of a 1 μm object than in the back of it

LIQUID FLOWS at ~100 m/s

THE GAS DYNAMIC NOZZLE HAS TWO APPLICATIONS

DePonte, D.P. et al. Gas dynamic virtual nozzle for generation of microscopic droplet streams. J. Phys. D 41, 195505 (2008).

HELIUM GAS

LIQUID

1. LIQUID JET for NANOCRYSTALLOGRAPHY

(high background from the jet)

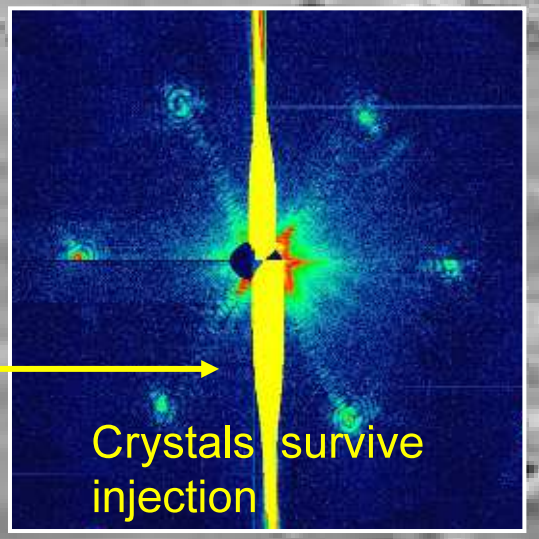

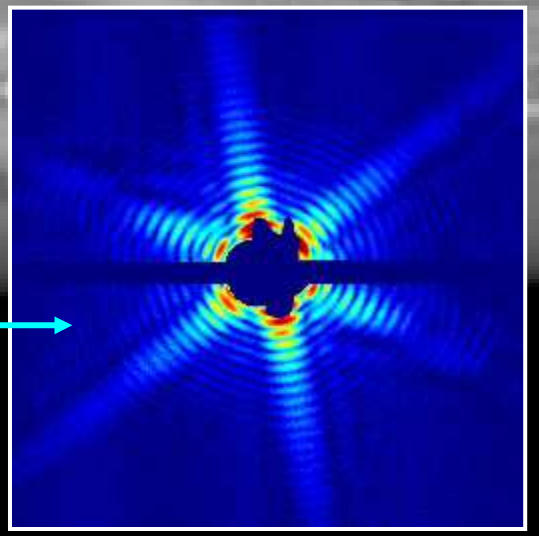

2. AEROSOLS FOR STUDIES ON SINGLE MOLECULES / PARTICLES (practically no added background)

AEROSOL SAMPLE INJECTION

Rick Kirian

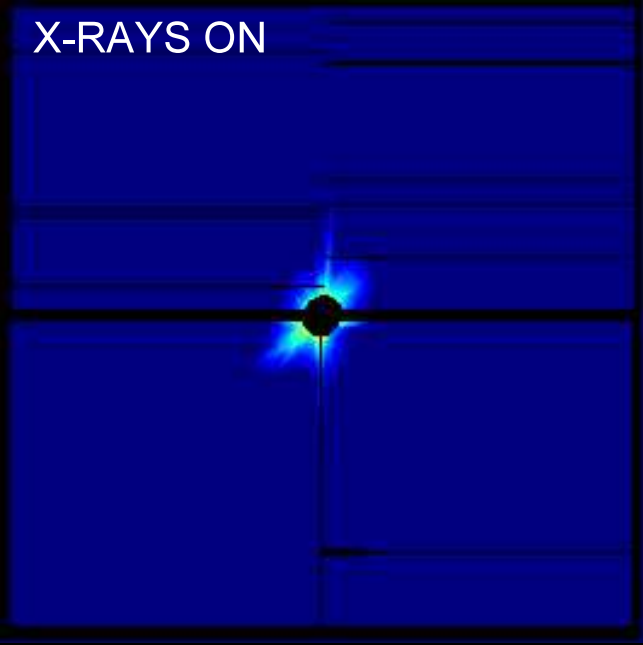

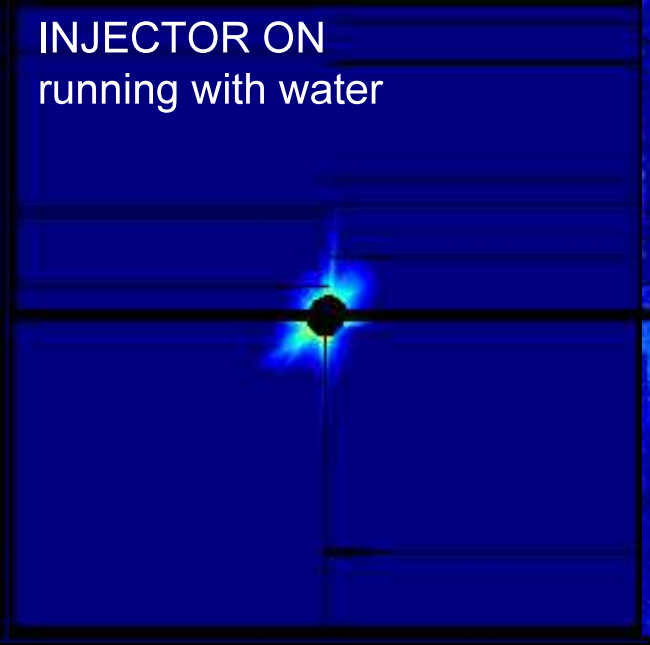

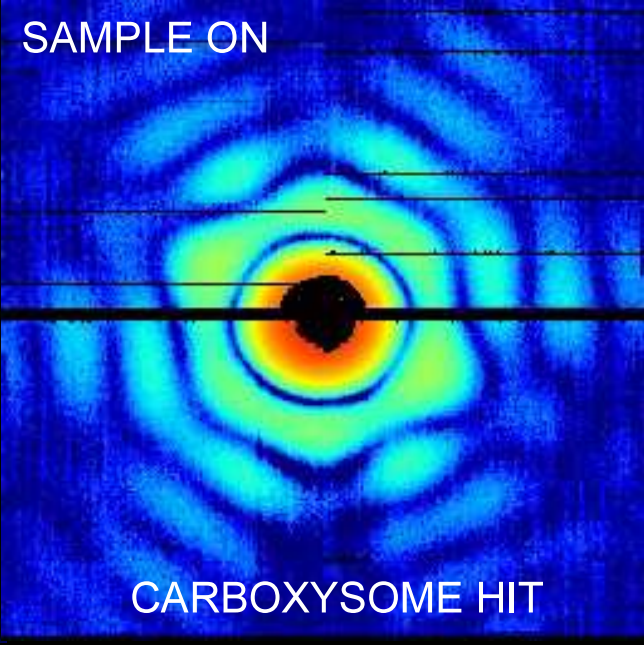

EVAPORATION CAN BE CONTROLLED BY ADJUSTING, PRESSURE, TEMPERATURE, LIQUID FLOW AND GAS FLOW. WE AVOID DROPLETS COMING THROUGH THE INJECTOR.

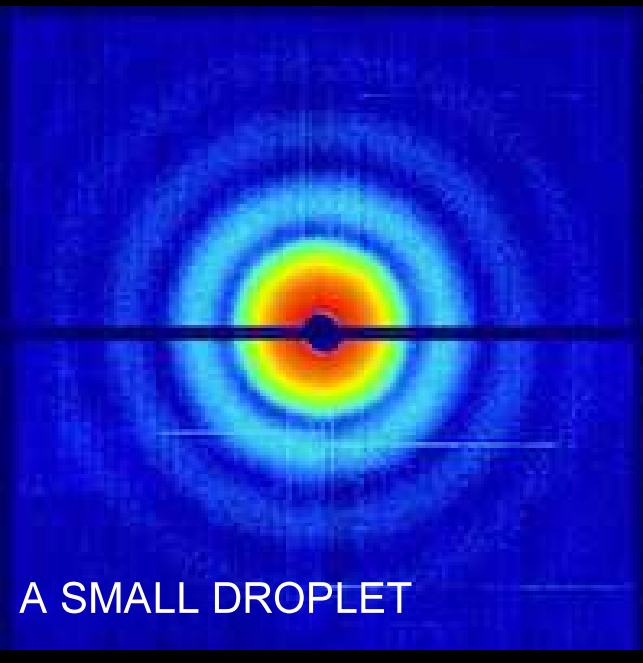

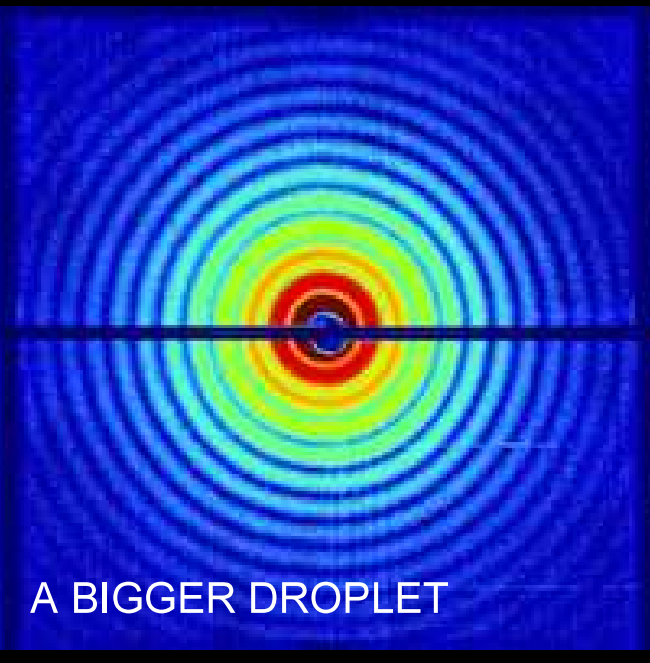

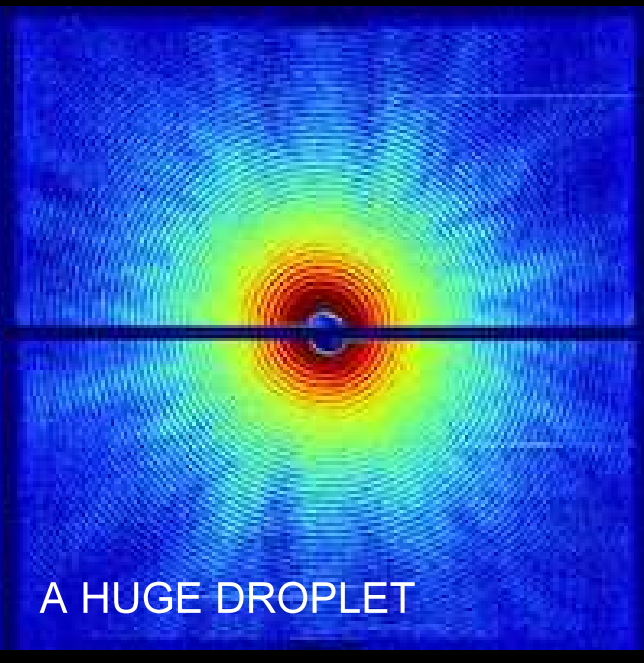

SAMPLES TESTED SO FAR

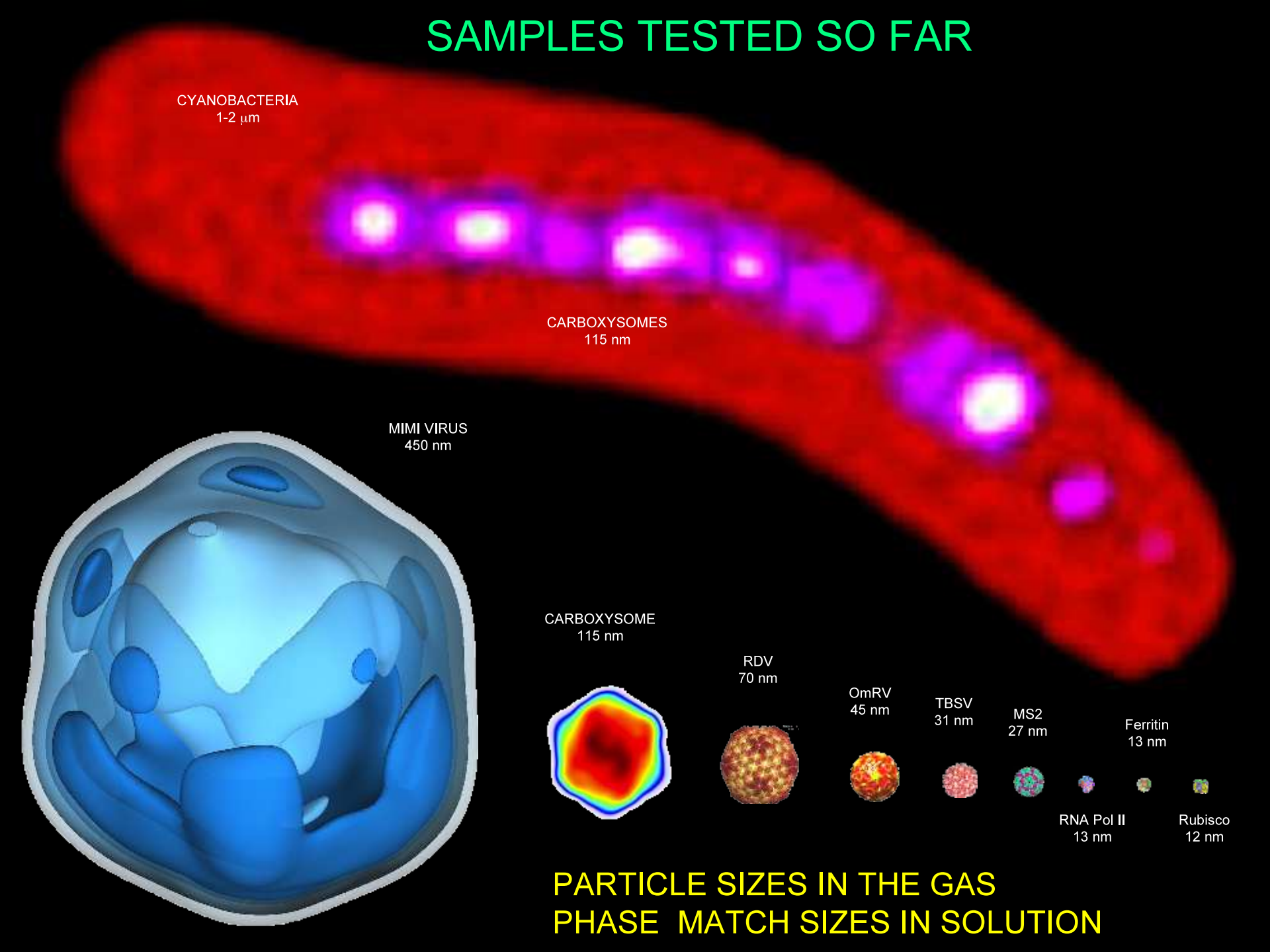

PARTICLE SIZES IN THE GAS PHASE MATCH SIZES IN SOLUTION

1st RESULTS from LCLS - SINGLE VIRUS PARTICLES

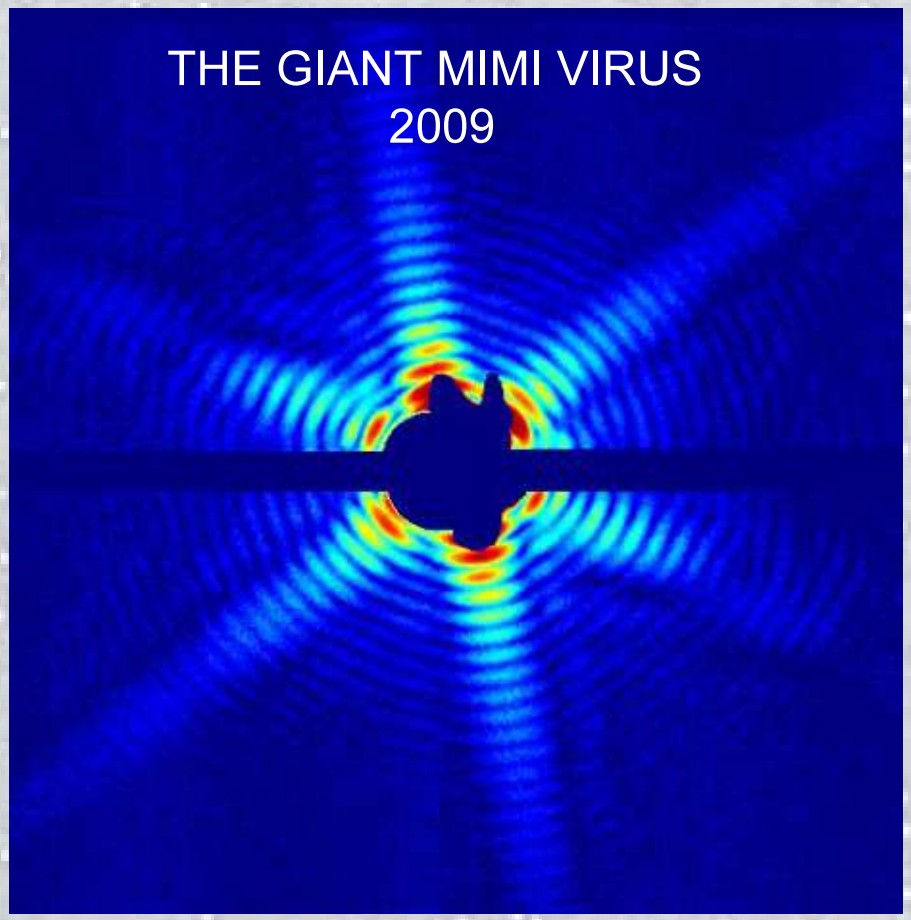

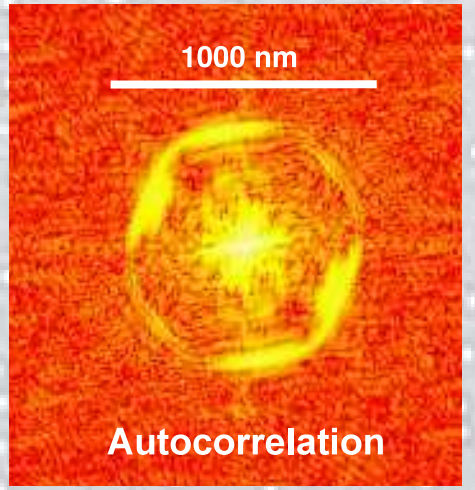

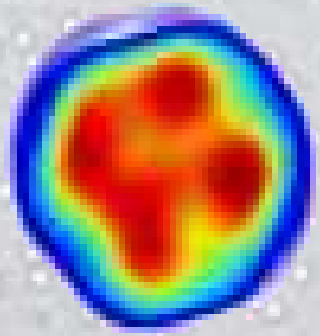

Projection image

Photon energy: 1.80 keV
Pulse length: 70 fs (FDHM)
Focus: 10 μm (FWHM)
1.6 x 10^{10} photons/μm²

Seibert, Ekeberg, Maia *et al*. *Nature* **470**, 78-U86 (2011).

From 2D to 3D structure determination

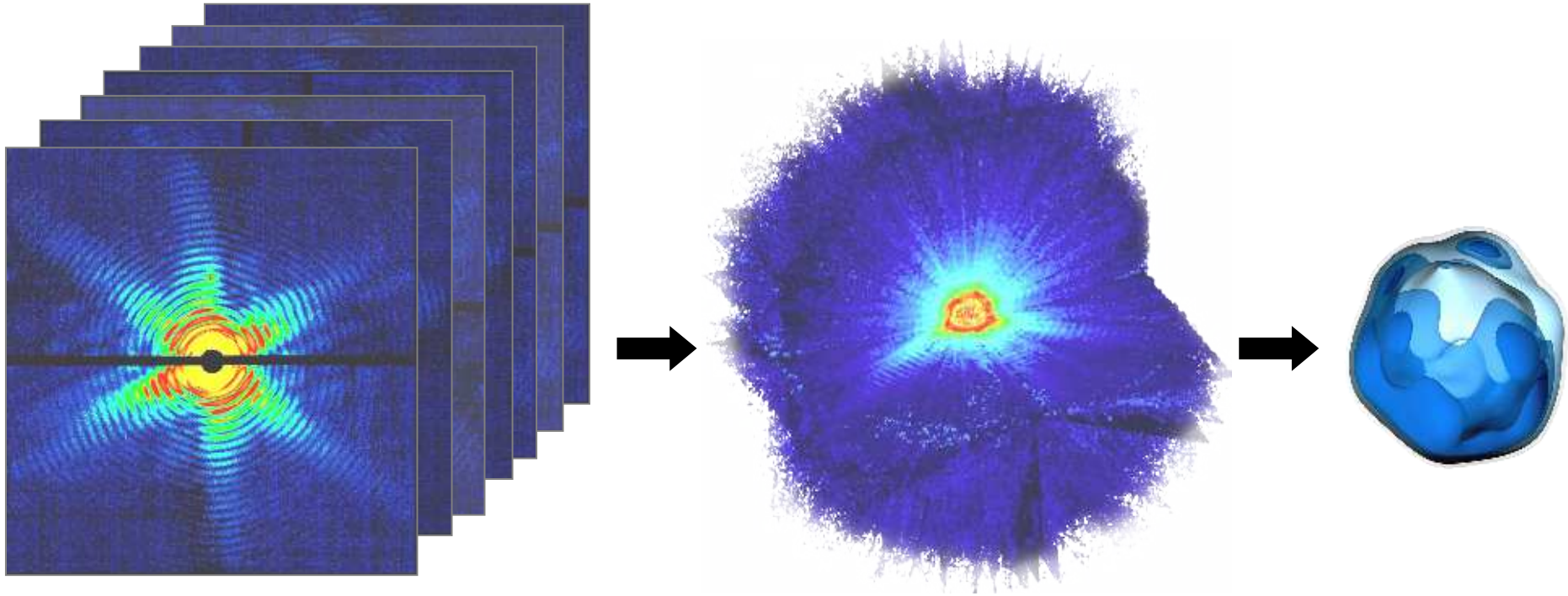

Individual exposures

Self-consistent 3D data set

Electron density map

EMC: Expectation Maximalisation and Compression

Based on Loh et al. *PRE* (2009)

PRL 114, 098102 (2015) Selected for a Viewpoint in *Physics* PHYSICAL REVIEW LETTERS week ending 6 MARCH 2015

Three-Dimensional Reconstruction of the Giant Mimivirus Particle with an X-Ray Free-Electron Laser

Tomas Ekeberg,[1,*] Martin Svenda,[1] Chantal Abergel,[2] Filipe R. N. C. Maia,[1,3] Virginie Seltzer,[2] Jean-Michel Claverie,[2] Max Hantke,[1] Olof Jönsson,[1] Carl Nettelblad,[1] Gijs van der Schot,[1] Mengning Liang,[4] Daniel P. DePonte,[4] Anton Barty,[4] M. Marvin Seibert,[1,5] Bianca Iwan,[1,6] Inger Andersson,[1] N. Duane Loh,[7] Andrew V. Martin,[8] Henry Chapman,[4,9] Christoph Bostedt,[5] John D. Bozek,[5] Ken R. Ferguson,[5] Jacek Krzywinski,[5] Sascha W. Epp,[10] Daniel Rolles,[10,11] Artem Rudenko,[11] Robert Hartmann,[12] Nils Kimmel,[13,14] and Janos Hajdu[1,15]

[1]*Laboratory of Molecular Biophysics, Department of Cell and Molecular Biology, Uppsala University, Husargatan 3 (Box 596), SE-751 24 Uppsala, Sweden*

[2]*Génomique & Structurale - IGS - UMR 7256, CNRS, Aix-Marseille Université, Institut de Microbiologie de la Méditerranée, Parc Scientifique de Luminy, Case 934, 13288 Marseille Cedex 9, France*

[3]*NERSC, Lawrence Berkeley National Laboratory, Berkeley, California 94720, USA*

[4]*Center for Free-Electron Laser Science, DESY, Notkestrasse 85, 22607 Hamburg, Germany*

[5]*LCLS, SLAC National Accelerator Laboratory, 2575 Sand Hill Road, Menlo Park, California 94025, USA*

[6]*Attophysics Group, CEA-Saclay, 91191 Gif sur Yvette Cedex, France*

[7]*Centre for BioImaging Sciences, National University of Singapore, 14 Science Drive 4 Blk S1 A, Singapore 117546, Singapore*

[8]*The University of Melbourne, Parkville, 3010 Victoria, Australia*

[9]*University of Hamburg, Notkestrasse 85, 22607 Hamburg, Germany*

[10]*Max Planck Advanced Study Group, Center for Free Electron Laser Science, Notkestrasse 85, 22607 Hamburg, Germany*

[11]*J. R. Macdonald Laboratory, Department of Physics, Kansas State University, 116 Cardwell Hall, Manhattan, Kansas 66506, USA*

[12]*PNSensor GmbH, Römmerstrasse 28, 80803 München, Germany*

[13]*Max-Planck-Institut Halbleiterlabor, Otto-Hahn-Ring 6, 81739 München, Germany*

[14]*Max-Planck-Institut für extraterrestrische Physik, Giessenbachstrasse, 85741 Garching, Germany*

[15]*European XFEL, Albert-Einstein-Ring 19, 22761 Hamburg, Germany*

(Received 3 October 2014; published 2 March 2015)

We present a proof-of-concept three-dimensional reconstruction of the giant mimivirus particle from experimentally measured diffraction patterns from an x-ray free-electron laser. Three-dimensional imaging requires the assembly of many two-dimensional patterns into an internally consistent Fourier volume. Since each particle is randomly oriented when exposed to the x-ray pulse, relative orientations have to be retrieved from the diffraction data alone. We achieve this with a modified version of the expand, maximize and compress algorithm and validate our result using new methods.

DOI: 10.1103/PhysRevLett.114.098102 PACS numbers: 42.30.-d, 87.64.-t, 87.64.Bx

FROM BIG TO SMALL: SINGLE PROTEIN MOLECULES

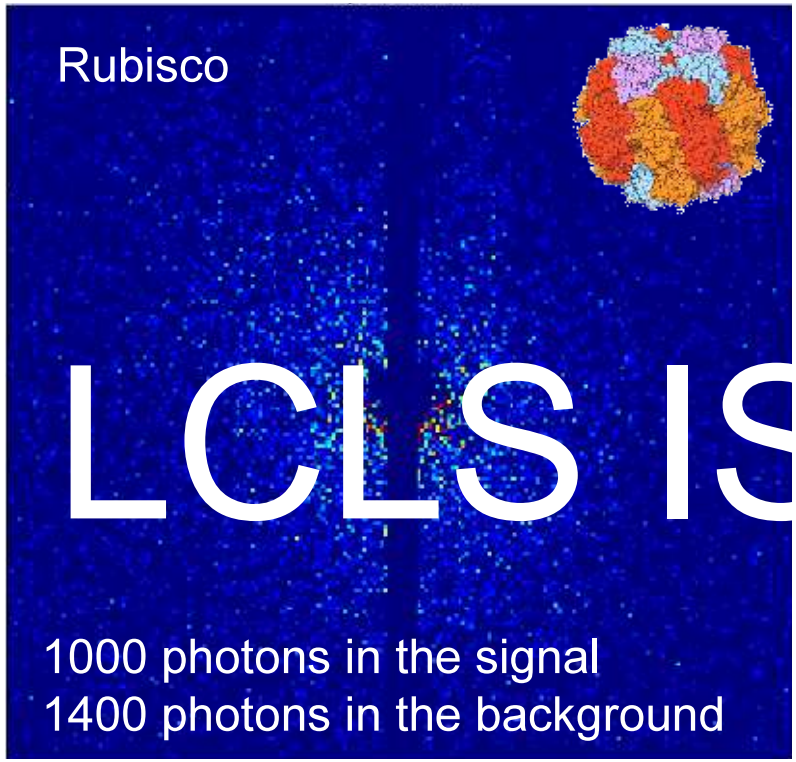

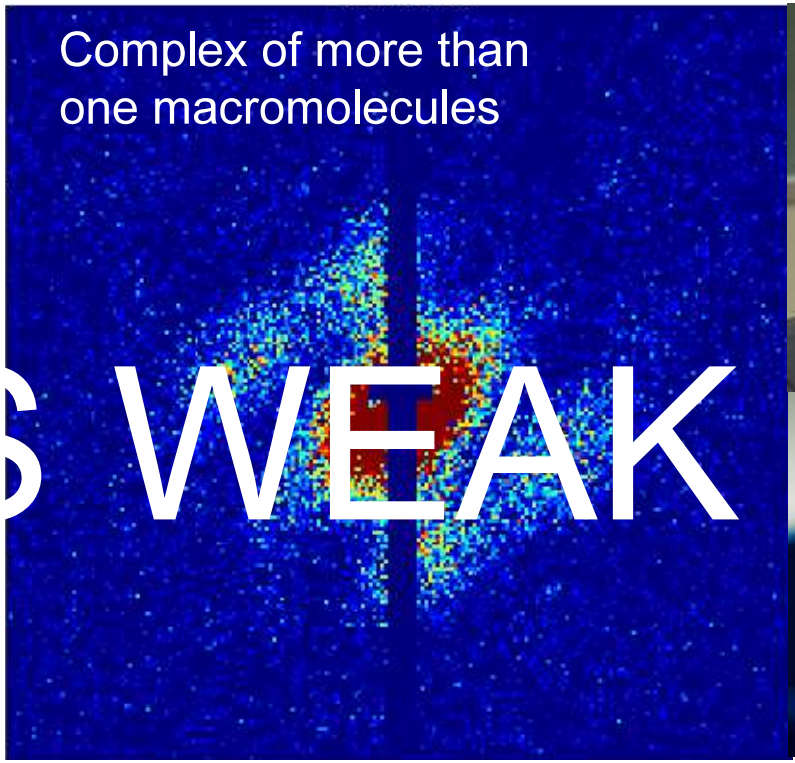

LCLS IS WEAK

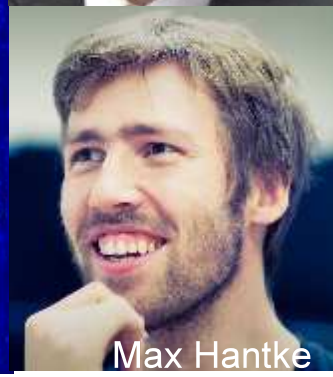

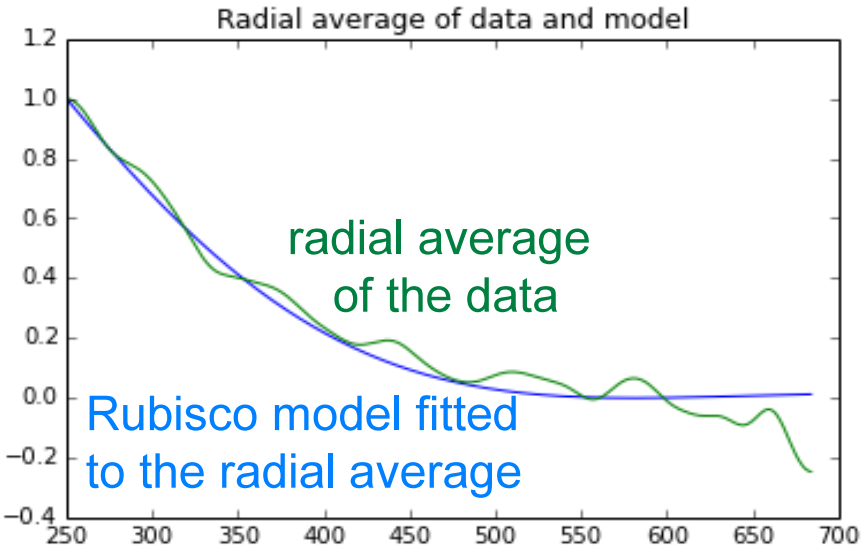

Pulse energy = 2.55 mJ
Focus = 3-5 μm
Wavelength = 1.55 nm (800 eV)
Resolution = 10.5 nm at the edge and 7.5 nm at the corner of the detector
Intensity on the sample: 0.01 mJ/μm^2

XFEL could give ~1000 x more photons

IMAGING LIVING CELLS

THE OTHER DREAM: IMAGING A LIVING CELL AT HIGH RESOLUTION

THE PROBLEM:

100,000,000 Grey is needed for a cell at 10 Å resolution

20 Grey kills a human

100 Grey kills a cell

25,000 kills all known germs

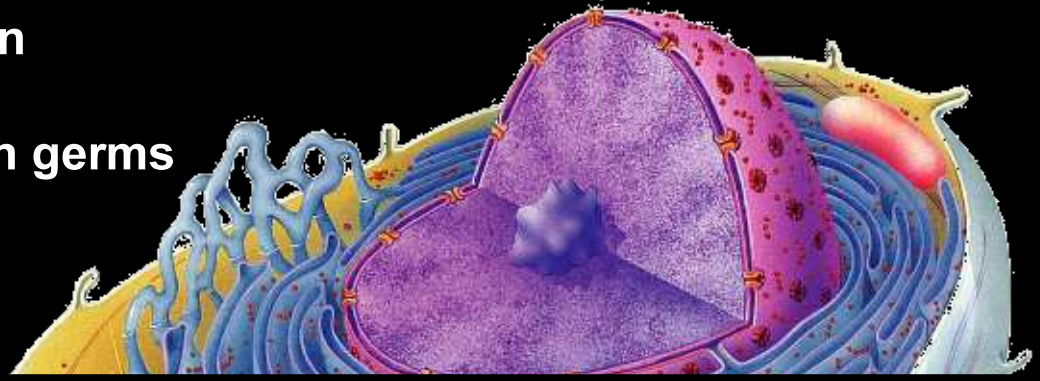

IN CONVENTIONAL STUDIES, THE FIRST HUNDRED MILLIONTH OF THE EXPOSURE KILLS THE CELL

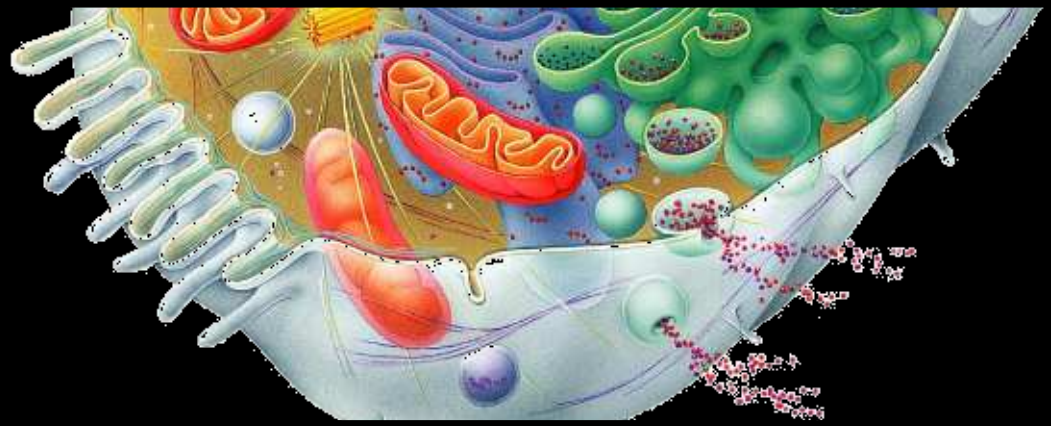

DIFFRACTION BEFORE DESTRUCTION CAN OVERCOME THIS PROBLEM


Shoot your own picoplankton
UMC
DNMI
METEOROLOGISKE OBSERVASJONER
PÅ MARITIME STASJONER
C_L


Half of all photosynthesis on the planet is done by microorganisms in the Arctic and Antarctic oceans

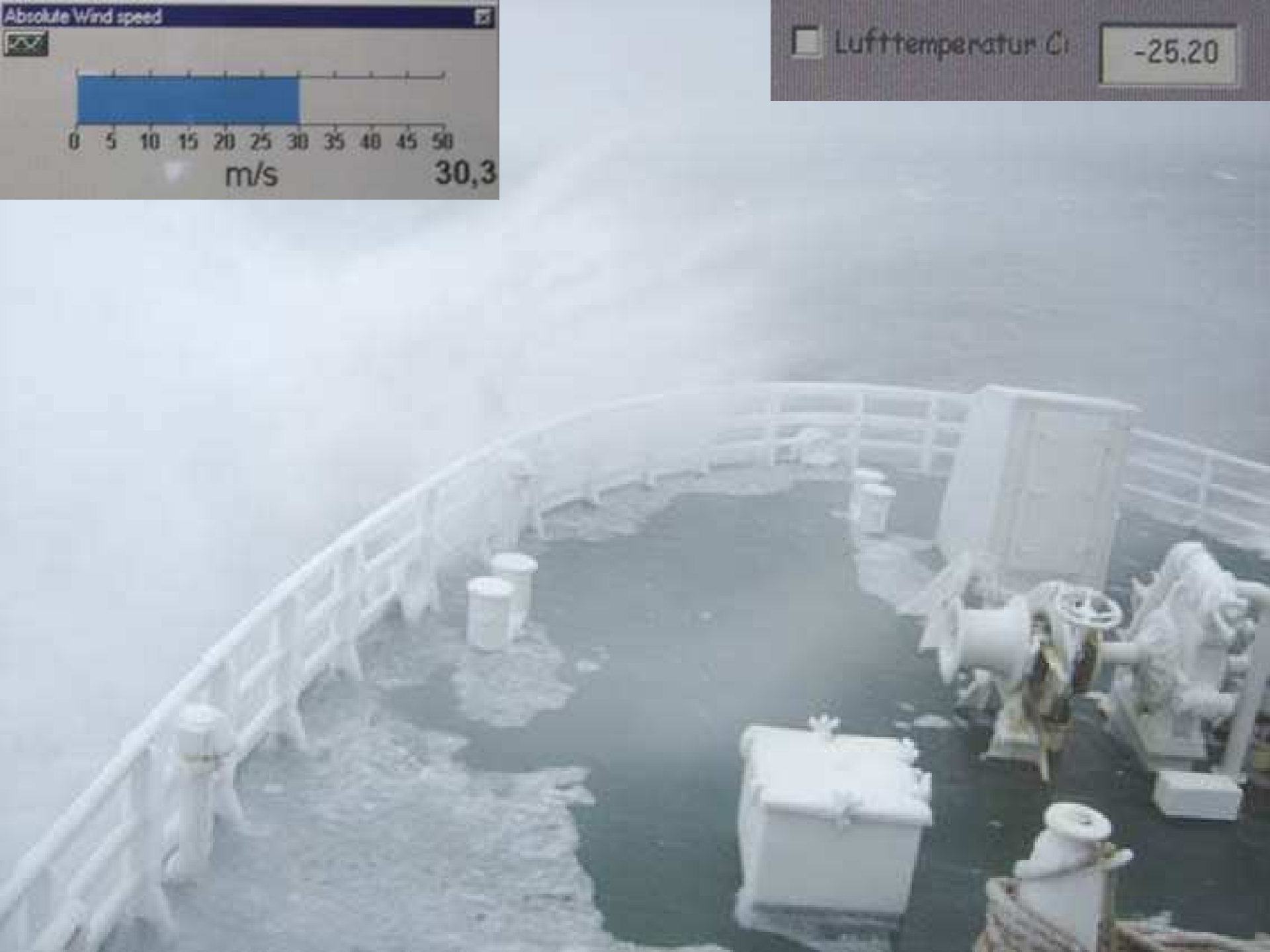
Absolute Wind speed
0 5 10 15 20 25 30 35 40 45 50
m/s
30,3
Lufttemperatur C
-25.20

85º North of Svalbard

The company


The probe

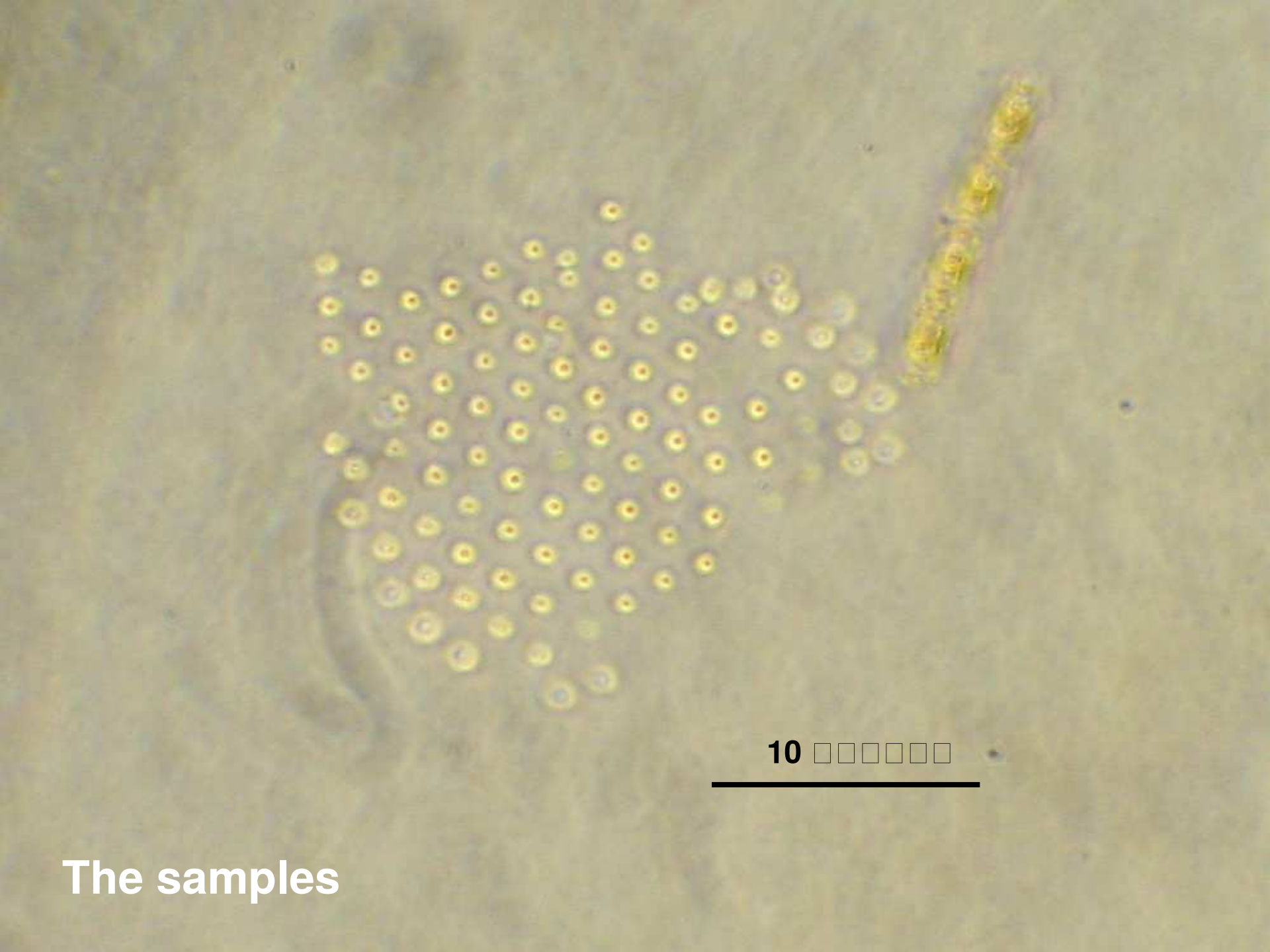

The samples

FIRST FLASH DIFFRACTION IMAGE OF A LIVING CELL

FLASH soft X-ray laser, Hamburg, Germany, 6 NOV 2006

FLASH pulse length: 10 fs
Wavelength: 13.5 nm

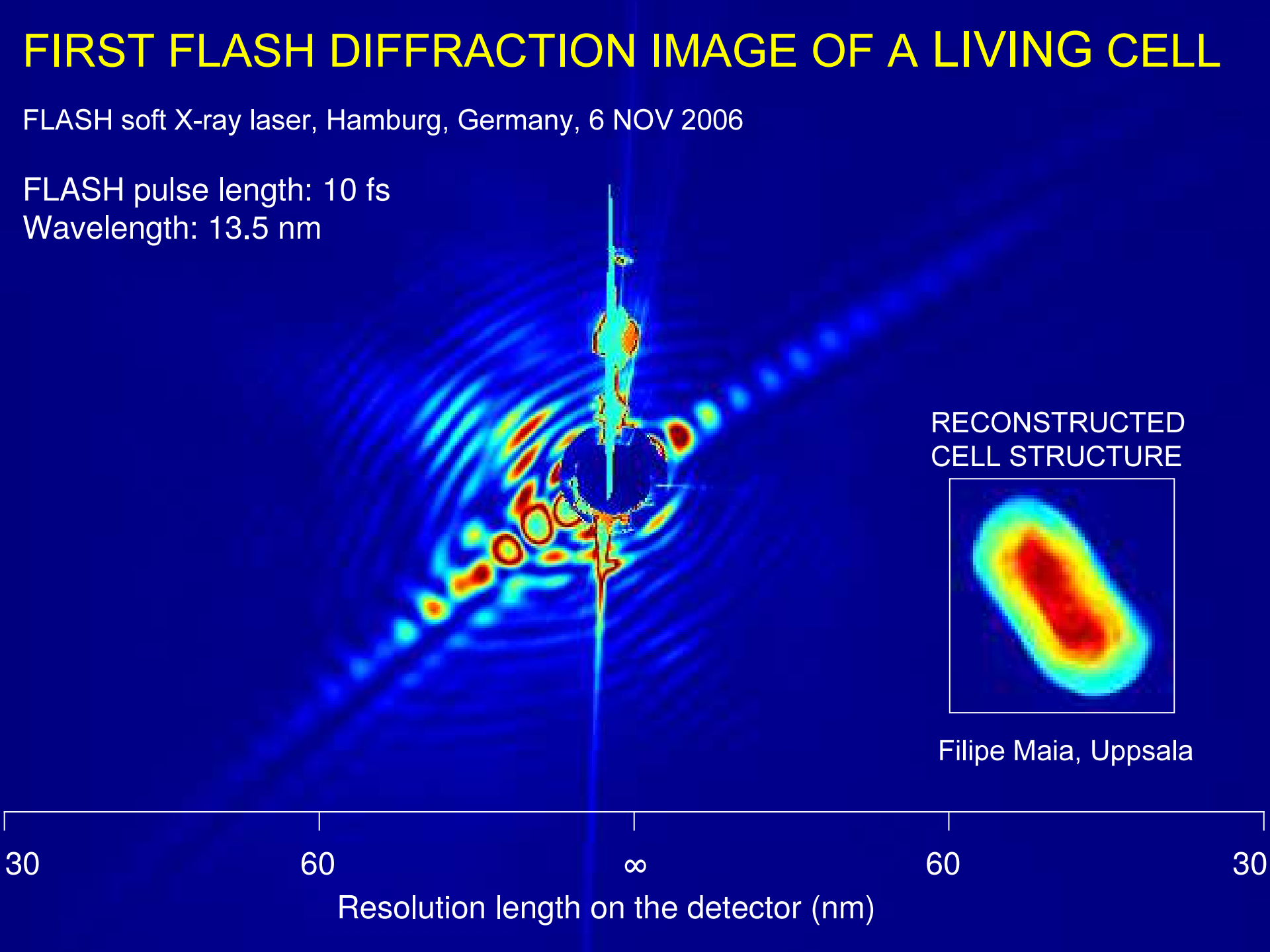

RECONSTRUCTED
CELL STRUCTURE

Filipe Maia, Uppsala

30 60 ∞ 60 30

Resolution length on the detector (nm)

nature COMMUNICATIONS

ARTICLE

Received 1 Apr 2014 | Accepted 29 Oct 2014 | Published 11 Feb 2015

DOI: 10.1038/ncomms6704

Follow up in 2016 at the LCLS

Imaging single cells in a beam of live cyanobacteria with an X-ray laser

Gijs van der Schot[1,*], Martin Svenda[1,*], Filipe R.N.C. Maia[1,2], Max Hantke[1], Daniel P. DePonte[3,4], M. Marvin Seibert[1,4], Andrew Aquila[3,5], Joachim Schulz[3,5], Richard Kirian[3], Mengning Liang[3], Francesco Stellato[3,6], Bianca Iwan[1], Jakob Andreasson[1], Nicusor Timneanu[1], Daniel Westphal[1], F. Nunes Almeida[1], Dusko Odic[1], Dirk Hasse[1], Gunilla H. Carlsson[1], Daniel S.D. Larsson[1], Anton Barty[2], Andrew V. Martin[3,7], Sebastian Schorb[4], Christoph Bostedt[4], John D. Bozek[4], Daniel Rolles[3], Artem Rudenko[3,8], Sascha Epp[3], Lutz Foucar[9], Benedikt Rudek[10], Robert Hartmann[11], Nils Kimmel[11,12], Peter Holl[11], Lars Englert[13], Ne-Te Duane Loh[14], Henry N. Chapman[3,15], Inger Andersson[1], Janos Hajdu[1,5] & Tomas Ekeberg[1]

There exists a conspicuous gap of knowledge about the organization of life at mesoscopic levels. Ultra-fast coherent diffractive imaging with X-ray free-electron lasers can probe structures at the relevant length scales and may reach sub-nanometer resolution on micron-sized living cells. Here we show that we can introduce a beam of aerosolised cyanobacteria into the focus of the Linac Coherent Light Source and record diffraction patterns from individual living cells at very low noise levels and at high hit ratios. We obtain two-dimensional projection images directly from the diffraction patterns, and present the results as synthetic X-ray Nomarski images calculated from the complex-valued reconstructions. We further demonstrate that it is possible to record diffraction data to nanometer resolution on live cells with X-ray lasers. Extension to sub-nanometer resolution is within reach, although improvements in pulse parameters and X-ray area detectors will be necessary to unlock this potential.

LIVE CELLS IN MOLECULAR DETAILS?

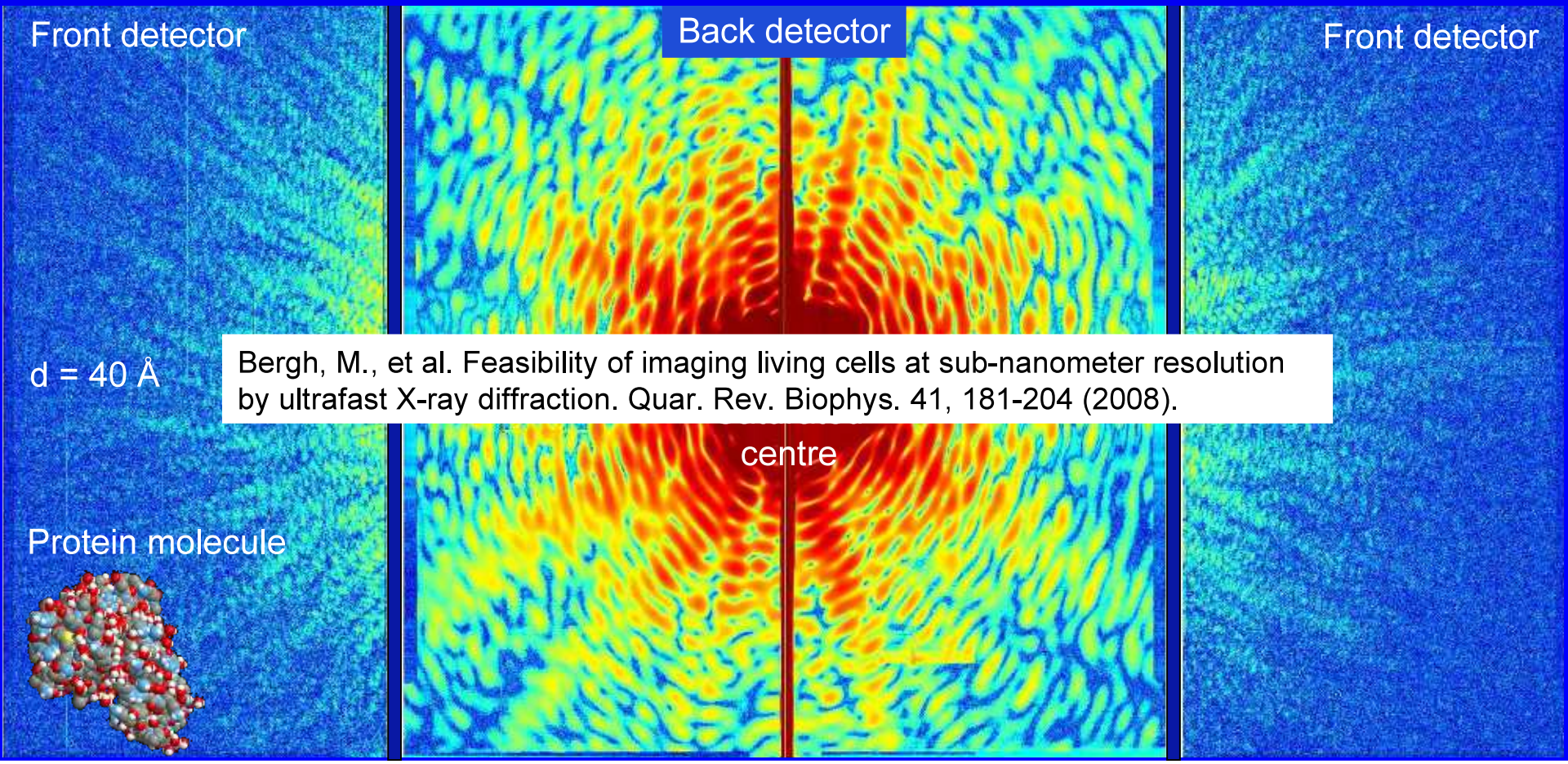

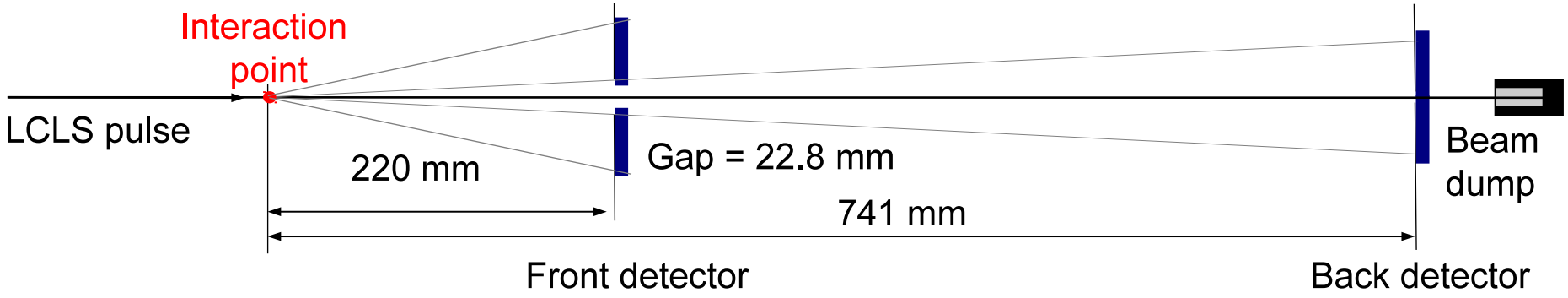

2017: the European XFEL

2.3 billion shots/day

Up to 10^{15} photons/shot expected

QuickTime™ and a
decompressor
are needed to see this picture.

First lasing on 4 May 2017

“To understand the whole you must look at the whole”

H. Kacser “On parts and wholes in metabolism” in: Welch GR, Clegg JS (eds) *The organisation of cell metabolism*, Plenum Press, New York, p 327, (1986).

Background image: http://biology.usf.edu/cmmb/undergrad/bi

Most of what has been presented here had to be established from scratch. And a lot more has to be done.

Alterelli: ”There is a steep learning curve to climb, for experiments and also for theory, in order to exploit these potentials”

RESERVE SLIDES

The ultimate impact of X-ray lasers must be considered in relation to recent developments in electron cryo-microscopy

Electron microscopy
Excellent cross sections
Phases
Long history
Great S/N from 2012 onwards
Many instruments
but
Short penetration depth (sample size)
Small field of view (small sample size)
Low scattered flux per exposure
Low temporal resolution
Frozen state, background from ice

Ultra-fast diffractive imaging
Long penetration depth, big objects
fs-as time resolution
fs-as pulses: Better cross sections !
Damage can be ~eliminated
Millions or billions of exposures/day
Access to fs-as DYNAMICS
but
Phases need to be determined
A few of these machines exists
New field and learning
FEL pulses are weak today…
…these pulses are great for xtals!

Both methods have tremendous potentials but none of them is perfect.

What is image reconstruction?

- Image reconstruction methods try to recover an image of an object from it's diffraction pattern alone.

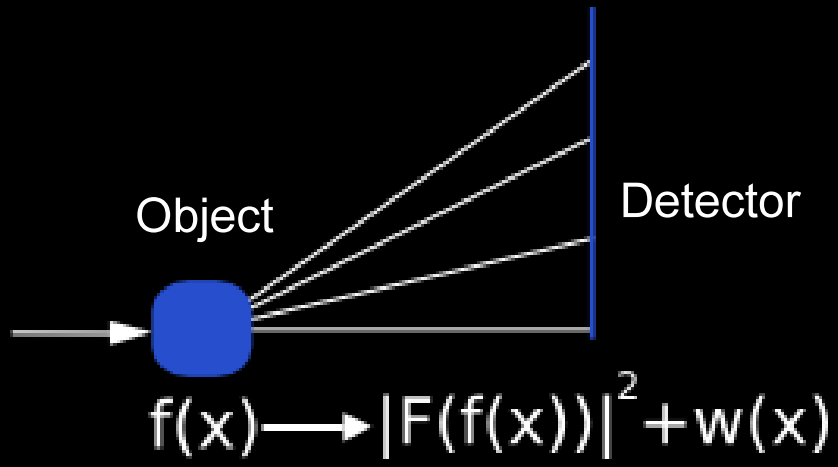

- This is done by solving the inverse of the problem of calculating the diffraction pattern of a given object, and as such fall under the category of inverse problems.

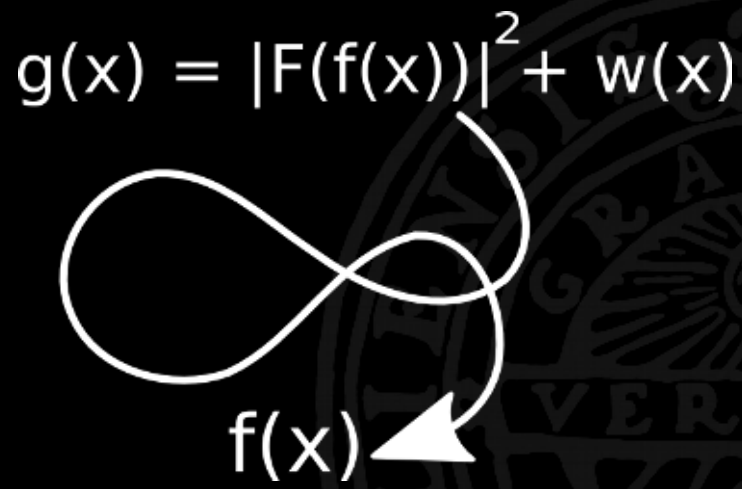

Fundamental difficulties

•Only the magnitude of the complex function F(f(x)) is known (famous phase problem).

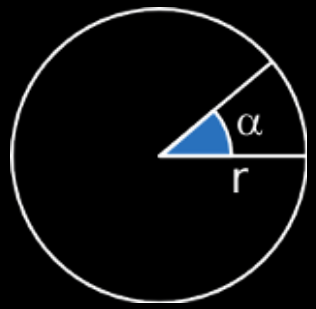

$r = |F(f(x))|$

$\alpha = ?$

•The problem is ill-conditioned, meaning that small variations in the input give rise to big variations in output.

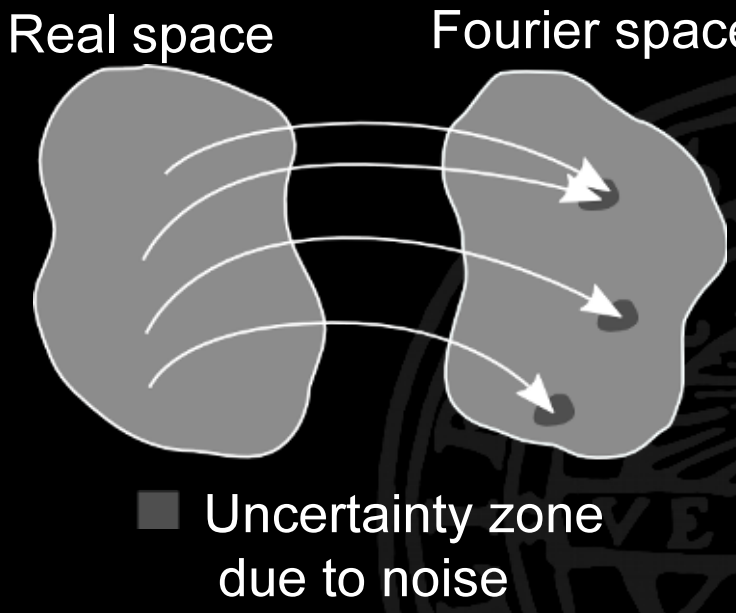

Fundamental difficulties

- The problem is further ill-posed due to noise in the diffraction pattern.

- Unless the diffraction pattern is oversampled (bandwidth limited), the problem is also underdetermined.

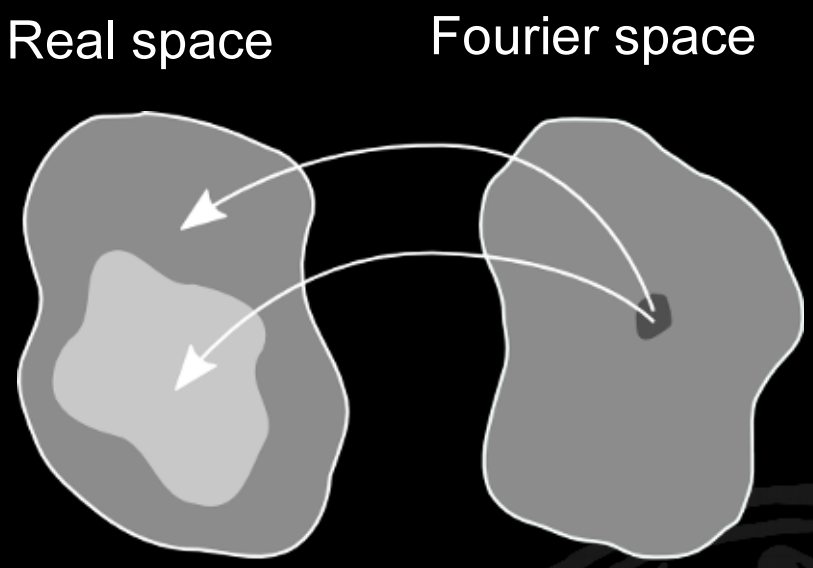

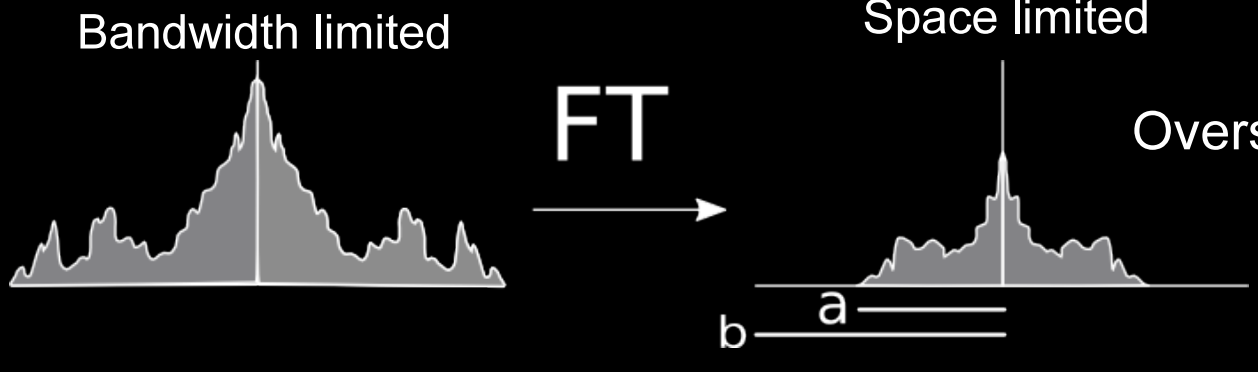

Oversampling degree (α)

$\alpha = b/a$

Additional difficulties

- The incident light is not perfectly monochromatic causing blurring of the diffraction pattern.
- Beamstops limit the availability of low resolution data.
- Radiation damage can cause changes in the object during exposure.
- Some pixels in the detector are usually saturated.

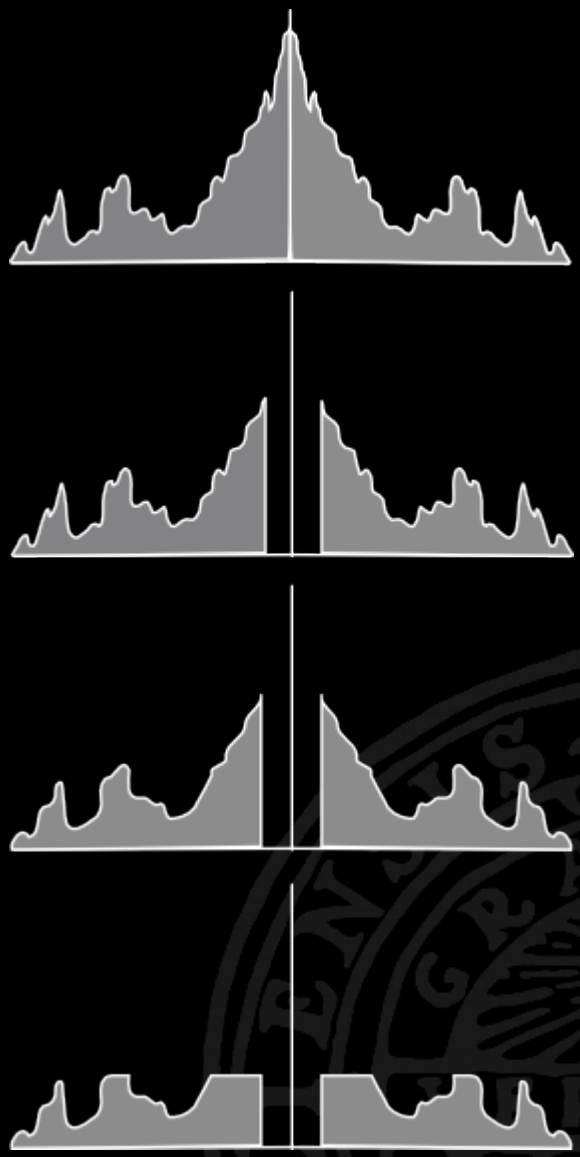

Phasing and deconvolution

- The problem of phasing |F(f(x))| is equivalent to the problem of deconvoluting f(x)*f(-x).

- Due to the convolution theorem the autocorrelation of f(x) can be directly calculated from the diffraction pattern.

- The autocorrelation function can be used as a starting point for the reconstruction.

$$F^{-1}|F(f(x))|^2 = f(x) * f(-x)$$

$$F^{-1}g(x) \approx f(x) * f(-x)$$

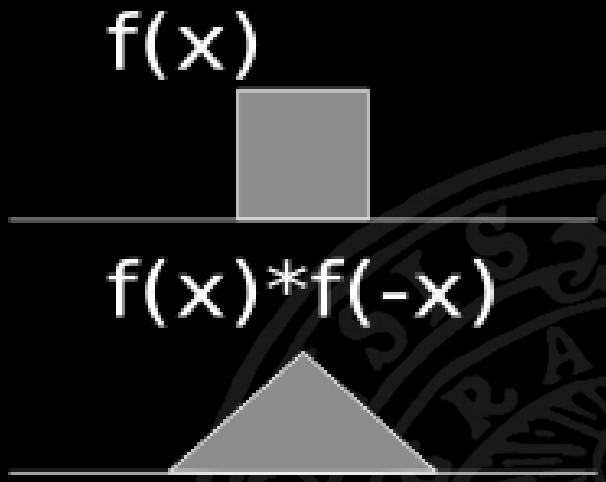

$$f(x) * f(-x) \neq 0$$

contains $f(x) \neq 0$

Reconstruction methods

- Almost all phase retrieval methods are iterative fixed point schemes.
- Based on the Gerchberg-Saxton error reduction algorithm.
- Use constraints in real space (support) and Fourier space (intensities)
- Make use of 2 projection operators, usually called P_s and P_m.

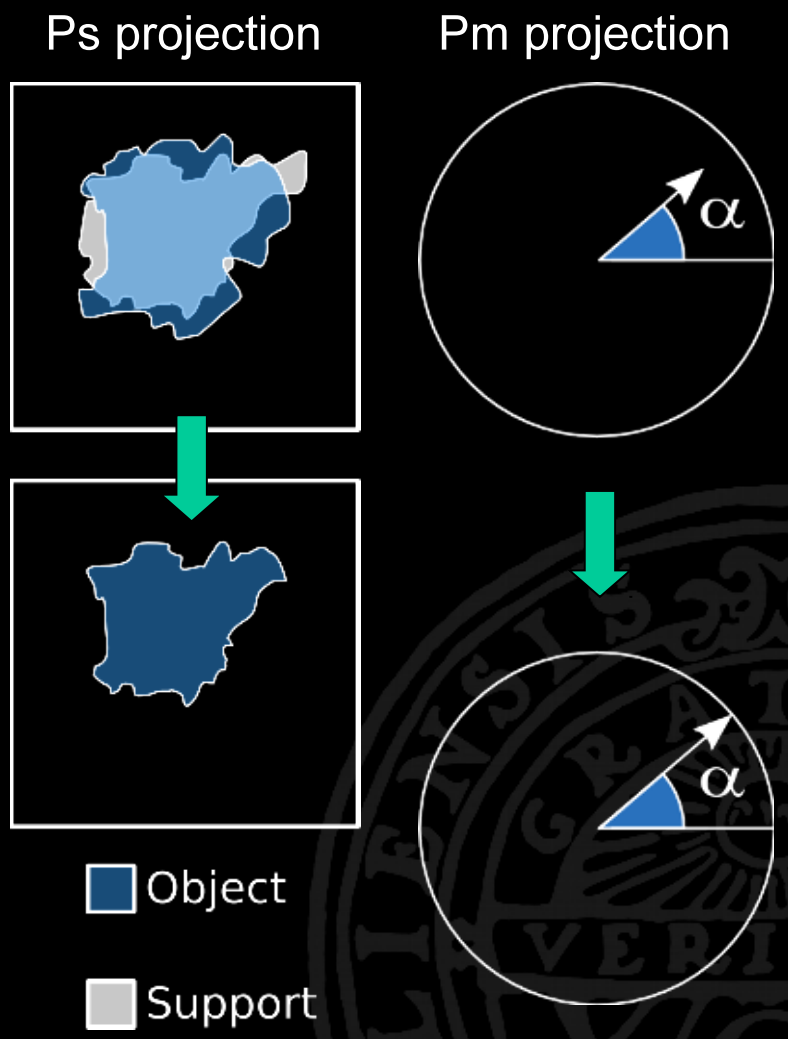

Algorithms overview

- Large number of existing algorithms.
- Addition of the relaxation parameter (β).
- HIO is still one of the more used ones.
- None of the existing algorithms by themselves is enough.

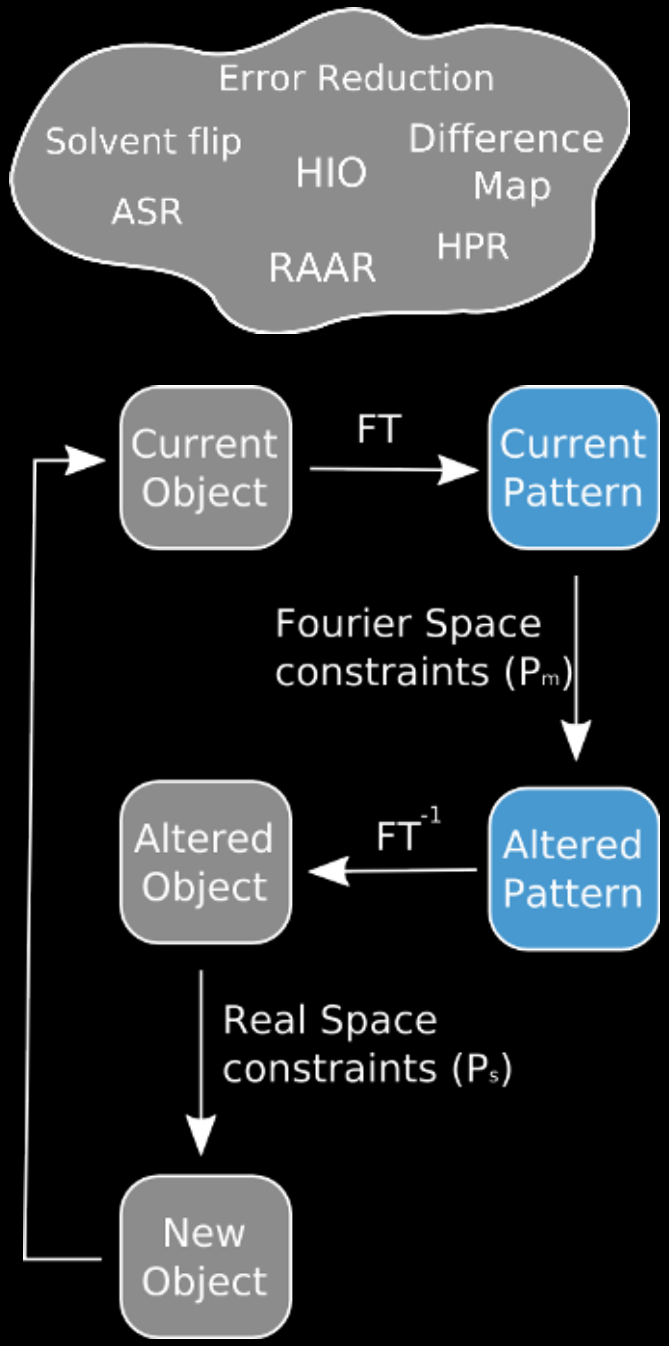

Resonant scattering beyond one photon at a time

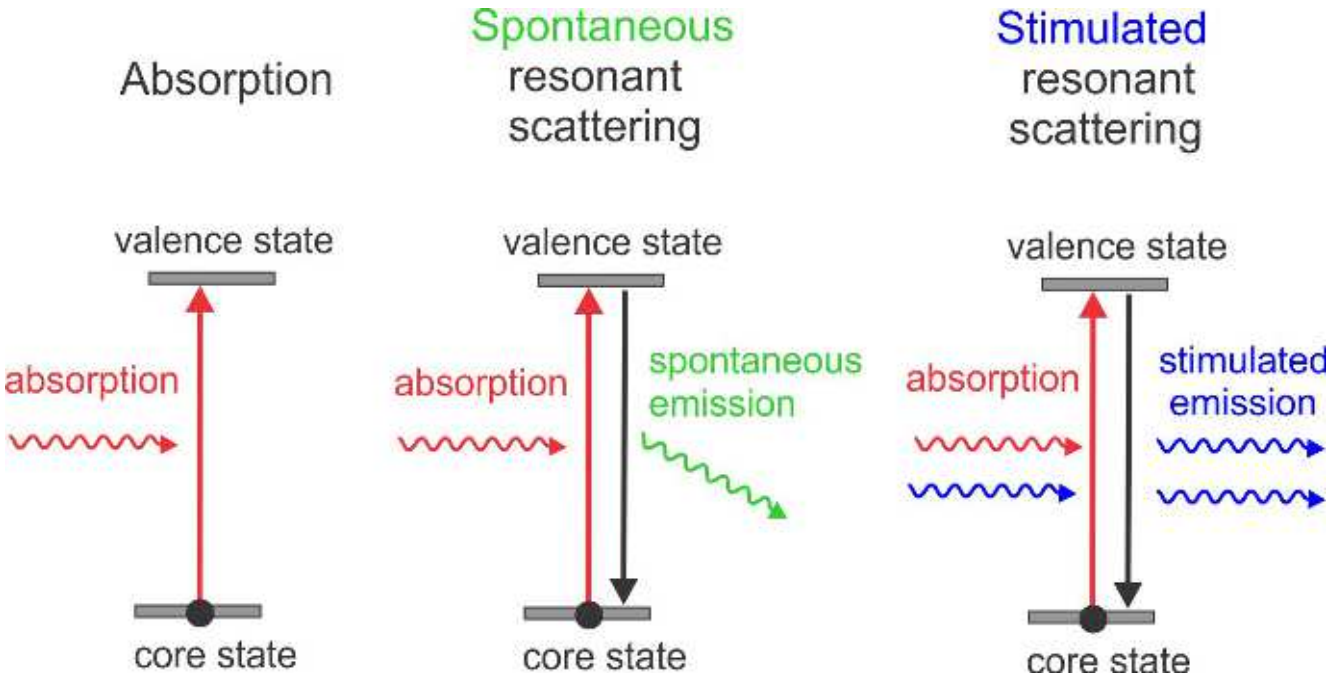

- **Spontaneous** scattering is random ⇨ on average a "spherical wave"
- **Stimulated** scattering is directional ⇨ cloned photon pair propagates in forward direction
- At high intensity all x-ray emission processes become stimulated ⇨ sample becomes transparent (Stöhr and Scherz, PRL **115**, 107402 (2015))

One-photon versus two-photon diffraction

Spontaneous diffraction - each photon interferes only with itself

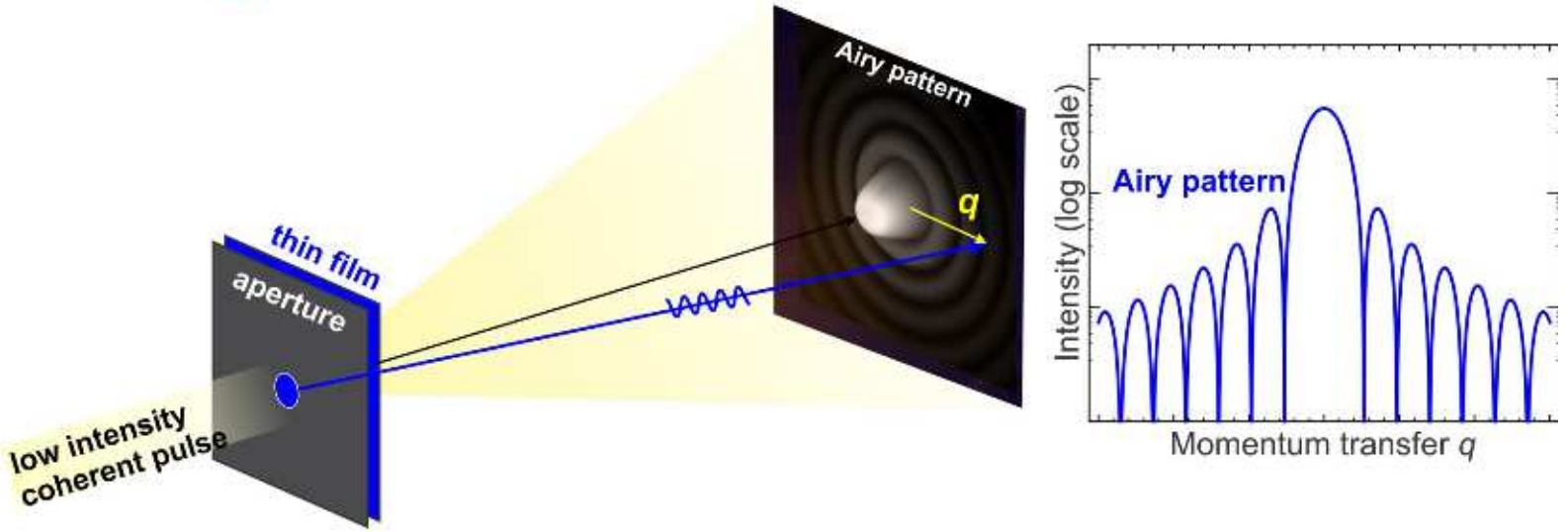

DIFFRACTION BEFORE DESTRUCTION has now been demonstrated to Ångström resolution on **CRYSTALS**, and to nm resolution on **VIRUS PARTICLES / BIOMOLECULES**

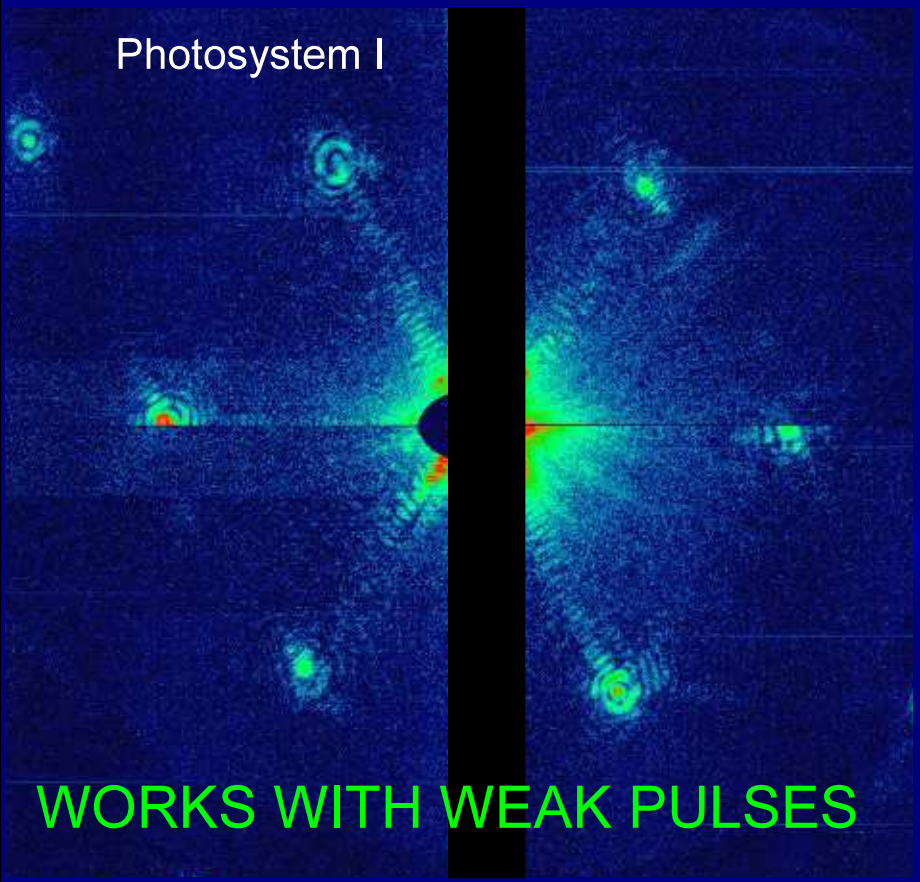

WORKS WITH WEAK PULSES

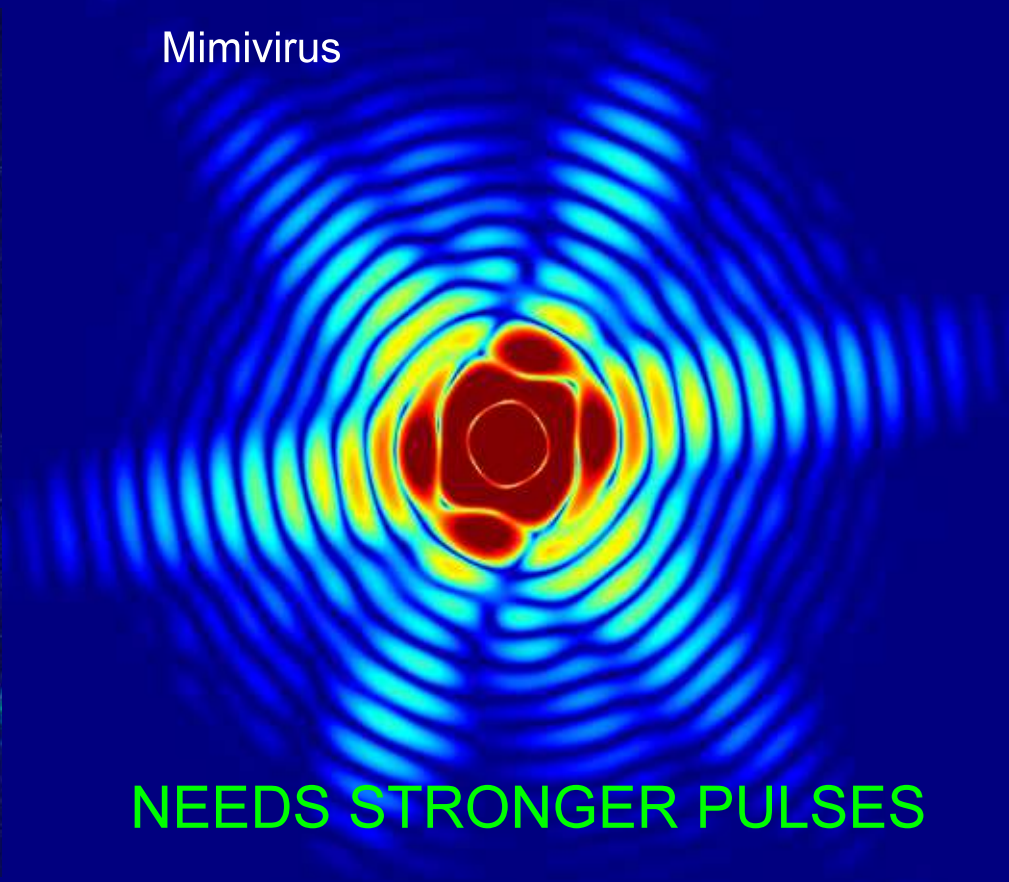

NEEDS STRONGER PULSES

Outrunning damage is routinely exploited in practically all applications of X-ray FELs